

Bis- and Tris(amidine)fluoroboron Cations and
Related Systems Studied by Multinuclear NMR
and Fast Atom Bombardment Mass Spectrometry

Zheng Yuan, B. Sc.
Beijing Institute of Technology, P. R. China

A thesis submitted to the
Department of Chemistry
in partial fulfilment of the requirements
for the degree of
Master of Science.

Brock University,
St. Catharines, Ontario
August, 1988

© Zheng Yuan

To my parents, my wife and my daughter
for their love

ABSTRACT

The formation and the isolation of fluoroboron salts, $(D_2BF_2^+)(PF_6^-)$, $(DD'BF_2^+)(PF_6^-)$ and $(D_3BF_2^+)(PF_6^-)_2$, have been carried out. 1,8-Diazabicyclo[5,4,0]undec-7-ene (**DBU**) and 1,5-diazabicyclo[4,3,0]non-5-ene (**DBN**), extremely strong organic bases, were introduced into the fluoroboron cation systems and induced a complicated redistribution reaction in the $D/BF_3/BCl_3$ systems. The result was the formation of all $BF_nCl_{4-n}^-$, $D.BF_nCl_{3-n}$ and fluoroboron cation species which were detected by ^{19}F and ^{11}B NMR spectrometry. The displacement reaction of Cl^- from these $D.BF_nCl_{3-n}$ ($n = 1$ and 2) species by the second entering ligand is much faster than in other nitrogen donor containing systems which have been previously studied. Tetramethylguanidine, oxazolines and thiazolines can also produce similar reactions in $D/BF_3/BCl_3$ systems, but no significant $BF_nCl_{4-n}^-$ species were observed. As well as influences of their basicity and their steric hindrance, $N=C-R(X)$ ($X = N, O$ or S) and $N=C-(X)_2$ ($X = N$ or S) structures of ligands have significant effects on the formation of fluoroboron cations and the related NMR parameters.

$D_3BF_2^+$ and some $D_2BF_2^+$ show the expected inertness, but $(DBU)_2BF_2^+$ shows an interestingly high reactivity. $(D_2BF_2^+)(X^-)$ formed from weak organic bases such as pyridine can react with stronger organic bases and form $DD'BF_2^+$ and $D'_2BF_2^+$ in acetone or nitromethane.

Fast atom bombardment mass spectrometry is doubly meaningful to this work. Firstly, FABMS can be directly applied to the complicated fluoroboron cation containing solution systems as an excellent complementary technique to multinuclear NMR. Secondly, the gas-phase ion substitution reaction of $(D_2BF_2^+)(PF_6^-)$ with the strong organic bases is successfully observed in a FABMS ion source when the B-N bond is not too strong in these cations.

Acknowledgements

The author would like to express his great thanks and gratitude to his supervisor Dr. J. S. Hartman for his guidance, encouragement and advice during all his time at Brock University. Deep thanks to Dr. M. F. Richardson for her patience and confidence in him in the field of inorganic chemistry; to Dr. J. M. Miller for his support and help, especially with the applications of FAB; and to Dr. H. L. Holland and Dr. M. S. Gibson for their constructive and helpful suggestions and discussions with respect to the organic synthesis.

Special thanks to Mr. T. R. B. Jones for his teaching and assistance with the analytical equipment; to Dr. Balasanmugam for the co-work and running of FAB samples; to Dr. Chenchiah for helping to set up the equipment for the organic synthesis.

All of the faculty and Staff of the department of chemistry and Brock University have made a deep impression on him.

Thanks to David for his time and patience in improving the author's written English in this thesis. The author can not forget these friends inside and outside of his Lab: all of the Chinese students, Bea, Doug, Caroline, Catherine, Ann, Lev, Adrian, and everyone else.

Thanks also to the Guelph Analytical Centre for the elemental analysis of the compounds; to McMaster University for AM-500 FT NMR instrumental time; and to Abbott and Air Products for the DBU sample.

Finally, a grant from N. S. E. R. C. has given the author an essential financial support.

Table of Contents

	Page
Dedication	ii
Abstract	iii
Acknowledgements	iv
Table of Contents	v
List of Tables	x
List of Figures	xi
Chapter I Introduction	1
A. Boron Trihalide Adducts and Redistribution Reactions	1
1) Boron Trihalides and Acceptor Behavior	1
2) Boron Trihalide Adducts	2
3) Redistribution Reactions	3
B. Tetracoordinated Fluoroboron Cations	4
1) Singly Charged Cations	5
2) Doubly Charged Cations	8
C. Strong Nitrogen Bases	9
1) Amidine Ligands	9
a. Basicity	9
b. DBU and DBN Complexes	12
2) Guanidine Ligands	13
a. Basicity	13
b. Intramolecular Exchange	15
c. Pentamethylguanidine (PMG)	15
d. Adducts of Guanidines in Main Group Chemistry	16
D. Nuclear Magnetic Resonance Spectroscopy	16
1) Background	16
2) Basic Principles	18
3) Chemical Shift	19
4) Spin-Spin Coupling	20
5) Spin-Lattice Relaxation, T_1	21
6) Fluorine and Boron NMR	22
E. Fast Atom Bombardment Mass spectrometry	23
1) Background	23
2) Basic Method and Ion Generation	24

Chapter II	Experimental	25
A. Materials		25
1) General		25
2) Boron Trihalides		25
3) Donors		26
4) Solvents		26
5) NMR References		26
6) Boron Trihalide Adducts		28
7) Other Materials		29
B. Formation and Isolation of Fluoroboron Cations		29
1) General Process and Methods		29
2) Salts of Fluoroboron Cations		31
C. Preparation of Pentamethylguanidine		34
D. NMR Instrumentation		37
E. Other Instrumentation		38
Chapter III	Boron Trihalide Adducts of DBU and DBU Fluoroboron Cations	40
A. General		40
B. Results		40
1) DBU/BF ₃ /BCl ₃ System		40
a. NMR Determination		40
b. FAB Confirmation of Cations		42
c. DBU Titration Monitored by ¹⁹ F NMR		45
d. A Search for (DBU) ₃ BF ₂ ⁺		45
e. Equilibrium in Ions and Adducts		49
2) System with B-Br Bond		49
C. Discussion		52
1) NMR Parameters		52
a. Adducts and Cation Species		52
b. Anion Species		55
c. ¹⁰ B Isotopic Pattern of BFCl ₃ ⁻ in ¹⁹ F NMR		56
2) Donor Strength Effect on B-X Bond		59
3) Redistribution Reaction		59
4) Some Properties of (DBU) ₃ BF ₂ ⁺ and [(DBU) ₃ BF ₂ ⁺](PF ₆ ⁻) ₂		62
5) Reactivity of (DBU) ₂ BF ₂ ⁺		65
6) Molecular Size Effect on Spin-Lattice Relaxation Time		66

Chapter IV	DBN Compared to DBU. Ring Size Effects	67
A. General		67
B. Results		68
1) ^1H , ^{13}C and ^{15}N NMR of DBU, DBN and Their Trifluoride Adducts		68
a. ^1H NMR		68
b. ^{13}C NMR		68
c. ^{15}N NMR		71
2) Formation of DBN-Containing Fluoroboron Cations		73
a. DBN/ BF_3/BCl_3 System		73
b. DBN/ BF_3/BBr_3 System		78
c. Low Temperature ^{11}B NMR		78
d. DBN/ $\text{BF}_3/\text{BCl}_3/\text{DBU}$ System		78
C. Discussion		81
1) Donor Ability		81
2) Reactivity of $\text{D.BF}_n\text{Cl}_{3-n}$ and Associate Reaction Mechanism		82
3) Why (DBN). BF_2Br and (DBN). BFBr_2 are Unfavourable		83
4) Comparison of DBN with DBU fluoroboron Cations		84
Chapter V	Systems with Low-Sterically-Hindered Guanidines	86
A. Introduction		86
B. Results and Discussion		87
1) Synthesis of Pentamethylguanidine		87
a. Brief Thermodynamic Study of PMG		87
b. Properties of Lithioguanidine, $\text{Li}[\text{N}=\text{C}(\text{NMe}_2)_2]$		88
c. Major Question of Synthesis of PMG		89
2) N-H Bond Effects on TMG/ BF_3/BCl_3 System		89
a. NMR Patterns of TMG/ BF_3/BCl_3 System and $(\text{TMG})_2\text{BF}_2^+$		89
b. N-H Bond Effect		90
Chapter VI	^{19}F Chemical Shift of D.BF_3 and D_2BF_2^+ Formed From $\text{N}=\text{C}-(\text{X})_2$ ($\text{X}=\text{N}, \text{S}$) and $\text{N}=\text{CR}-\text{X}$ ($\text{X}=\text{N}, \text{O}, \text{S}$) Containing Bases	94
A. Introduction		94
B. Results		96
C. Discussion		97
Chapter VII	Mixed-Ligand Difluoroboron Cations	101

A. Introduction	101
B. Results	101
1) DD'BF ₂ ⁺ Formed From D.BF ₂ Cl	101
2) DD'BF ₂ ⁺ Formed From D ₂ BF ₂ ⁺	105
C. Discussion	107
1) Basicity Effect on Cation Formation From D.BF ₂ Cl	107
2) Correlation of NMR Parameters	108
3) Basicity Effect on Ligand Substitution Reaction of Fluoroboron Cations	110
 Chapter VIII Fast Atom Bombardment Mass Spectrometry	 112
Studies of Fluoroboron Cations	
A. General	112
B. Results and Discussion	112
1) Singly Charged Difluoroboron Cations	113
a. Mass Spectra	113
b. The Value of the Application of FAB to Complicated Solution Systems	113
c. The Effect of Cation Size on the Formation of Ion Clusters	119
d. The stability of N-B Bonds in the Gas-Phase	119
2) Doubly Charged Fluoroboron Cations, D ₃ BF ₂ ²⁺	120
a. Background	120
b. Mass spectra	120
c. Mechanism of Ionization	124
d. Stability of Ions in the Gas-Phase	125
e. Doubly Charged Intact Cations	127
3) Singly Charged Monofluoroboron Cations	127
4) DH ⁺ X ⁻	128
5) Gas-Phase Chemistry of Fluoroboron Cations	128
6) Determination of Hexamethylguanidium (HMG ⁺)	133
 Chapter IX Conclusions and Proposals	 135
A. Conclusions	135
B. Proposals For Further Work	136
 References	 138
 Appendix 1	 145

Appendix 2	146
Appendix 3	147
Appendix 4	148
Appendix 5	149
Appendix 6	150
Appendix 7	151

List of Tables

	Page
1. Bonding Distances and Energies of Boron Trihalides	2
2. Basicity of Amidines, $R_x-N=C(Me)-N(Me)_2$	10
3. Basicity of Amidines, $R_y-N=C(R_z)-N(Me)_2$	10
4. Basicity of Alkyl Substituted Guanidines	14
5. Nuclear Properties of Fluorine and Boron	21
6. Nitrogen Donors Used in This Work	27
7. Elemental Analyses of $(D_3BF_2^+)(PF_6^-)_2$	33
8. Elemental Analyses of $(DD'BF_2^+)(PF_6^-)$	34
9. Operating Conditions of ^{19}F , ^{11}B , 1H ^{13}C and ^{15}N NMR in Bruker AC-200 FT NMR Spectrometer	37
10. ^{19}F and ^{11}B NMR Parameters for the DBU/ BF_3/BCl_3 System	41
11. The Change of Peak Areas of All Species in the DBU/ BF_3/BCl_3 System with Time at 50 °C, Monitored by ^{19}F NMR	51
12. $[(DBU)_3BF_2^+](PF_6^-)_2$ in Acetone Acted on by Strong Organic Bases	63
13. T_1 value of ^{19}F of Species in the DBU/ BF_3/BCl_3 System	66
14. 1H and ^{13}C NMR Chemical Shifts of DBN and $(DBN)BF_3$	70
15. ^{13}C Chemical Shifts of DBU and $(DBU)BF_3$	70
16. ^{15}N Chemical Shifts of DBN and DBU	71
17. ^{19}F and ^{11}B NMR Parameters for the DBN/ BF_3/BCl_3 System	73
18. The Change of the Intensity of Species in the DBU/ $BF_3/BCl_3/DBN$ System with Increasing DBU monitored by ^{19}F NMR	79
19. ^{19}F and ^{11}B NMR Parameters for the TMG/ BF_3/BCl_3 System	90
20. ^{19}F Chemical Shifts of Some Amidine Containing $D.BF_3$ and $D_2BF_2^+$	95
21. ^{19}F Chemical Shifts of Species in $N=C-X$ ($X=O, S$) Containing $D/BF_3/BCl_3$ System	96
22. Coupling Constant, $J^{19}F-^{11}B$, of Species in $N=C-X$ ($X=O, S$) Containing $D/BF_3/BCl_3$ System	96
23. ^{19}F and ^{11}B NMR Parameters of Ligand-Mixed Difluoroboron Cations	104
24. Pyridine Titration of the DBU/ BF_3/BCl_3 System Monitored ^{19}F NMR	105
25. The Linear Correlation of ^{19}F Chemical Shift and $J^{19}F-^{11}B$ of $D_2BF_2^+$, $DD'BF_2^+$ and $D'_2BF_2^+$ (D: oxazoline and D': thiazoline)	109
26. Major Ion Peaks and Their Intensity of $[(DBN)_3BF_2^+](PF_6^-)_2$ and $[(DBU)_3BF_2^+](PF_6^-)_2$	124
27. The Ion Intensity Percentage of B-F Containing Species of $(D_3BF_2^+)(PF_6^-)_2$ in FABMS	125

List of Figures

	Page
1. $[(\text{Me}_2\text{N})_2\text{C}=\text{NLi}]_6$ Structure with Chain-Shaped Li_6 Ring	16
2. Instrumental Determination of Pentamethylguanidine	36
3. 188.2 MHz ^{19}F NMR Spectrum of a typical DBU/ BF_3/BCl_3 System (mole ratio 2:1:1)	43
4. 160.4 MHz ^{11}B NMR Spectra of the DBU/ BF_3/BCl_3 System	44
5. The Change of the species in the DBU/ BF_3/BCl_3 System with increasing DBU, Monitored by ^{19}F NMR	46
6. Formation of $(\text{DBU})_2\text{BF}_2^+$ from $(\text{DBU})\cdot\text{BF}_3/\text{BCl}_3$ in 0.1 mmol:0.1 mmol by Stepwise Reaction, Monitored by Fluorine-19 NMR	47
7. Search for Optimum Sample Composition for D_3BF_2^+ Preparation in DBU/ BF_3/BCl_3 System	48
8. ^{11}B and ^{19}F NMR Spectra of $(\text{DBU})_3\text{BF}_2^+$ and $(\text{DBU})_2\text{BF}_2^+$	50
9. 188.2 MHz ^{19}F NMR Spectra of the DBU/ BF_3/BBr_3 System	53
10. Linear Correlation of ^{19}F and ^{11}B NMR Parameters of $(\text{DBU})\cdot\text{BF}_3$, $(\text{DBU})_2\text{BF}_2^+$ and $(\text{DBU})_3\text{BF}_2^+$	54
11. $\Delta\delta$ of ^{19}F NMR of $\text{BF}_n\text{Cl}_{4-n}^-$ Species in CD_2Cl_2 and CDCl_3	55
12. Splitting Pattern of F-on- ^{10}B and F-on- ^{11}B in ^{19}F NMR Spectrum of BFCl_3^- in CDCl_3	57
13. Selective Solvolysis of $(\text{DBU})_2\text{BF}_2^+$ and Solvent Effect on ^{19}F NMR Signal of $(\text{DBU})_3\text{BF}_2^+$	64
14. ^1H NMR Spectra of DBN and $(\text{DBN})\text{BF}_3$	69
15. ^{15}N Spectra of DBN and DBU	72
16. 188.3 MHz ^{19}F NMR Spectrum of a Typical DBN/ BF_3/BCl_3 System (mole ratio 2:1:1)	74
17. 160.4 MHz ^{11}B NMR Spectra of the DBN/ BF_3/BCl_3 System at Ambient and Low Temperatures	75
18. The Change of Peak Areas of Adducts and Cations with Increasing DBN for DBN/ BF_3/BCl_3 System	77
19. ^{19}F NMR spectrum of the DBN/ $\text{BF}_3/\text{BCl}_3/\text{DBU}$ System	80
20. ^{19}F NMR Spectra Sequence of $(\text{DBN})_2\text{BF}_2^+$ and $(\text{DBN})_3\text{BF}_2^+$ in CDCl_3 and Water	85
21. ^{19}F NMR Spectrum of the TMG/ BF_3/BCl_3 System	91
22. ^{19}F NMR Spectra of the MOZ/ BF_3/BCl_3 System	98
23. ^{19}F NMR Spectrum of the MTTZ/ BF_3/BCl_3 System	99

24.	Quinuclidine Titration of (DBU)BF ₃ /BCl ₃ in 0.1 mmol:0.1 mmol Monitored by ¹⁹ F NMR	102
25.	The formation of (DBU)(Q)BF ₂ ⁺ Monitored by ¹⁹ F NMR	103
26.	The formation of (Q)(Py)BF ₂ ⁺ from Ligand Substitution Reaction Monitored by ¹⁹ F NMR	106
27.	Linear Correlation of Amidine Difluoroboron Cations	109
28.	The Complicated ¹⁹ F NMR Pattern Formed from DBN Added to (Py) ₂ BF ₂ ⁺ PF ₆ ⁻ in Acetone	111
29.	FAB Spectrum of (DBU) ₂ BF ₂ ⁺ in Solution	114
30.	FAB Spectrum of [(DBN) ₂ BF ₂ ⁺](PF ₆ ⁻)	115
31.	FAB Spectra of (Quinuclidine)(Pyridine)BF ₂ ⁺ in Solution and in the Solid State	116
32.	FAB Spectrum of the DBN/BF ₃ /BCl ₃ /DBU System	118
33.	FAB Spectrum of [(DBN) ₃ BF ₂ ²⁺](PF ₆ ⁻) ₂	121
34.	FAB Spectrum of [(DBU) ₃ BF ₂ ²⁺](PF ₆ ⁻) ₂	122
35.	FAB Spectrum of DBU/BF ₃ /BCl ₃ System with High Cl/F Ratio	123
36.	FAB Spectrum of [(DBN)H ⁺](BPh ₄ ⁻)	129
37.	MS-30 Brock Dual Target and Sample Preparation	130
38.	Gas-Phase Reaction of Py ₂ BF ₂ ⁺ PF ₆ ⁻ with DBN in FAB-MS Ion Source	132
39.	FAB and EI-MS Spectra of HMG ⁺	134

CHAPTER I

INTRODUCTION

The purpose of this thesis is to set up the new fluoroboron cation systems which are formed from strong nitrogen bases and to characterize these cations, the related chemical reactions and the bonding situation by using multinuclear NMR and fast atom bombardment mass spectrometry (FABMS).

A. Boron Trihalide Adducts and Redistribution Reactions

1) Boron Trihalides and Acceptor Behavior

Since the chemical properties of boron are influenced primarily by its small size (its covalent radius for trihalides is about 0.85 - 0.90 Å) and high ionization energy (The first ionization potential is 8.296 eV and the next two are much higher), the covalent bond formation is of major importance^{<1>}.

Structurally, all boron trihalides are trigonal planar molecules with D_{3h} symmetry in which the boron atom is assumed to be sp^2 hybridized with its 2s, $2p_x$ and $2p_y$ orbitals and the remaining $2p_z$ orbital being formally vacant. The availability of only three electrons per boron atom to contribute to the sp^2 orbitals involved in covalent bonding leads to electron-pair acceptor behavior or Lewis acidity on $2p_z$ which is perpendicular to the plane formed by the halogens^{<2>}.

The actual B-X distances for all trihalides (X = halogen) are shorter than the estimated single B-X bond. This has been interpreted in terms of appreciable $p\pi$ - $p\pi$ interaction and confirmed by the increase in bond length upon the formation of tetrahedral compounds. Of course, steric effects are also present. The much shorter B-F distance has also been explained in terms of the ionic-covalent resonance in BF_3 ; this being due to the large electronegativity difference between

boron and fluorine (~ 2)^{<3>}. Bonding energies of boron trihalides are listed in Table 1^{<4>}.

TABLE 1
BONDING DISTANCES AND ENERGIES OF BORON TRIHALIDES

PROPERTIES	BF ₃	BCl ₃	BBr ₃	BI ₃
r(B-X)/pm	130	175	187	210
E(B-X)/KJ.mol ⁻¹	646	444	368	267

2) Boron Trihalide Adducts and Bonding Situations

The electron configuration of the boron atom in the boron trihalides is a sextet. This is the most important aspect of the boron trihalides, as with other tri-coordinated boron compounds. The coordinatively unsaturated trihalides are known to be able to form a great many adducts^{<5>}.

The relative strengths of the boron trihalides as Lewis acids are as follows: BF₃ < BCl₃ < BBr₃ < BI₃. This is the opposite of the order expected, based on electronegativity consideration and steric grounds. The trend is explained by the loss of π bonding upon the structural reorganization from planar (Boron: sp²) to tetrahedral geometry (Boron: sp³)^{<4>}. The stability of the coordinative bond for a given BX₃ mainly depends on the chemical nature of the donor atom, ligand properties and steric effects^{<4>}. Boron trihalides form 1:1 adducts with a wide range of Lewis bases. However, in some cases, complexes of 2:1 and other stoichiometries are also obtained^{<5>}.

Far more BF₃ complexes are known than complexes of the other trihalides, due to the great strength of the B-F bond and due to the fact that other BX₃ (X = Cl, Br and I) complexes easily to lose HX by reacting with the active H atom on ligands or other reagents^{<4>}. Based on their stability, the BF₃ adducts are of widespread use as model compounds for investigating Lewis acid-base interactions

and the nature of the donor-acceptor bond^{<6,7>}. Usually, BF₃ as a "hard acid" can form stronger complexes with "hard bases", N, O, and F donor atoms, than with P, S and Cl^{<4>}. Boron trihalide adducts are capable of forming weaker complexes with As, Sn^{<8>} and Se^{<9,10>}. The weak Van der Waals complexes were yielded by "supersonic expansion" with CO, N₂ and Ar^{<11>}. Certain electron-rich transition metal complexes can also act as donors to form complexes with boron trihalides^{<4>}.

The B-F bond does not vary significantly among the D.BF₃ compounds, normally being in the 1.33 ~ 1.36 Å range^{<12>}. Some B-N bond lengths in their coordination compounds have been measured by microwave, electron diffraction and X-ray diffraction^{<5>}. For D.BX₃, the B-N bond length is affected by the heavy halogen substitution pattern on the boron atom site and the substituent on the nitrogen atom site, but the value does not change much, always being around 1.6 Å^{<13>}.

3) Redistribution Reactions

Making the weak B-X bond containing fluoroboron adducts is a key step in the formation of fluoroboron cations, since the weak B-X bond can be broken easily by an appropriately strong base as a nucleophile attacking^{<5>}. Specifically, forming mixed boron trihalide adducts, D.BF_nX_{3-n}, is important for this work.

Several different ways to make mixed boron trihalide adducts have been summarized^{<14>}. Halogen redistribution reactions greatly contribute to the formation of mixed boron trihalide adducts, including nitrogen donor containing mixed boron trihalide adducts^{<14,15,16>}. The redistribution reactions for mixed boron trihalide adducts do not always follow the statistical rule with D.BX₃:D.BX₂Y:D.BXY₂:D.BY₃ = 1:3:3:1 when X/Y is in a 1:1 ratio; they are influenced by the properties of the donors to a large extent, especially, for F,Cl and F,Br in the sulfur-donor systems^{<17>}. It seems to obey "the Symbiotic

Principle"<18>. In the $D.BF_nI_{3-n}$ system, $D.BF_3$ and $D.BI_3$ are much more favourable than mixed-halogen adducts<12>.

The rapid halogen redistribution at ambient temperature makes the isolation of many mixed boron trihalide adducts difficult. Only a few amine adducts have been isolated<15,19>. Most studies have to be limited to dealing with solution chemistry. The application of multinuclear NMR has greatly simplified these studies and shown an incomparable superiority in the detection and characterisation of these mixed-halogen boron trihalide adducts<14>. A combination of ^{11}B with ^{19}F NMR is a very efficient method for using with the fluorine containing system. 1H , ^{13}C and ^{15}N NMR were also used to study the donor site and donor-acceptor bond strength. "Pairwise interaction" parameters used for calculating the NMR chemical shifts and $J^{19}F-^{11}B$, combined with the experimental parameters, were successful in these systems<14,20,21,22>.

B. Tetracoordinated Fluoroboron Cations

Since the structure elucidation of the "diammoniate of diborane"<23>, the cationic boron complexes have really received attention.

Most comprehensive studies in the last thirty years related to the singly charged tetracoordinated cations. The number of known species of $D_2BX_2^+$, $D_3BX_2^+$ and D_4B^3+ decreases with the increasing charge on the cation<24,25>.

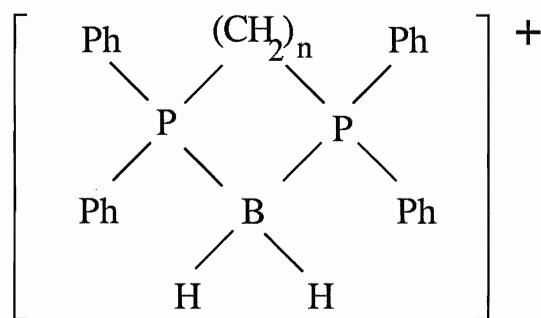
The chemistry of borinium (dicoordinated boron cation) and borenium (tricoordinated boron cation) has received increased attention in recent years<24,26>. In a very recent report, Doyle found that three-coordinated BO_3 units and two-coordinated $-B=O$ units containing boron oxide cations have been produced by particle-induced desorption from vitreous boron trioxide in the ion source of the FAB mass spectrometer<27>. The development of these areas not only contributes to cationic boron chemistry, but also offers a new way to prepare

tetracoordinated boron cations, due to the coordinative unsaturation of borinium and borenium salts<28,29,30>.

1) Singly Charged Cations

Singly charged cationic boron complexes have been reviewed in the 1960's<2,31,32>, 1970's<14,25> and 1980's<5>. Boron cations formed with nitrogen, phosphorus, arsenic, oxygen and sulphur donor ligands have been studied<5,14>. Especially, the species, $[H_2B(NR_3)_2]^+$, have been greatly developed<25>. However, not much new work has been done recently<33>.

New progress in recent years has been made on phosphorous hydroboron cation systems, probably due to the P-B bond being weaker than the N-B bond<5>, which results in hydroboron cations being not "too stable" to do the further study. Martin and co-workers synthesized some new chelating boron cations with the P-B Bond<34>, bis(diphenylphosphino)alkanedi hydroboronium ions (Their cation species are shown in Structure I) as their iodide salts, based on earlier work<35,36>. Kameda and Kodama reported a series of polyboron cationic complexes with the formula $B_nH_{n+3}.2P(CH_3)_3^+$, where $n = 3, 4, 5$ and 6 , very recently<37,38>. The structures of these clusters were studied by ^{11}B , 1H and ^{31}P NMR.



$n = 1, 2, 3$ and 4

I

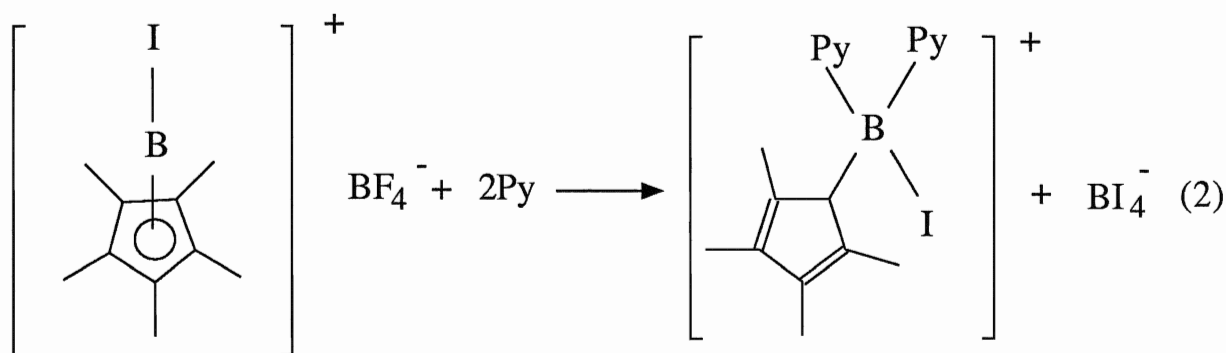
Haloboron cations were not equally well studied. It was reported that BCl_3 and BBr_3 adducts were in equilibrium spontaneously in solution with the ionic forms of the adducts, $\text{D}_2\text{BX}_2^+ + \text{BX}_4^-$ ^{<14,39>}. For boron trifluoride adducts, the ionic-covalent equilibrium (Equation 1) is not general but does occur in BF_3 adducts of ureas^{<40>}, thioureas, selenoureas,^{<11>} dialkylamides and hexamethylphosphoramide^{<41>}, all of which contain a grouping of the type $\text{R}_2\text{N-E-X-BF}_3$ ($\text{E} = \text{C OR P}$; $\text{X} = \text{O, S or Se}$).



Halogenation of tetrahedral dihydroboron cations is one of the important methods used to synthesize haloboron cations^{<35,42,43,44,45>}. However, only two fluoroboron cations, $[\text{N}(\text{CH}_3)_3]_2\text{BF}_2^+$ and $[\text{N}(\text{CH}_3)_3]_2\text{BFCl}^+$ have been made by this method, and elemental fluorine is required for this preparation^{<35>}.

With the bidentate molecules, 2,2'-bipyridine and 1,10-phenanthroline, the chloroboron cation salts were prepared recently from dichloro(η -pentamethylcyclopentadienyl) borane^{<30>}. $[\text{D}_2\text{BF}_2^+][\text{BF}_4^-]$ is also can be favoured by chelation^{<46>}, but ethylenediamine and tetramethylethylenediamine do not form cations^{<47>}.

The formation of $[\text{4-pic.}(\text{CH}_3)_3\text{N.BCl}_2^+]\text{PF}_6^-$ is the first example of the preparation of haloboron cation salts from tricoordinated boron cations by adding neutral adducts^{<29>}. Recently, a new boronium salt was formed from iodo(η^5 -pentamethylcyclopentadienyl) boron cation (1+) tetraiodoborate (Equation 2) and detected by ^{11}B and ^1H NMR^{<30>}.



Heavy halogen ion replacement from D.BH₂X or D.BX₃ (X = Br or Cl) by a second neutral donor is the most widely used method for preparing tetrahedral boron cations <5,25,35>. Analogous to this method, difluoroboron cations can be formed from D.BF₂X (Equation 3).



An earlier work by Hartman and Schrobilgen explored this route<40>. They reported that tetramethylurea almost quantitatively displaced chloride from (tetramethylurea).BF₂Cl. Later on, it was found that difluoroboron cations of carboxylic esters were much easier to form from D.BF₂Br than from D.BF₂Cl, due to the weaker B-Br bond<48,49>. All of the oxygen containing donors used in these systems seem to have the ability to delocalize negative charge toward the donor atom site.

Heavy halogen replacement from D.BF₂X was also used to form nitrogen-donor difluoroboron cations. Analogous to the double bond containing oxygen-donor ligands, a few amidines and imines have been used to form fluoroboron cations from their BF₂Cl adducts by the substitution of chloride<50>. A diastereomeric (amine)₂BF₂⁺ cation was prepared from BF_nI_{3-n} (n = 0-3) adducts of benzyl(ethyl)methylamine by adding excess donor, although the F,I redistribution equilibrium results in less BF₂I and BF₂I₂ <16>.

Studies of tertiary amine and pyridine containing fluoroboron cations have been greatly developed in this laboratory recently<51,52>. Over 60 difluoroboron cations and over 40 monofluoroboron cations have been formed in the solution and detected by both ¹¹B and ¹⁹F NMR. Five difluoroboron cations have been successfully isolated by precipitation as BPh₄⁻, BF₄⁻ and PF₆⁻ salts, the anion of choice depending on the individual cation<53>. These studies confirmed the former studies indicating the relative rates for D₂BF₂⁺ formation being D.BF₂I >> D.BF₂Br >> D.BF₂Cl. It was found that the steric hindrance of the second entering donor greatly affected the formation of difluoroboron cations<51>, and pyridine

displaces X^- from $(\text{pyridine})\text{BF}_2X$ much faster than R_3N does. Variations in base strength are not as critical for the formation of fluoroboron cations. The properties of these cations have not been studied in depth. Only $(Q)_2\text{BF}_2^+\text{Br}^-$ was found to be stable in H_2O , EtOH , DMF , and CHCl_3 solvents.

2) Doubly Charged Cations

Doubly charged and triply charged boron cations are less-well known. Doubly charged chloroboron cations, $[(\text{amine})_3\text{BCl}]^{2+}(\text{Cl}^-)_2$, have been postulated, based on the elemental analysis of $\text{BCl}_3 \cdot 3(\text{amine})$ ^{<54>}, but the method of preparation and lack of structural proof leave doubt as to the identity of these materials. A series of doubly charged bromoboron cations were synthesized through trimethylamine-boron tribromide with pyridine or various substituted pyridines. Cationic charge is retained as confirmed by conductivity data^{<55>}. Using this method, triply charged boron cations, D_4B^{3+} , were also prepared. All of these cations were isolated as bromide, hexafluorophosphate and hexafluoroarsenate salts^{<55>}.

Nucleophilic displacement is thought to be a general method for synthesizing the weak B-X bond containing multiply charged boron cations (e.g. B-Br, B-I, B-SR, and B-OSO₃CF₃)^{<5>}(Equation 4).



Similar to the formation of the singly charged fluoroboron cations, the formation of doubly charged fluoroboron cations can be analogous to the formation of the doubly charged hydroboron cations from $\text{D} \cdot \text{BHX}_2$ ($X = \text{Br}$ or I)^{<56,57>}. In a recent work^{<52>}, $(\text{pyridine})_3\text{BF}_2^+$ was detected by both ^{19}F and ^{11}B NMR spectra. NMR parameters were consistent with "pairwise interaction" calculations. It was also studied as one of the species for ^{19}F spin-lattice relaxation times. Some mixed-ligand doubly charged fluoroboron cations, $\text{D}_2\text{D}' \cdot \text{BF}_2^+$, were probably observed

by ^{19}F and ^{11}B NMR. The present work extends these studies to the isolation of D_3BF_2^+ salts.

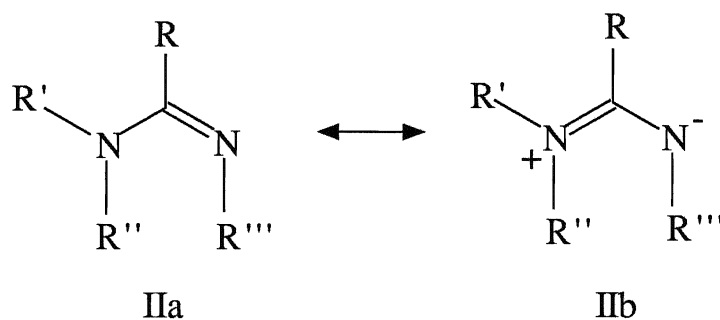
C. Strong Nitrogen Bases

1) Amidine Ligands

Amidines, with the functional group $-\text{N}=\text{CR}-\text{N}<$, are strong organic bases. They have been of interest to coordination chemists for many years. Monomeric, dimeric and cluster systems of metal amidine complexes have been studied^{<58>}.

a. Basicity

The main contribution to the basicity of amidines results from their electron resonance structure and electron delocalization toward to imino nitrogen, which is shown in Structure II.



The basicity of amidines also depends on the substitution at three sites, which are the functional carbon atom, amino and imino nitrogen atoms. The later one is the site of protonation. Thus, the strongest influence on pKa value of amidines (note: the most papers use pKa instead of pKb, so the pKa values are used in this thesis) is always from the substituent on the imino nitrogen atom ^{<59>}. As clearly shown in Table 2, if Rx is an electron-attracting group such as $\text{p-C}_6\text{H}_4\text{NO}_2$, the pKa value is small; in contrast, if Rx is an electron-offering group such as an alkyl group, the pKa value is much greater. The substituent at the amidine carbon atom

<60> and amino nitrogen atom <61> influence the pKa value of amidines to a small extent (Table 3).

All of the alkyl substituted amidines have a strong basicity. The effect of the size of the substituents among all these three sites is very small, due to the proton having a very small space requirement.

TABLE 2
BASICITY OF AMIDINES, $R_x-N=C(Me)-N(Me)_2$

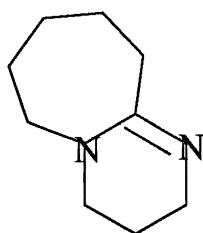
R_x	pKa*
p-C ₆ H ₄ NO ₂	5.69(0.02)
Ph	8.32(0.02)
p-C ₆ H ₄ OMe	8.96(0.08)
Bu ⁿ	12.34(0.05)
Pr ⁿ	12.46(0.07)
Pr ⁱ	12.56(0.05)

TABLE 3
*BASICITY OF AMIDINES: $R_y-N=C(R_z)-N(Me)_2$

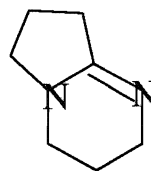
R_z	pKa*(R_y =allyl)	pKa*(R_y =Pr ⁱ)
H	10.18(0.01)	
CH ₃	11.75(0.03)	
CH ₂ CH ₃	11.59(0.04)	12.30(0.09)
CH(CH ₃) ₂	11.88(0.05)	12.26(0.06)
C(CH ₃) ₃	10.65(0.03)	10.88(0.06)

*Values in brackets are the calculated errors.

The amidine bases studied in this work are 1,8 - diazabicyclo (5,4,0) undec-7-ene (DBU) and 1,5 - diazabicyclo (4,3,0) non-5-ene (DBN). Their structures (Structure IIIa for DBU and IIIb for DBN) show that the unique potential reaction centre for a ligand is at the imino nitrogen atom, which is different from those N-H containing acyclic amidines which can form amidinium $[R'-N=CR-N-R'']^-$ as bridging ligands in the binuclear complex systems^{<62>}.



IIIa, DBU



IIIb, DBN

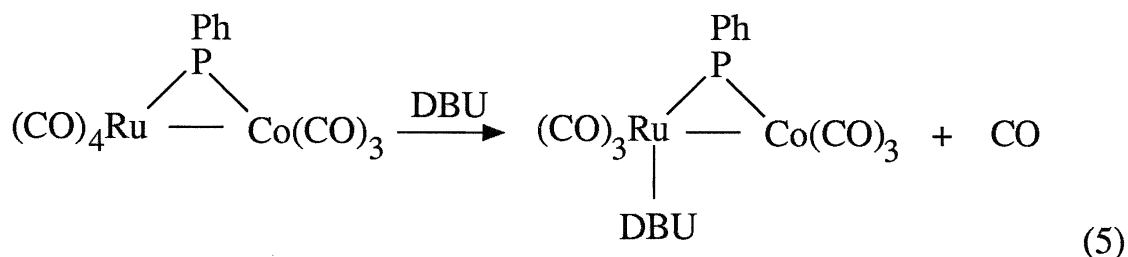
DBN and DBU were first synthesized in the middle 1950's^{<63>} and the middle 1960's^{<64>}, respectively. The pK_a value of DBN is 13.5 (ca.) in 50% aqueous ethanol^{<65>}. It is one of the strongest amidine bases. DBU has a basicity similar to DBN, pK_a: 12.9, in 1M aqueous solution and 13.4, in 10% aqueous solution^{<66>}. Both of them received equal attention in the early 1970's as catalysts in organic synthesis^{<67>}, but later on, DBU was found to have a high catalytic ability in many areas, hundreds of applications have been reported^{<68>} and reviewed recently^{<67>}.

b. DBU and DBN Complexes

DBU and DBN metal complexes are involved in catalysts, by-products and middle products such as (DBU)CuX (X=Cl, Br and I), (DBN)CuI^{<69>}, GeCl₂(DBU)^{<70>} and [(CH₃)C-Si(CH₃)₂-DBU]Cl^{<71>}. (DBU)LiCl phosphonate adduct was detected by ³¹P NMR, but the spectrum has not been completely interpreted^{<72>}.

It was noted that only (DBU)HCl and $M(\text{CO})(\text{PPh}_3)_3$ were obtained when DBU was added to $\text{MClH}(\text{CO})(\text{PPh}_3)_3$ ($M=\text{Ru}$, Os and Pt)^{<73>}. DBU did not form complexes with these metals in these cases. However, DBU did successfully replace $[\text{PCl}(\text{mesityl})(\text{CHPh}_2)]$ from $\text{trans-PtCl}_2(\text{PEt}_3)[\text{PCl}(\text{mesityl})(\text{CHPh}_2)]$ to give $\text{Pt}(\text{DBU})\text{Cl}_2(\text{PEt}_3)$ and did not form (DBU)HCl^{<74>}. The possible reason for these phenomena is whether or not the active M-H bond is in the system.

Few studies of metal complexes with DBU as a ligand have been reported. The important role of DBU as a basic ligand in the oxidative coupling of an alkene with carbon dioxide at a nickel centre has recently been demonstrated^{<75>}. Only very recently, a preliminary communication focussed on DBU as a ligand^{<76>}, in which DBU selectively displaces one carbonyl ligand at the ruthenium site of the Ru-Co complex $(\text{CO})_4\text{Ru}(\mu\text{-PPh}_2)\text{Co}(\text{CO})_3$ (Equation 5) and can be selectively substituted by phosphorus ligands in the presence of acid. The structure of this unstable DBU ruthenium-cobalt complex was determined by ^1H and ^{31}P NMR.



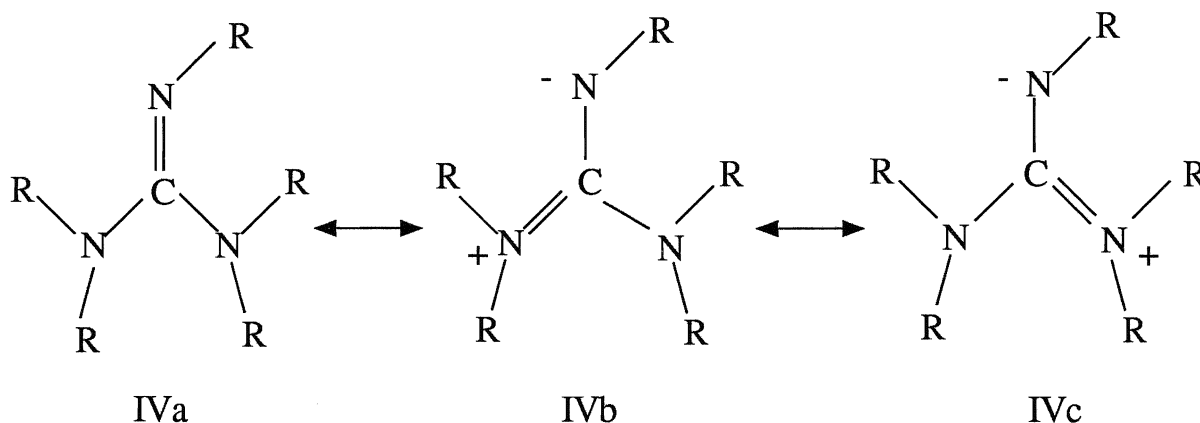
Reaction with the solvent can be a problem, since both of DBU and DBN reacted with carbon tetrachloride at 40-45 °C under a nitrogen atmosphere in the dark^{<77>}. However it was found that the deuterium of DBU in $[\text{}^2\text{H}_6]$ DMSO with CDCl_3 as deuterium source reacted very slowly^{<77>}. CDCl_3 is chosen as the major solvent for NMR studies in our system in order to be able to make a comparison with our previous work.

2) Guanidine Ligands

a. Basicity

Guanidines have a fundamental group $(>\text{N})_2\text{C}=\text{N}-$. Normally, the reaction centre also is on the imino nitrogen. It was well known that guanidines as ligands form complexes with metal atoms and cations in coordination chemistry^{<58>}.

Guanidine, $\text{H}_2\text{NC}(=\text{NH})\text{NH}_2$, is one of the strongest organic bases with $\text{pK}_\text{a}=13.6$ ^{<78>}. It exists almost exclusively as cationic species in neutral hydrolysis systems^{<79>}. Many substituted guanidines are also strong organic bases^{<58>}, due to their resonance structure (Structure IV).



Analogous to amidine, the basicity of guanidines strongly depends on the properties of the substituted groups on imino nitrogen, especially, the short - range localized electron - attracting group. For instance, $-\text{NO}_2$ substituted guanidine has the pK_a value less than zero^{<80>}. Similarly to those alkyl substituted amidines, most alkyl substituted guanidines have the higher pK_a value. The basicity of various methyl substituted guanidines is around $\text{pK}_\text{a}=13.4 \sim 13.9$ ^{<78>} in 50% aqueous ethanol. Only with very high steric hindrance, the basicity of alkyl substituted guanidines is reduced, due to the protonation being difficult, such as NNN'-tetra(iPr)-N''-methylguanidine, $\text{pK}_\text{a}=11.35$ ^{<81>}. The basicity of NNN'-tetramethylguanidine (TMG) and pentamethylguanidine (PMG) are listed

in Table 4. The greater steric hindrance makes protonation difficult and reduces the basicity of alkyl substituted guanidines.

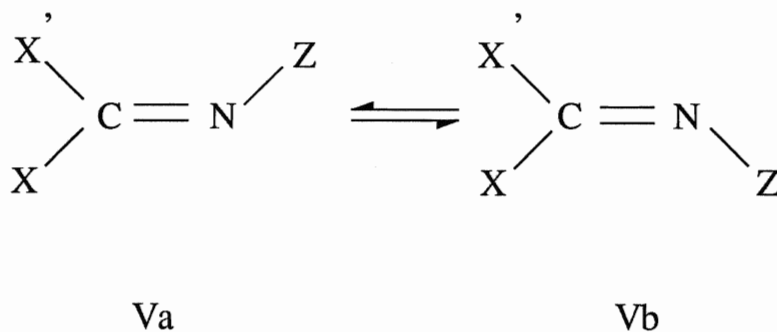
TABLE 4
BASICITY OF ALKYL SUBSTITUTED GUANIDINES

Guanidine	pKa	*ref.
NNN'N'-tetramethyl	13.6	<79>
NNN'N'-tetramethyl	13.3	<63>
Pentamethyl	13.8	<76>
Pentamethyl	13.15	<79>

*Ref.<63>, 50% aqueous ethanol. Ref.<76>, at 25 °C, water. Ref.<79>, at 20 °C, 2-methoxyethanol.

b. Intramolecular Exchange

For guanidine, the intramolecular proton exchange occurs on the different nitrogen atoms<79>. For the substituted guanidines, the intramolecular exchange has two different mechanisms, inversion and rotation<82,83>. Both of these mechanisms result in the interconversion of the isomers Va and Vb. ¹H NMR studies of the substituted phenylguanidines (Z=C₆H₄R) found that the large substituents R in the o-position of the phenyl ring made the inversion easier<82>.



c. Pentamethylguanidine (PMG)

Pentamethylguanidine was first reported in the 1920's^{<84>}. Recently, it has been used in the field of biochemistry^{<85>} and in epoxy resin synthesis^{<86>} in some laboratories. However, up to now the commercial product is still not available, although a great deal of interest has been exhibited recently by the Aldrich Chemical Company.

Barton's group has synthesized a series of sterically hindered pentaalkylguanidines in the early 1980's^{<65,87>}. The basic process is the reaction of tetra-alkylureas or tetra-alkylthioureas with phosgene to form Vilsmeier salts. Then these salts are reacted with amines to produce the hindered guanidines. The smallest hindered guanidine in this series is 2-*t*-butyl-1,1,3,3-tetramethylguanidine.

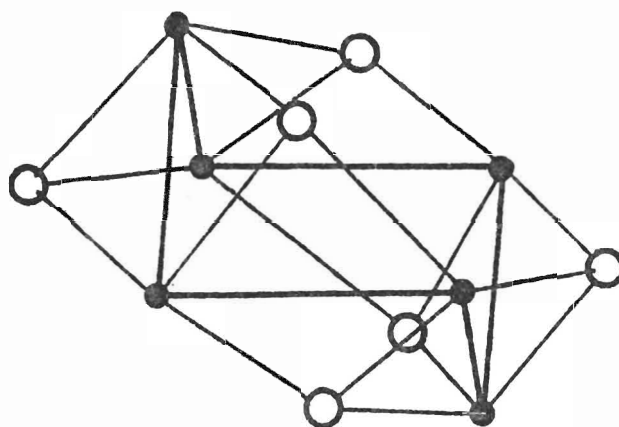
Later on, this work was developed by Wieland and Simchen^{<81>}. Some more hindered pentaalkylguanidines were synthesized. Using the same method as Barton's, Kantelehner's group synthesized thirteen new pentaalkylguanidines^{<88>}, in which 2-methyl-1,1,3,3-ethylguanidines had the smallest steric hindrance. They found that hexaalkylguanidium formed easily, rather than pentaalkylguanidine, when substituent groups on all of the nitrogen atoms have the small size.

d. Adducts of Guanidines in Main Group Chemistry

Unlike with the transition metals, complexes of main group elements with guanidines as ligands have only been the objects of a few studies during the last twenty years^{<58>}. In the early 1970's, Wade's group began to synthesize and characterize tetramethylguanidine adducts of Me_3Al , Et_3Al and AlCl_3 ^{<89>}. They also synthesized $(\text{Me}_2\text{N})_2\text{C}=\text{NLi}$ ^{<90>}, and the correct molecular structure was determined in 1983 by X-ray crystallography: chain-shaped Li_6 rings held by triply-bridging guanidine imino nitrogen atoms. (Figure 1) ^{<91>}.

Very recently, TMG halosilane adducts were obtained and characterized by Chaudhry and Kummer^{<92>}. The basic reaction was the replacement of TMG to a halogen (Equation 6, Hal: Cl or Br).

FIGURE 1
[(Me₂N)₂C=NLi]₆ STRUCTURE WITH CHAIN-SHAPED Li₆ RING



○ N

● Li



No analogous reaction occurred between TMG and Me_3SiF . This is due to the Si-F bond being much stronger than the Si-Cl and Si-Br bonds.

The boron trifluoride adduct of TMG has been briefly studied in this laboratory^{<93>}. The tri-coordinated boron compound, $(\text{TMG-H})\text{BF}_2$, generated by cleavage of N-H bond was proposed.

D. Nuclear Magnetic Resonance Spectroscopy

1) Background

Nuclear Magnetic Resonance was demonstrated by several physicists in the middle 1940's ^{<94>}. The development of commercially available high resolution nuclear magnetic resonance (NMR) spectrometers in the late 1950's provided chemists with a new tool of enormous power. With the introduction^{<95>} of stable superconducting magnets, the application of pulse techniques and the used of the Fourier transform method, the last decade of NMR spectroscopy has seen the opening up of completely new areas of application, especially, in solids (MASNMR)^{<96>} and in medicine and biology (NMR imaging)^{<97>}. During the last two decades, the magnetic field of the instrument has increased 10 times (60 MHz to 600 MHz for protons). At the same time, NMR has been applied routinely to almost all possible NMR active nuclei. Multinuclear NMR has become an important method in many chemical fields^{<98,99,100>}.

Our present fluoroboron systems are ideal for NMR study since five major elements in these systems have NMR active isotopes, ^1H , ^2H , ^{10}B , ^{11}B , ^{13}C , ^{14}N , ^{15}N and ^{19}F . In fact, it was through the application of NMR that the study of the mixed boron trihalide adducts and fluoroboron cations became significant^{<14>}.

2) Basic Principles<101>

Nuclei, when they spin, possess angular momentum (p), as described in Equation 7:

$$p = I\hbar / 2\pi \quad (7)$$

Where I is the nuclear spin quantum number and \hbar is Plank's constant. Some nuclei have zero net spin, $I = 0$, and many nuclei have $I \neq 0$, in which the nuclei possess a magnetic moment, μ ,

$$\mu = \gamma p \quad (8)$$

γ is a unique constant for each nucleus, called the magnetogyric ratio.

In an applied magnetic field (H_0), the nuclei with a magnetic moment tend to precess around the direction of this field (H_0). The frequency, ν_0 , of this Larmor precession relates to H_0 as in the Larmor Equation.

$$\nu_0 = \gamma H_0 / 2\pi \quad (9)$$

The related nuclear energy levels in this applied magnetic field are :

$$E = -\mu H_0 \quad \text{or} \quad E = -m\mu H_0 / I \quad (10)$$

The number of energy levels is restricted by the number of allowed orientations for the angular momentum. For a nucleus with a spin of I , the number m can be taken as $I, I - 1, \dots, -(I - 1), -I$. The splitting of energy levels is called "nuclear Zeeman splitting". For $I = 1/2$, application of the selection rule result in $m = \pm 1/2$. The NMR experiment consists of inducing transitions between these energy levels by the application of electromagnetic radiation in the form of RF (radio frequency) current perpendicular to H_0 .

3) Chemical Shift

A chemical shift (δ) is due to a shielding difference between two nuclei of the same species. The shielding of a nucleus is caused by the motion of electrons in the molecule induced by H_0 . The induced motion of these electrons sets up a local

magnetic field opposed to the direction of H_0 . The magnitude of the effective field perceived by a set of equivalent nuclei will be proportional to the applied field as in the following equation:

$$H = H_0(1 - \sigma) \quad (11)$$

σ is the screening or shielding constant which can be described as following:

$$= \sigma_d + \sigma_p + \sigma_x$$

where: σ_d is diamagnetic effects, σ_p is paramagnetic effects and σ_x is extraneous effects involving anisotropy and ring currents.

Actually, σ can not generally be determined experimentally, as this would require measurement of a "bare" nucleus stripped of all electrons. All nuclei are "shielded" to a certain extent from H_0 . If one particular "shielded" nucleus in a molecule such as ^1H in $\text{Si}(\text{CH}_3)_4$ is chosen as a reference, the extent to which the other nuclei are shielded can be obtained by an exact measurement of this shielding difference - the chemical shift. Chemical shift is measured in a dimensionless unit parts per million (ppm), which is independent of the frequency or magnetic field strength.

$$\begin{aligned} \delta &= (\sigma_R - \sigma_S) / (1 - \sigma_R) \cdot 10^6 \approx (\sigma_R - \sigma_S) \cdot 10^6 \\ \text{or } \delta &= (V_S - V_R) / V_R \cdot 10^6 \end{aligned} \quad (12)$$

4) Spin - Spin Coupling

Actual NMR spectra are not always present as individual lines(singlets). In many cases, groups of lines, named multiplets, are present. Multiplets result from splitting of the energy levels and hence represent several transitions, instead of the original single transition, brought about by interaction between nuclei. This type of interaction is called spin - spin coupling or spin - spin splitting.

A mechanism for the spin - spin coupling interaction that involves electrons which form a chemical bond was described by Ramsey and Purcell in the early 1950's^[102]. Consider a system with two spin 1/2 nuclei, A and X, bonded

covalently. If nucleus A has its spin oriented parallel to H_0 , an electron near nucleus A will tend to orient its spin antiparallel to that of A, due to the tendency of magnetic moments to pair in antiparallel fashion. Another electron in this orbital is antiparallel to this electron in the most favourable situation. However, these magnetic interactions are so small that the parallel orientation of spin A and X is a state of only slightly higher energy and occurs with almost equal probability. Thus when nucleus A undergoes resonance, two slightly different energies are required to match the effect from nucleus X in order to resonate. Thus, we can see two peaks (a doublet) and the difference in their frequency, expressed as J_{AX} , is proportional to the energy of interaction between A and X. From the above explanation, J_{AX} is independent of the applied magnetic field. If several bonds intervene between A and X, such as A-B-M-X, spin-spin coupling is also present. It will decrease with increasing numbers of intervening bonds.

When nuclei have $I > 1/2$, $2I + 1$ possible orientations of a nuclear spin relative to the applied magnetic field can occur and a multiplet with $2I + 1$ lines will certainly be present in the NMR spectrum. On the other hand, if a nucleus couples to more than one nearby equivalent nuclei, the resonance signal will be split into $(2nI + 1)$ components, in the case of a first-order spectrum.

5) Spin-Lattice Relaxation Time, T_1

Nuclei establish a Boltzmann distribution which tends to equalize the populations in the $2I+1$ levels which are formed by means of Zeeman splitting. In this situation, intramolecular and intermolecular (including the involvement of solvent molecules) vibrational changes take place around these nuclei. The random tumbling of molecules and the vibrations of bonds and electrons will produce many fluctuating magnetic dipoles; these are proportional to the magnitude of the interaction with high energy nuclei and absorb excess energy from them. This

process of the transition of spin energy to the surrounding lattice is named spin-lattice relaxation.

Spin-lattice relaxation is a first-order rate process and the time constant for it is defined as T_1 .

$$(n - n_{eq})_t = (n - n_{eq})_0 \exp(-t / T_1) \quad (13)$$

$(n - n_{eq})$ is the displacement from the equilibrium distribution n_{eq} at time t or 0.

6) Fluorine and Boron NMR

For our fluoroboron cation system, ^{19}F and ^{11}B NMR were the major methods used. Nuclear properties of fluorine and boron are listed in Table 5^{<98>}.

None of these three nuclei create a problem in sensitivity. For ^{19}F nuclei, the range in chemical shifts is around 800 ppm^{<103>}. This nucleus can strongly couple to other nuclei. In our system, normally, ^{19}F spectra show 1:1:1:1 quartets split by a ^{11}B nucleus which is directly bonded to fluorine. Coupling to ^{10}B nuclei of spin $I = 3$ is usually not observed because of the much more intense ^{11}B - ^{19}F coupling pattern in the ^{19}F NMR spectra.

TABLE 5
NUCLEAR PROPERTIES OF FLUORINE AND BORON

Nucleus	Spin	Abundance	Magnetogyric Ratio	Quadrupole Moment	Receptivity
		(%)	($10^7 \text{ rad T}^{-1}\text{S}^{-1}$)	(10^{-28}m^2)	Referred to ^{13}C
^{19}F	1/2	100	25.1665	-	4730
^{10}B	3	19.58	2.8748	0.074	22
^{11}B	3/2	80.42	8.5827	0.036	754

Boron has two isotopes, ^{10}B and ^{11}B , The range of ^{11}B chemical shift is around 250 ppm. Both of them have a high natural abundance. As ^{10}B has a lower relative sensitivity, NMR measurements of boron usually deal with ^{11}B isotope^{<104>}.

E. Fast Atom Bombardment Mass Spectrometry (FABMS)

1) Background

Fast atom bombardment mass spectrometry, as one of the "soft" ionization methods, was explored in the early 1980's^{<105>}. Up to 1987, more than 1000 papers relating to the FAB technique were reported^{<106>}. The instrumentation and experimental technique have been extensively developed^{<106,107>}. The applications of FABMS have been widely extended to many areas of chemistry, biochemistry and industry^{<108>} to deal with those involatile, thermally labile, polar and high molecular weight materials which previously were not suitable to be studied by conventional mass spectrometry.

In a comparative study^{<109>} of the soft ionization techniques such as Field Desorption (FD), Laser (LMS), Californium-252 Plasma Desorption (PDMS), Fast Atom Bombardment (FAB) and Secondary Ion Mass Spectrometry (SIMS) on a series of internal salts, FAB is unique with respect to high order cluster-ion formation. Fragmentation is observed for FAB and the complete structure elucidation is made possible by using both the positive- and the negative-ion FAB. Of course, more complete information will be given by the complementary studies of the several different ionization methods.

The facility available at Brock University, and the previously successful work done in this laboratory^{<52,53>}, led to the use of this technique in the present work. The applications of FAB in other inorganic chemical systems also encourage

our work. Inorganic chemists have recognized that FABMS is a potentially useful tool in transition metal, main group and f-block element chemistry^{<110,111,112,113>}. The papers related to this present work will be discussed in Chapter VIII. Understanding the basic method of this technique seems fundamental for an inorganic chemist^{<111,112>}.

2) Basic Method and Ion Generation

Normally, in this technique, a sample is dissolved in a relatively nonvolatile matrix liquid such as glycerol and placed on the tip of a small stainless steel probe which is inserted into the FAB source. Fast pumping is required. A focussed high intensity beam of Argon or Xenon serves as the typical atom gun. It produces the primary beam which is directed onto the sample, about 60 - 70 ° with the surface normal. The atom beam sputters or desorbs secondary neutrals and ions from the sample surface; the secondary ions (positive and negative) are analyzed mass spectrometrically. The liquid matrix provides a renewable source of intact molecular species, when the samples are subjected to radiation damage from the energetic primary beam. The spectra can be stable over a period of several minutes. No heating of the sample is required other than the localized energy implanted in the sample by the atom beam. Although a background of the matrix is usually obtained in the practical spectra, it can be removed on a spectrometer equipped with a computerised data system by digital subtraction.

In positive ion spectra, the highest ion for organic compounds is generally $[M+H]^+$ or ionic aggregates, and sometimes is $[M+matrix]^+$; In negative ion spectra, similarly, $[M-H]^-$ is present. Salts $[A^+][B^-]$ give $[A^+]$ and $[B^-]$ in the positive ion spectra and the negative ion spectra, respectively. Particularly, for $[D_2BF_2^+][X^-]$, $[D_2BF_2^+]$ was found as the parent ion peak, and also $[D_2BF_2^+]_2[X^-]$ ^{<52>}. Salts $[C^{2+}][D^-]_2$ give the ionic aggregate $[C+D]^+$ as the highest monopositive ion,

normally. In fact, ion generation is very complicated for the different compounds, the studies related to the present systems will be discussed in Chapter VIII.

CHAPTER II

EXPERIMENTAL

A. Materials

1) General

Almost all important compounds utilized in this work are moisture-sensitive materials. They were handled with the standard inert-atmosphere techniques, mainly using the Schlenk line and the glove bag^{<114>}. The high vacuum line was used only for distillation of BBr_3 . Carefully dried solvents were used.

2) Boron Trihalides

Boron trifluoride was not pretreated. When it was used, boron trifluoride gas was passed through a glass tube packed with sodium fluoride in order to remove trace HF which may be mixed with BF_3 from the lecture bottle (Matheson) or cylinder.

Boron trichloride gas (Matheson), b.p. 12.7°C , was condensed with a slush bath at -63°C on the Schlenk line. A trap-to-trap distillation was performed under this condition. The purified liquid BCl_3 which is clear and colorless was diluted to 0.5 M with CDCl_3 in a scaled Schlenk vessel and stored in the freezer.

Sealed ampoules of boron tribromide (Alfa Inorganics) were broken in the glove bag. BBr_3 was treated with an excess of metallic mercury to remove bromine. A high vacuum line was utilized to transfer boron tribromide into the small ampoules by trap-to-trap distillation at -196°C . Then these ampoules were sealed and stored in the dark to prevent bromine from reappearing.

3) Donors

All donors used in this work, with their sources and the methods used to purify them are listed in Table 6. Many donors were used without further purification. The market pure compounds were satisfactory for our study.

Initially, yellow DBU (Abbott) was distilled under reduced pressure and dry nitrogen (130-134 °C at 20 mmHg ^{<115>}), due to its higher boiling point, 249 °C at 1 atm., and moisture-sensitivity^{<115>}. The equipment for micro-distillation was used^{<114>}. All of the equipment was sealed with Apiezon M grease and linked on to a Schlenk line. The very narrow glass tube for passing nitrogen gas was passed to the bottom of the flask. The purified DBU is clear and almost colourless.

4) Solvents

Hexane was dried with sodium wire. Nitromethane(Fisher) and acetonitrile (Matheson) were distilled at 101 °C - 102 °C and 80 °C - 81 °C, respectively. THF and ether were dried by distillation from benzophenone/sodium under argon (Organic Lab, Brock University). Deuterated chloroform (Merck, min. isotopic purity atom 99.8% D) was dried by Linde 5 Å Molecular Sieves which were baked in advance in the muffle furnace at 400 °C for more than 3 hours and then cooled over a period of 0.5 hours in a vacuum dessicator.

5) NMR References

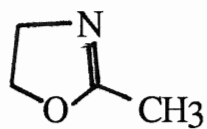
C₆F₆ (Whittaker) as a secondary internal reference was used for ¹⁹F NMR, at -162.7 ppm from CFCl₃. Et₂O.BF₃ was used for ¹¹B as external reference. TMS (Merck) as the internal reference was used for ¹H, CDCl₃ as the secondary internal reference was used for ¹³C, at 77.0 ppm, and nitromethane for ¹⁵N as

TABLE 6
NITROGEN DONORS USED IN THIS WORK

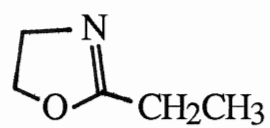
DONORS (Abb.)	SOURCES	PURIFICATION
1,8,-Diazabicyclo[5,4,0] undec-7-ene (DBU)	Abbott and *A.P.C.	Distilled under N ₂ (see page)
1,5-Diazabicyclo[4,3.0] non-5-ene (DBN)	Aldrich (95%)	Stored in Linde 5 Å Molecular Sieves
1,1,3,3-Tetramethylguanidine (TMG)	Aldrich (97%)	Same as above
Quinuclidine (Q)	Aldrich	
Triethylenediamine (DABCO)	*A.P.C.	
Pyridine	BDH	
2-picoline	BDH	
4-picoline	BDH	
2,4-lutidine	Aldrich (96%)	
2,6-lutidine	BDH	
2-Ethylpyridine	Aldrich (97%)	
2-Methyl-2-oxazoline (MOZ)	Aldrich (98%)	
2-Ethyl-2-oxazoline (EOZ)	Aldrich (99%)	
2-Methyl-2-thiazoline (MTZ)	Aldrich (99%)	
2-(Methylthio)-2-thiazoline (MTTZ)	Aldrich (98%)	

*A.P.C. Air Products and Chemicals, Inc.

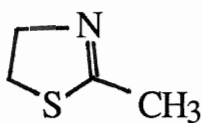
2-Methyl-2-oxazoline



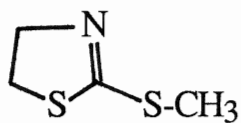
2-Ethyl-2-oxazoline



2-Methyl-2-thiazoline



2-Methyl(thio)-2-thiazoline



external reference. STP, sodium 3-trimethylsilpropionate-2,2,3,3,-d₄, was used as internal reference for ¹H NMR of aqueous samples.

6) Boron Trihalide Adducts

The reaction equipment for the syntheses of boron trihalide adducts was set up according to reference^{<16>} (also see ref.^{<52>}, Page 33), and with a bubbler added to control the flow rate of nitrogen gas. Generally, BF₃ or BCl₃ was slowly bubbled into an anhydrous hexane solution of the donor ligand (hexane:donor = 5:1 to 10:1) under the positive nitrogen atmosphere until no additional precipitation occurred. The reaction took place at 0 °C in an ice bath, with stirring.

The new boron trihalide adducts prepared in this work include boron trifluoride adducts of DBU, DBN, TMG, MOZ, EOZ, MTZ and MTTZ, and the boron trichloride adduct of DBU, as well as known boron trihalide adducts of triethylenediamine(DABCO) and quinuclidine. All of them were detected by ¹⁹F and ¹¹B NMR. (DBU).BF₃ and (DBN).BF₃ are very stable in water. (DBU).BF₃ did not change over one month in air. However, (MOZ).BF₃, (MTZ).BF₃ and (MTTZ).BF₃ rapidly decomposed in water and in air over 10 hours, changing to the liquid state.

2-Ethyl-2-oxazoline did not form a precipitate with BF₃, but gave a second liquid phase instead. (EOZ).BF₃ which is clear and colourless was separated from hexane and stored at 0 °C. At -63 °C, (EOZ).BF₃ shows a very high viscosity.

Initially, the separation of boron trifluoride adducts from the solution was carried out by the syringe/septum system^{<52>}. In the cases of (DBU).BF₃ and (DBN).BF₃ which were very stable to hydrolysis, they were simply filtered using filter paper and washed with hexane and water, in order to remove organic and inorganic impurities, and then dried in air and under vacuum, and then stored under nitrogen in a Schlenk vessel.

Boron trihalide adducts of (DABCO) were also synthesized by two other different methods^{<116>}, in order to obtain (DABCO).BF₃ and (DABCO).2BF₃. Firstly, Et₂O.BF₃ was added to DABCO in ethyl ether and secondly, Et₂O.BF₃ was added in THF. The white precipitate which occurred in these reactions exhibits a very poor solubility in water and in most organic solvents: C₆H₆, toluene, chlorobenzene, C₆H₅Cl₃, acetone, acetonitrile, CH₂Cl₂, CHCl₃, CCl₄ and C₂H₅OH. Only in DMSO (CH₃SOCH₃) does it show a good solubility. [DMSO might have reacted with (DABCO).BF₃ in this situation]. The insolubility problem led to the abandonment of further work.

7) Other Materials

N-butyllithium (2.5 M or 1.6 M) solution in hexane which was stored under nitrogen (Aldrich) and Iodomethane (BDH) were used for the synthesis of pentamethylguanidine. Sodium tetraphenylborate (Fisher, 99.6%), sodium hexafluorophosphate (Alfa, 98%) and Ammonium hexafluorophosphate (Aldrich, 99.5%) were used for crystallization.

Two salts, (quinuclidine)₂BF₂⁺PF₆⁻ and (pyridine)₂BF₂⁺PF₆⁻, which were isolated in this Laboratory in 1985^{<53>}, were used to study the ligand substitution reactions.

B. Formation and Isolation of Fluoroboron Cations

1) General Process and Methods

Both difluoroboron cation, (D₂BF₂⁺), and monofluoroboron cation, (D₃BF₂⁺), were formed by similar methods. In most situations, a solution of 0.05 - 0.10 ml 1.0 M BCl₃ in CDCl₃ was added to a solution of 0.3 - 0.4 ml 0.3 - 0.5 M D.BF₃ in CDCl₃ which was in a 5 mm NMR tube. Both of these solutions were kept

at $-63\text{ }^{\circ}\text{C}$ in a slush bath. After 10 - 20 minutes during which time $\text{D.BF}_n\text{Cl}_{3-n}$ formed, a solution of 0.2 - 0.4 ml of 1 M donor, D or D', in CDCl_3 was added. One-millilitre and micro scale (50 μl) syringes were used at all times to inject various reagents. A very narrow glass rod with an enlargement at the bottom was especially useful for mixing reagents in the NMR tube. The whole process was carried out in a glove bag under nitrogen atmosphere. The fluorine-19 NMR internal reference, C_6F_6 , was only added to certain reactions. A very small drop was required for each sample. Since the redistribution of mixed boron trihalide adducts is a rapid dynamical equilibrium, a short time is required for the cation formation.

The optimized ratio of Cl/F for the formation of D_2BF_2^+ cations is 0.8/1 and for D_3BF^{+2} cations (only bicycloamidine) is 1.2 - 1.5 /1 under the present experimental conditions. The reaction was monitored by ^{19}F NMR. The optimized condition for the formation of D_2BFCl^+ is similar to the used in the formation of D_3BF^{+2} cations. But only half free donor as much as was used for D_3BF^{+2} was needed to have one Cl attach to D.BFCl_2 . In fact, D_2BFCl^+ was always present with D_3BF^{+2} .

Neither D_2BF_2^+ nor D_3BF^{+2} were isolated directly in the mother solution (CHCl_3) by precipitating as $\text{D}_2\text{BF}_2^+\text{X}^-$ or $\text{D}_3\text{BF}^{+2}\text{X}^{2-}$. A precipitate which occurred in a $(\text{DBU})_2\text{BF}_2^+$ containing mother solution was collected in a centrifuge and dried on the Schlenk line after separating. The FAB spectrum only gave $(\text{DBU})\text{H}^+$. The precipitate might be $[(\text{DBU})\text{H}]^+\text{Cl}^-$.

BPh_4^- was introduced to attempt to isolate fluoroboronium salts. However, only $\text{DH}^+\text{BPh}_4^-$ (D = DBU or DBN) were isolated in 1:1 $\text{CHCl}_3/\text{EtOH}$ solution, which was determined by FABMS. These will be discussed in Chapter VIII.

In this work, three types of fluoroboron cations, D_3BF^{+2} , D_2BF_2^+ and $\text{DD}'\text{BF}_2^+$ were isolated with hexafluorophosphate (PF_6^-). For DBU and DBN fluoroboron cations systems, PF_6^- selectively precipitates fluoroboron cations. The white precipitate occurred immediately when the saturated Na^+PF_6^- or $\text{NH}_4^+\text{PF}_6^-$

ethanol solution was added to cations containing 1:1 $\text{CHCl}_3/\text{EtOH}$ solution. A recrystallization procedure was performed in a 1:1 acetone/EtOH solution, since all fluoroboronium hexafluorophosphate are soluble in acetone and insoluble in EtOH.

The high quality single crystals examined with the microscope and suitable for X-ray crystallography determination were grown by a solvent diffusion process. The key to growing these crystals is that the absolute EtOH must be very gently dropped into fluoroboronium hexafluorophosphate-containing acetone solution along the glass wall of a 10 cm-diameter tube to keep the surface in a basically undisturbed state. The acetone solution is required to be a little less than saturated. The slower the diffusion process, the higher the quality of the crystal grown. In our experiment, after 20 hours of solvent diffusion, excellent crystals began to appear.

Since $(\text{DBU})_2\text{BF}_2^+$ decomposed in water and alcohol, it could not be isolated by the general method. Two other methods have been tried, but both were unsuccessful. One of them involved using a large amount of non-polar solvent, hexane, to precipitate the ionic compounds from a mother solution's residue. Another was the direct addition of a saturated solution of Na^+PF_6^- or $\text{NH}_4^+\text{PF}_6^-$ in CHCl_3 to the mother solution.

2) Salts of Fluoroboron Cation

Since the following fluoroboron cationic salts were not prepared and isolated using exactly the same method, the procedures will be described, individually.

Tris(DBU)monofluoroboronium hexafluorophosphate

In a -63°C slush bath, a solution of BCl_3 in CHCl_3 was added to a solution of $(\text{DBU})\cdot\text{BF}_3$ in CHCl_3 with a 1:0.8 molar ratio. After stirring for 10 minutes, a four-fold excess of 1 M DBU to BCl_3 added in CHCl_3 and stirred for another 10 minutes. This solution was mixed with the absolute EtOH in 1:1 volume ratio. $\text{NH}_4^+\text{PF}_6^-$, saturated in EtOH, was slowly added with vigorous stirring, until no

additional precipitate formed. This white solid was washed with several portions water and EtOH. In acetone, ^{19}F NMR spectrum: $\delta = -129.9$ ppm, 1:1:1:1 quartet and $\delta = -70.8$ ppm, 1:1 doublet, (q:d ~ 1:12). ^{11}B NMR spectrum: $\delta = 4.7$ ppm, 1:1 doublet. $J^{11}\text{B}-^{19}\text{F} = 50.7$ Hz. $J^{19}\text{F}-^{31}\text{P} = 710.6$ Hz. Both ^{19}F and ^{11}B spectra show only peaks expected for $[(\text{DBU})_3\text{BF}^{+2}](\text{PF}_6^-)_2$. The elemental analysis is listed in Table 7.

Tris(DBN)monofluoroboronium hexafluorophosphate

Needle-like transparent crystals of tris(DBN)monofluoroboronium hexafluorophosphate were obtained by using a procedure similar to that which was used to prepare tris(DBU)monofluoroboronium hexafluorophosphate. Since $(\text{DBN})_3\text{BF}^{+2}$ was always present with $(\text{DBN})_2\text{BF}_2^+$, and both of them could be precipitated by PF_6^- , the amount of PF_6^- was controlled so that only the doubly charged cation was isolated with PF_6^- and singly charged cation was still in the liquid phase. Both ^{19}F and ^{11}B NMR spectra had the expected peaks, referred to $(\text{DBN})_3\text{BF}^{+2} + \text{PF}_6^-$. In acetone, ^{19}F NMR: $\delta = -141.1$ ppm, 1:1:1:1 quartet; $\delta = -70.8$ ppm, 1:1 doublet. ^{11}B NMR: $\delta = 3.6$ ppm, 1:1 doublet. $J^{11}\text{B}-^{19}\text{F} = 47.8$ Hz. The elemental analysis is listed in Table 7.

Bis(DBN)fluoroboronium hexafluorophosphate

In a typical preparation, 1 M of BCl_3 in CHCl_3 was added to a solution of $(\text{DBN})\cdot\text{BF}_3$ in CHCl_3 , with a 1:3 molar ratio, in a -63°C slush bath. After stirring for five minutes, a two-fold excess of 1 M DBN CHCl_3 solution, related to BCl_3 , was added, and the solution was stirred for five minutes. A two-fold excess of water, related to the volume of CHCl_3 , was added to the mother solution to extract ionic compounds. After shaking for five minutes and separating in a separatory funnel, the saturated sodium hexafluorophosphate was dropped into the water phase with stirring. The white precipitate was collected on a filter paper, washed with several portions of water and CHCl_3 , and then recrystallized in 1:1 acetone/EtOH. The ^{19}F and ^{11}B NMR spectra show only the peaks referred to $(\text{DBN})\text{BF}_2^+ + \text{PF}_6^-$. In acetone, ^{19}F NMR spectrum: $\delta = -146.5$ ppm, 1:1:1:1 quartet, and $\delta = -70.8$ ppm,

1:1 doublet. (q:d ~ 1:6). $J^{11}\text{B}-^{19}\text{F} = 31.6 \text{ Hz}$. FAB spectrum: m/z at 297 $[(\text{DBN})_2\text{BF}_2]^+(100\%)$ and 173 $[(\text{DBN})\text{BF}_2]^+$. The elemental analysis is listed in Table 8.

(Quinuclidine-pyridine)difluoroboronium hexafluophosphate

In a typical ligand substitution reaction, excess quinuclidine solid was added to 33 mg $\text{Py}_2\text{BF}_2^+\text{PF}_6^-$ in 0.5 ml of acetone in an NMR tube. After putting this capped tube in a 50 °C oil bath for one hour, the reaction went to completion with only $(\text{Q})(\text{Py})\text{BF}_2^+$ being produced. The process was monitored by ^{19}F NMR. (Ligand substituted reaction will be discussed in Chapter 7). The solvent was evaporated naturally and the residues were washed with two portions of CHCl_3 to remove substituted pyridine and excess quinuclidine. The remaining precipitate was separated from CHCl_3 and recrystallized in 1:1 acetone/EtOH. FAB spectrum: m/z 623 $[(\text{QPyBF}_2^+)\text{PF}_6^-]^+$, 239 $[(\text{QPyBF}_2)^+]$ (100%), 160 $[\text{QBF}_2^+]$ and 112 $[\text{PyBF}_2^+]$. The elemental analysis is listed in Table 8.

TABLE 7
ELEMENTAL ANALYSES OF $[\text{D}_3\text{BF}_2^+](\text{PF}_6^-)_2$

ELEMENT	D = DBU			D = DBN		
	CALC'D	FOUND(%)		CALC'D	FOUND(%)	
C	41.75	43.05	42.92	36.42	37.17	37.33
H	6.23	6.44	6.59	5.24	5.32	5.43
N	10.83	10.47	10.51	12.14	11.66	11.93
F	31.82	31.67	32.07	35.68	36.42	36.13
B	1.39	1.59	1.83	1.56	0.96	1.05

TABLE 8
ELEMENTAL ANALYSES OF (DD'BF₂⁺)(PF₆⁻)

ELEMENT	D = D' = DBN			D = Pyridine; D' = Quinuclidine		
	CALC'D	FOUND(%)		CALC'D	FOUND(%)	
C	38.01	37.47	37.16	37.50	37.56	37.86
H	5.47	5.05	4.97	4.72	4.83	4.73
N	12.68	12.56	12.47	7.29	7.13	7.16

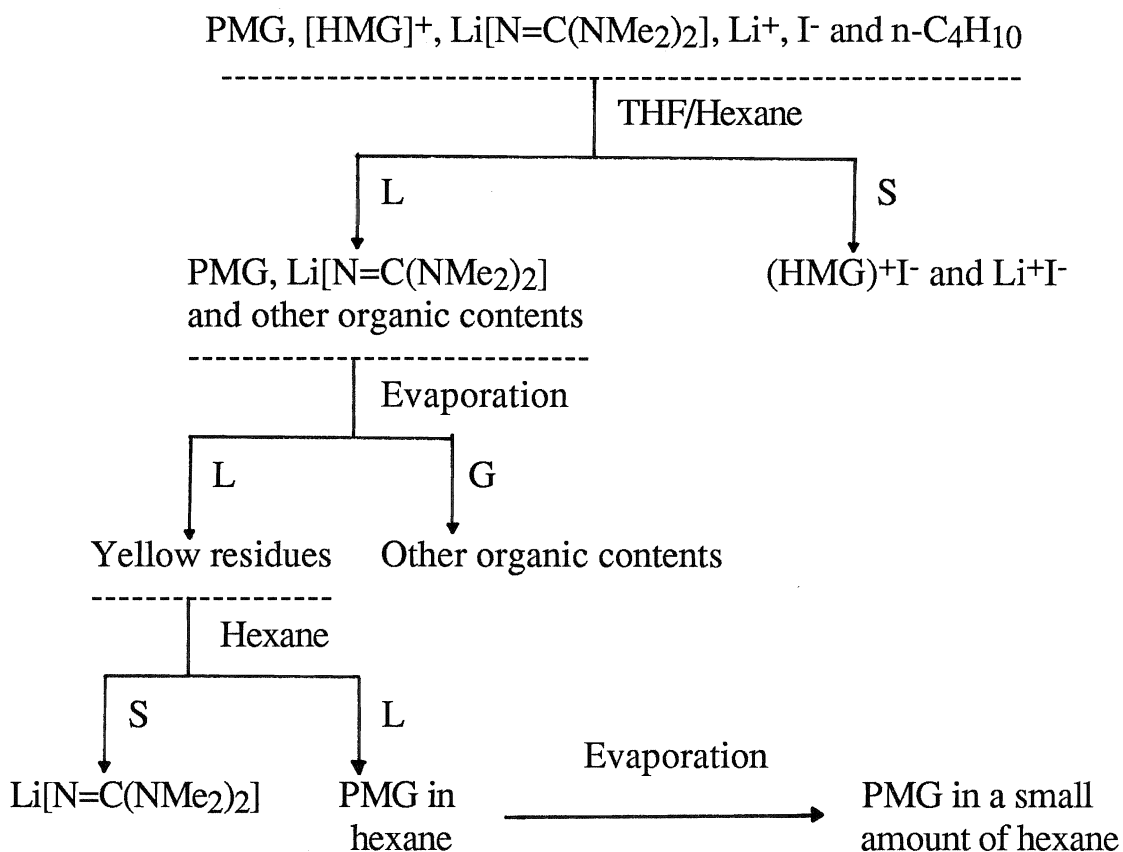
C. Preparation of Pentamethylguanidine

The synthetic process for making pentamethylguanidine includes two major steps; Step 1 is the formation of the lithoguanidine, Li[N=C(NMe₂)₂], and Step 2 is the formation of pentamethylguanidine. The whole reaction process was performed under scrupulously anhydrous conditions, with a nitrogen atmosphere. The reaction solution was stirred.

In step 1, 5 ml of 1,1,3,3-tetramethylguanidine was injected in 50 ml of THF, ether and hexane, respectively, at low temperature, in a dry ice-acetone bath or a ice-water bath. Nitrogen gas, dried by passing through Linde 5 Å Molecular Sieves packed in a 30 centimetre long U-style tube, was passed through the reaction apparatus over five hours in advance. One equivalent of 2.5 M or 1.6 M n-butyllithium in hexane was added slowly. After twenty minutes, the low temperature bath was removed. The precipitate was formed in ether and hexane. No separation was needed in this step. From a safety point of view, a dry ice-acetone bath was suggested.

Step 2 was continued in THF, due to the reaction taking place more easily in a homogeneous solution. The different amount of iodomethane was injected slowly at room temperature, 0 °C and -40 °C, respectively. The white precipitate occurred under all experimental conditions designed for this reaction. This stage was

maintained until no additional precipitate occurred. The best conditions were obtained by using a molar ratio of Li/CH₃I of 1:0.9 and a reaction temperature of -40 °C (Iodomethane was diluted in THF). A fritted glass filter (F grade) was required to separate the very fine solid formed in this reaction. The separation process and the determination of products are summarized in Scheme 1. (HMG)⁺I⁻ (HMG: hexamethylguanidinium ion) and Li⁺I⁻ were detected by FAB mass spectrometry. The details are reported in Chapter VIII. Pentamethylguanidine was detected by EI mass spectrometry and ¹H NMR. The EI-MS shows a parent ion peak, m/z at 129, (PMG⁺) with higher intensity (Figure 2a). ¹H NMR: 2.95 ppm (3H, -N=CH₃), 2.76 ppm / 2.65 ppm [12, -N(CH₃)₂], the ratio of peak areas: 1:2:2 in Hexane/CDCl₃ (1:1) (Figure 2b). These data can be referred to a reference^{<82>}, 2.72 ppm / 2.63 ppm in 1:1 in CDCl₃. However, the very low yield makes it difficult to use as a starting material.



SCHEME 1

FIGURE 2
THE INSTRUMENTAL DETERMINATION OF PMG

Fig. 2a, EI-MS

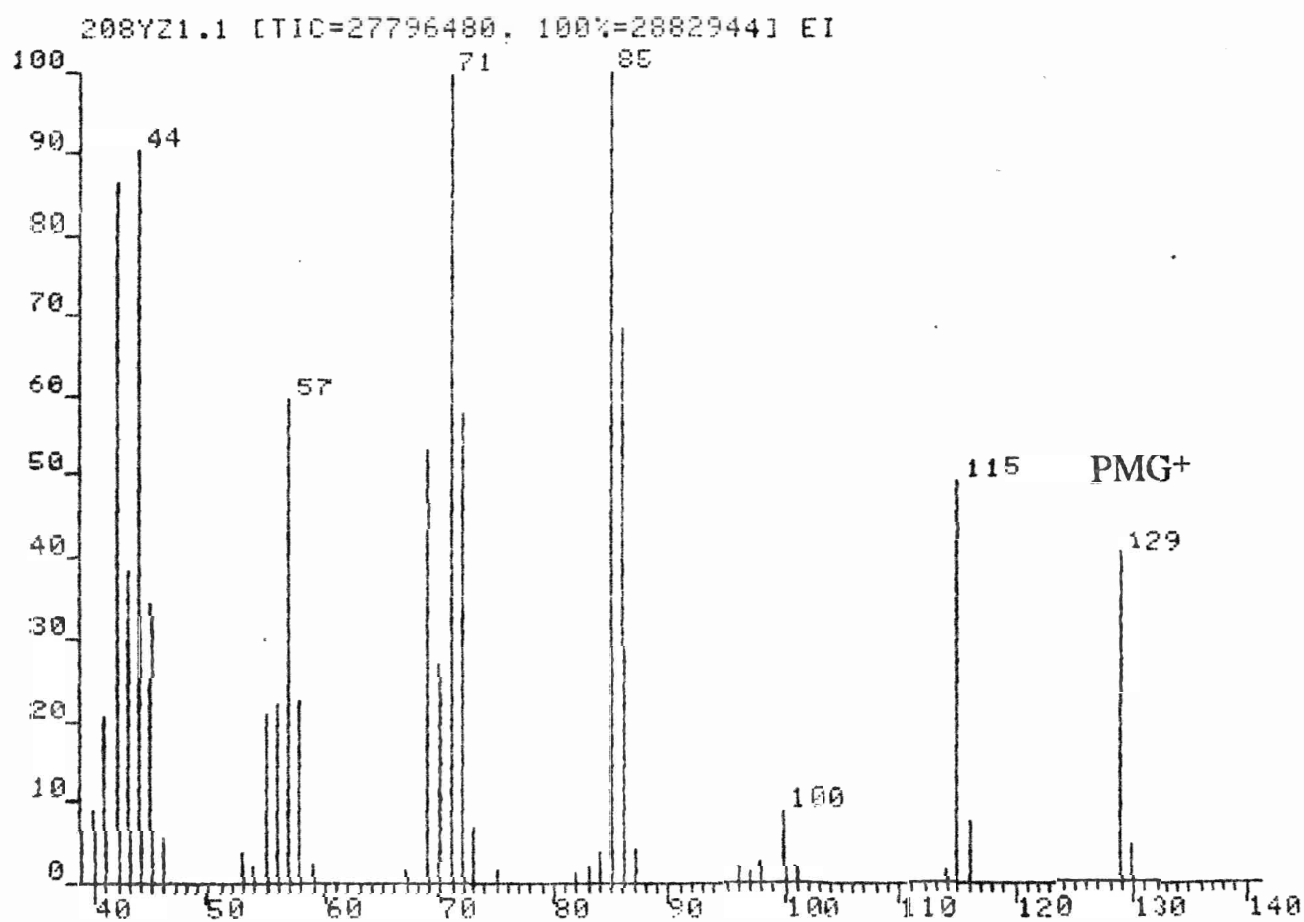
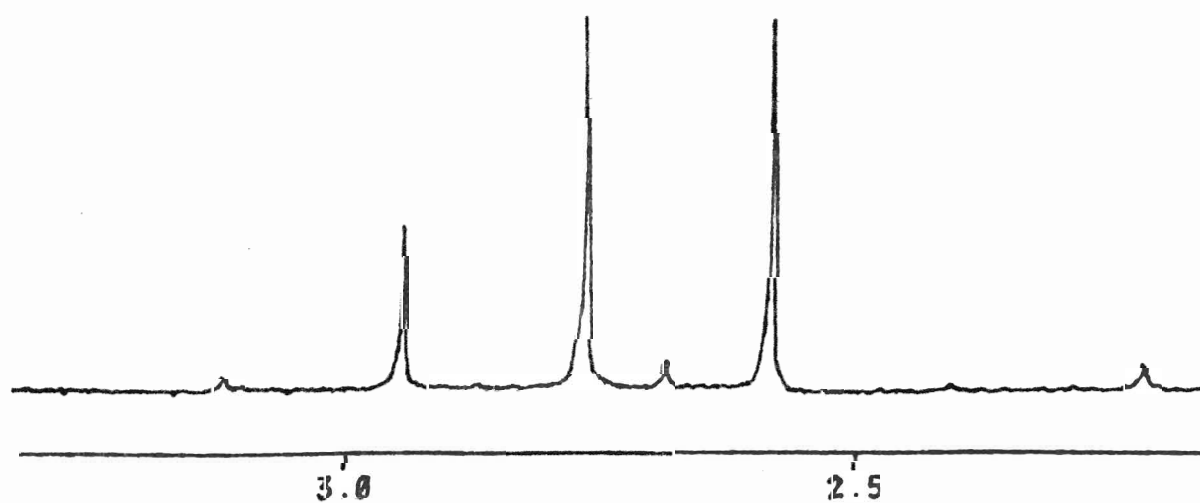


Fig. 2b, ^1H NMR



D. NMR Instrumentation

Most spectra were obtained on a Bruker AC-200 FT NMR spectrometer. The operating conditions are listed in Table 9. ^{19}F and ^{11}B NMR were used as the major methods, especially, ^{19}F NMR as a routine technique. ^1H , ^{13}C and ^{15}N NMR were used only in a few situations.

TABLE 9
OPERATING CONDITIONS OF ^{19}F , ^{11}B , ^1H , ^{13}C AND ^{15}N
NMR IN BRUKER AC - 200 FT NMR SPECTROMETER

	^1H	^{11}B	^{13}C	^{15}N	^{19}F
Operating Frequency (MHz)	200.13	64.20	50.32	20.29	188.31
Spectral Width (Hz)	2500	6000	12500	20000	35000
Repetition rate (Second)	1.6	1.7	1.3	0.2	1.1
FID	8K	8K	8K	8K	8K
*Block Size	16K	16K	16K	16K	16K
Pulse Number	16	500-5000	500-1000	1000-1200	200-2000
Pulse Angle	30°	30°	30°	30°	30°
Line Broadening (Hz)	0.3	1-3	1.5	1.5	0-1.5
Average Chemical Shift Deviation(ppm)	±0.002	±0.01	±0.03	±0.12	±0.02

* Block Size: The FID's with 8K of zero filling were transformed into 8K spectra .

Some ^{11}B spectra were obtained from the Bruker AM-500 FT NMR spectrometer at McMaster University, with an operating Frequency of 160.64 MHz and spectral width of 20000 Hz. 8K and 16K FID and Block Size were also used, respectively. Satisfactory spectra were obtained with 1000-2000 scans and with line broadening of -8 treated by a resolution enhancement method. The average chemical shift deviation was ± 0.015 ppm. The chemical shifts and ^{11}B - ^{19}F coupling constants obtained from this high field instrument are consistent with the data from our 200 MHz instrument.

The Bruker WP-80 FT NMR instrument was specially used for doing a high temperature ^1H NMR study, since the Bruker AC-200 does not at present have a variable temperature accessory.

^{19}F spin-lattice relaxation times have been investigated using the AC-200 FT NMR instrument. The microprogram of inversion recovery T_1 which generates the standard 180° - τ - 90° pulse sequence was used to measure the spin-lattice relaxation time T_1 of the individual lines in a spectrum. A stacked plot of inversion recovery experiment is shown in Appendix 1.

E. Other Instrumentation

FAB spectra were obtained from AEI MS-30 (Kratos Ltd, Manchester) double beam mass spectrometer coupled to a saddle field atom gun (Ion Tech Ltd, Teddington, U.K.), retrofitted with a Kratos FAB source in beam 1. The resolution was 1000 and accelerating voltage 4 KV. The instrument was operated by T. R. B. Jones and Dr. K. Balasannmugam. NBA, 3-nitrobenzyl alcohol, was used as a liquid matrix in most cases. Data were collected on a DS-55 Kratos Data System. A Hewlett-Packard 2631G printer was used to plot the spectra and mass intensity data. Signals from the matrix were subtracted automatically in the computer system in most situations. The BMASROS program was utilized for helping with the interpretation of the isotope pattern.

An Analect FX-6260 FT-IR spectrometer was used to obtain the infrared spectra.

CHAPTER III

BORON TRIHALIDE ADDUCTS OF DBU AND DBU FLUOROBORON CATIONS

A. General

To extend the previous studies of fluoroboron cations formed from low-steric-hindrance tertiary amines and pyridines^{<51,52>}, 1,8-Diaza-bicyclo-(5,4,0)undec-7-ene, DBU, as an extremely strong organic base is studied in the DBU/BF₃/BX₃ system (X = Cl or Br). DBU's properties such as its steric factors, basicity and stability, and some previous studies of its complexes have been described in Chapter I. In a brief attempt, DBU has given some interesting results in the DBU/BF₃/BCl₃ system^{<117>}. The extensive investigation will be reported in detail in this Chapter, based mainly on ¹⁹F and ¹¹B NMR studies.

B. Results

1) (DBU)/BF₃/BCl₃ System

a. NMR Determination

When the solution of DBU in CDCl₃ was gradually added to the mixed solution of (DBU).BF₃ and BCl₃ in CDCl₃, a series of B-F bond-containing species occurred with different intensities under the different conditions in both ¹⁹F and ¹¹B NMR spectra. These species are identified (shown in Table 10) as (DBU).BF_nCl_{3-n} (n: 0 - 3) species and BF_nCl_{4-n}⁻ (n: 0 - 4) species, as well as the fluoroboron cations, (DBU)₂BF₂⁺, (DBU)₂BFC⁺ and (DBU)₃BF²⁺. These are based on the known NMR parameters of BF_nCl_{4-n}⁻ species^{<118>}, the general chemical shifts sequence and coupling patterns of the D.BF_nCl_{3-n} species in ¹⁹F and ¹¹B NMR spectra and the change of the intensity of (DBU).BF₃Cl_{n-3}

*TABLE 10
 ^{19}F AND ^{11}B NMR PARAMETERS FOR
 DBU/ BF_3 / BCl_3 SYSTEM

SPECIES	CHEMICAL SHIFTS (ppm)		$J^{19\text{F}-^{11}\text{B}}$ (Hz)
	^{19}F	^{11}B	
(DBU). BF_3	-144.3	-0.4	17.3
(DBU). BF_2Cl	-124.6	2.9	36.3
(DBU). BFCl_2	-112.8	5.8	62.7
(DBU). BCl_3	-	6.7	-
(DBU) $_2\text{BF}_2^+$	-138.4	1.4	34.0
(DBU) $_2\text{BFCl}^+$	-121.6	~5.4	-
(DBU) $_3\text{BF}^{2+}$	-132.8	3.6	50.1
BF_4^-	-154.1	-2.3	~0
BF_3Cl^-	-126.2	1.8	24.3
BF_2Cl_2^-	-105.4	4.6	54.7
BFCl_3^-	-95.4	6.8	81.6
BCl_4^-	-	6.7	-

*a. ^{19}F chemical shifts are internally referred to C_6F_6 -162.7 ppm from CFCl_3 .

b. ^{11}B chemical shifts are externally referred to $\text{Et}_2\text{O}.\text{BF}_3$.

species and fluoroboron cation species during the reaction process (details are in the following section).

The ^{19}F chemical shift range of all species is about 60 ppm from BFCl_3^- to BF_4^- . Except for $(\text{DBU})_2\text{BFCl}^+$ and $(\text{DBU})_3\text{BF}^{+2}$, all signals are 1:1:1:1 quartets (for BF_4^- , $J^{11}\text{B}-^{19}\text{F}$ is too small to be observed when CDCl_3 is used as the solvent) in the Bruker AC-200 NMR spectrometer, which is characteristic of coupling to boron-11 ($I=3/2$). A typical fluorine-19 NMR spectrum is shown in Figure 3.

Since all boron containing species have ^{11}B chemical shifts within 7 ppm, overlapping of the multiplets occurs at the 64.0 MHz operating frequency. Particularly, $(\text{DBU})_2\text{BFCl}^+$ and BF_3Cl^- could not be observed under any experimental conditions. The 160.4 MHz NMR instrument for the ^{11}B nucleus helps in the determination of these "missing peaks". Spectra are shown in Figure 4. BF_3Cl^- and $(\text{DBU})\cdot\text{BF}_3$ are quartets; BF_2Cl_2^- , $(\text{DBU})\cdot\text{BF}_2\text{Cl}$ and $(\text{DBU})_2\text{BF}_2^+$ are triplets; BFCl_3^- , $(\text{DBU})_2\text{BFCl}^+$, and $(\text{DBU})_3\text{BF}^{+2}$ are doublets; BCl_4^- and $(\text{DBU})\cdot\text{BCl}_3$ are singlets but probably overlapping each other. $(\text{DBU})_2\text{BFCl}^+$ also overlaps with $(\text{DBU})\cdot\text{BFCl}_2$. The $^{11}\text{B}-^{19}\text{F}$ coupling constants are consistent in both ^{11}B and ^{19}F spectra, except $(\text{DBU})_3\text{BF}^{+2}$ and $(\text{DBU})_2\text{BFCl}^+$ which only show broad signals in ^{19}F NMR spectra.

b. FAB Confirmation of Cations

All fluoroboron cations were observed with fast atom bombardment mass spectrometry, under our experimental conditions, by showing parent ion peaks, $(\text{DBU})_2\text{BF}_2^+$, m/z at 353 and $(\text{DBU})_2\text{BFCl}^+$, m/z at 369 cluster. $(\text{DBU})_3\text{BF}^{+2}$ was not directly detected from the mother solution. When the isolation of $(\text{DBU})_3\text{BF}^{+2}$ became available, its salt, $[(\text{DBU})_3\text{BF}^{+2}](\text{PF}_6^-)_2$, was detected in the matrix NBA as an isotope pattern of $[(\text{DBU})_3\text{BF}^{+2}](\text{PF}_6^-)^+$, m/z at 631. Since FAB studies for these systems have some special features and problems, all details will be reported and discussed in Chapter VIII.

FIGURE 3

188.2 MHz ^{19}F NMR SPECTRUM OF A TYPICAL
DBU/ BF_3/BCl_3 SYSTEM (mole ratio 2:1:1)

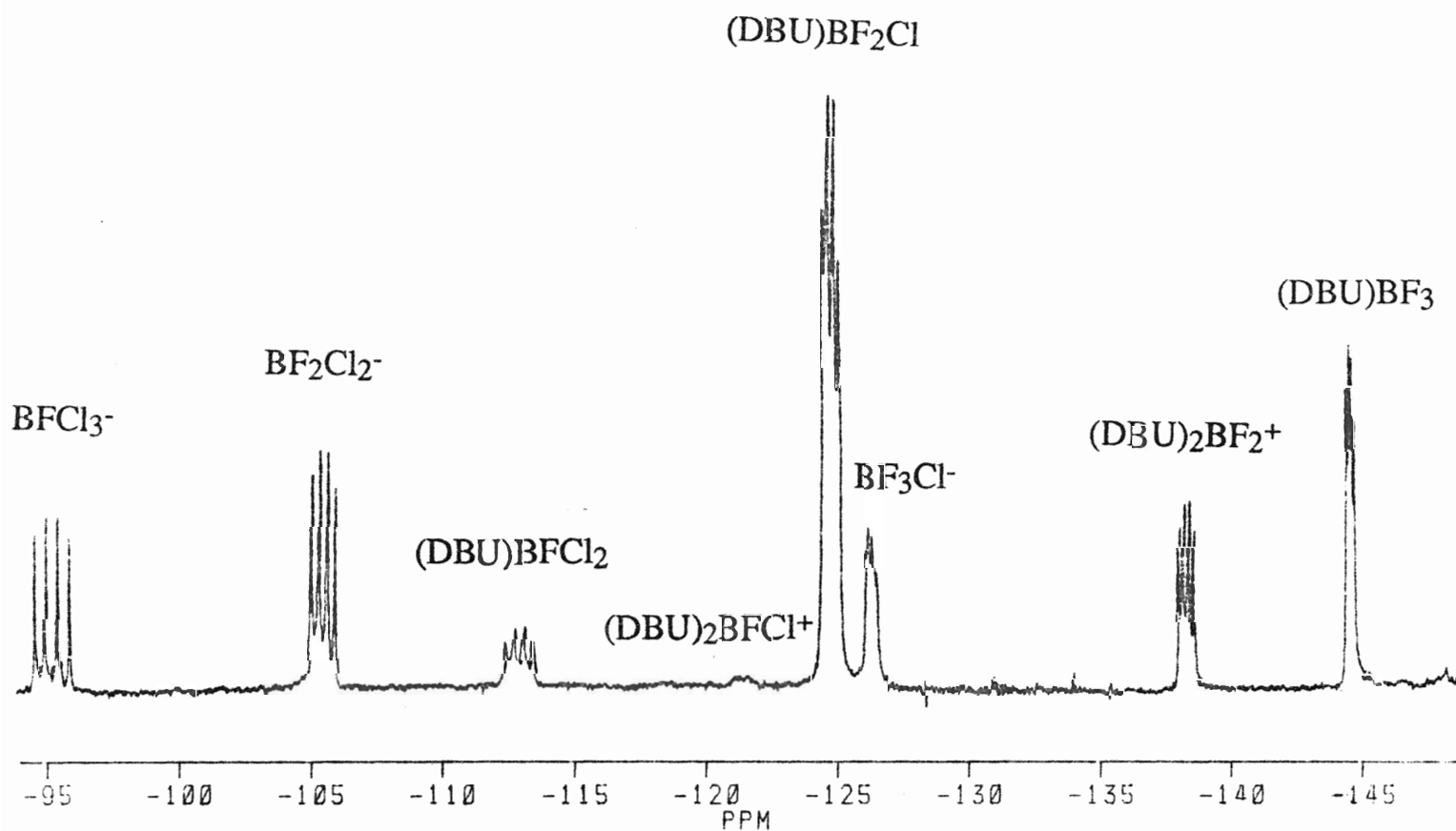
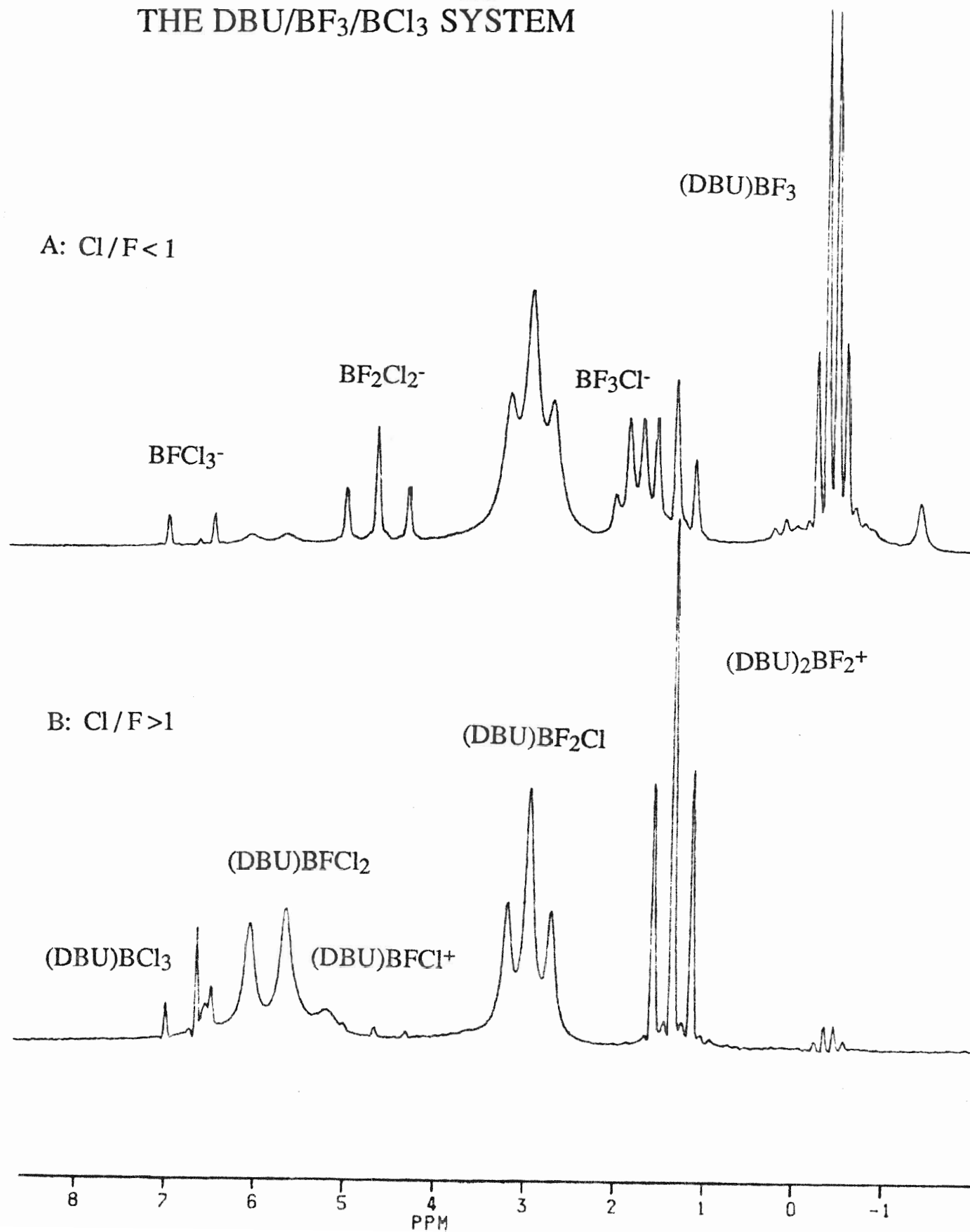


FIGURE 4
160.4 MHz ^{11}B NMR SPECTRA OF
THE DBU/ BF_3/BCl_3 SYSTEM



c. DBU Titration Monitored by ^{19}F NMR

(DBU). BF_3 and BCl_3 in a 1:1 mole ratio were prepared in CDCl_3 . The redistribution reaction occurred rapidly, so that the signals were not observed in the ^{19}F NMR spectrum, even at very low temperature. When 1 M DBU in CDCl_3 was gradually added to this system, the rapid redistribution was quenched. The first identifiable spectrum was obtained with $\text{DBU}:\text{BF}_3:\text{BCl}_3 = 1.6:1:1$, although the system still contained the excess Lewis acid in this case. The broad singlets for (DBU). BF_3 and BF_3Cl^- indicates that the rapid exchange reaction between (DBU). BF_3 and BF_3Cl^- was taking place. When the system was in the fully quenched state ($\text{DBU}:\text{BF}_3:\text{BCl}_3 = 2:1:1$), all of the peaks were well resolved, which means that chemical exchange reactions are slower than the NMR time scale. Up to $\text{DBU}:\text{BF}_3:\text{BCl}_3 = 3.4:1:1$, only the signals for $(\text{DBU})_2\text{BF}_2^+$ and (DBU). BF_3 are present, evidently. This process is shown in Figure 5. Throughout the whole process, the fluorochloroborate decreased and finally vanished. (DBU). BF_2Cl and (DBU). BFCl_2 increased first and then decreased, and also finally vanished. The result is consistent with the equilibrium shown in equations 14 and 15.

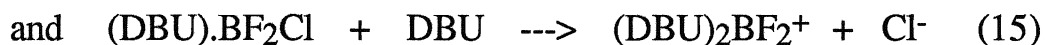


Figure 6 shows the stepwise formation process of $(\text{DBU})_2\text{BF}_2^+$ as the major reaction with increasing DBU, although redistribution reactions between $\text{BF}_n\text{Cl}_{4-n}^-$ species were still taking place.

d. A Search for $(\text{DBU})_3\text{BF}_2^+$

$(\text{DBU})_3\text{BF}_2^+$ and $(\text{DBU})_2\text{BFCl}^+$ were not readily recognized initially, due to their very low intensity and very poor resolution in primary ^{19}F NMR spectra. A search for $(\text{DBU})_3\text{BF}^{+2}$ was designed. The ratio of Lewis base, DBU, with Lewis acids, BF_3 and BCl_3 , was always 1:1 in equivalents in this experiment; only the proportion of Cl/F changed. The changing of the different B-F bond containing species in the system vs. the Cl/F proportion are shown in Figure 7. BF-

FIGURE 5
THE CHANGE OF THE SPECIES IN THE DBU/BF₃/BCl₃ SYSTEM
WITH INCREASING DBU, MONITORED BY ¹⁹F NMR

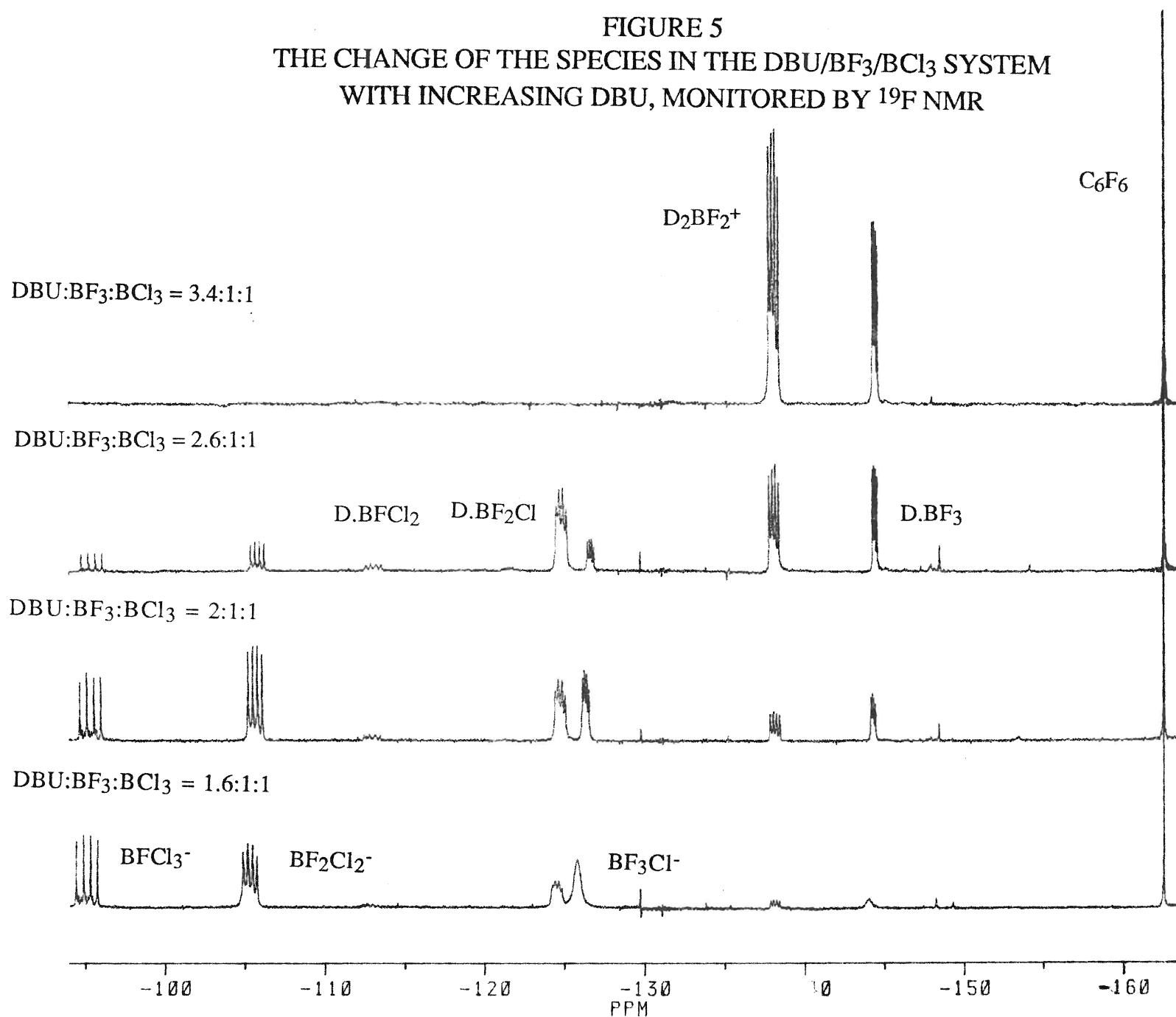


FIGURE 6
 FORMATION OF $(\text{DBU})_2\text{BF}_2^+$ FROM $(\text{DBU})\text{BF}_3/\text{BCl}_3$ IN 0.1 mmol:0.1 ml
 BY STEPWISE REACTION, MONITORED BY FLUORINE-19 NMR

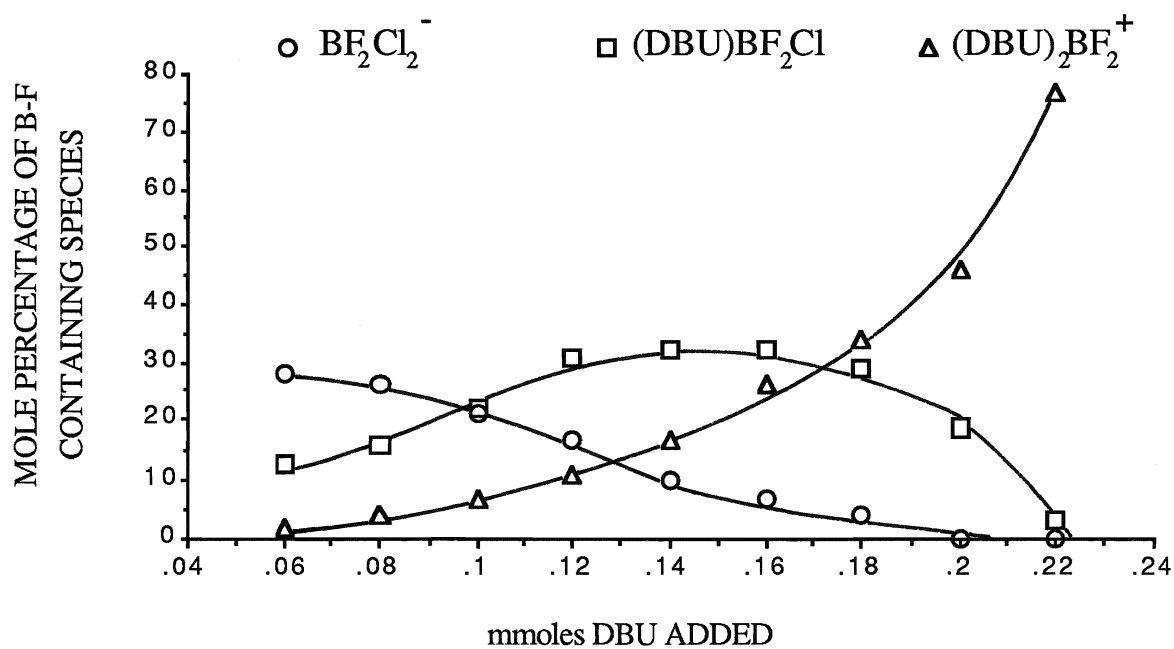
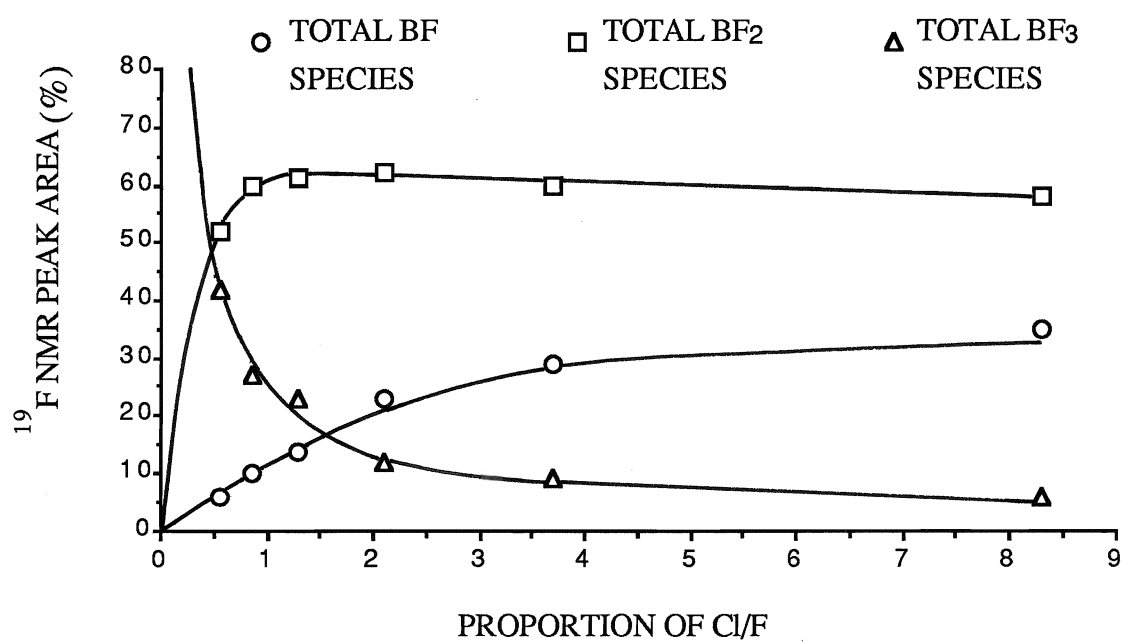


FIGURE 7
SEARCH FOR OPTIMUM SAMPLE COMPOSITION FOR
 D_3BF^{2+} PREPARATION IN $(\text{DBU})/\text{BF}_3/\text{BCl}_3$ SYSTEM



containing species increased with increasing Cl/F proportion. $(\text{DBU})_2\text{BFCl}^+$ and $(\text{DBU})_3\text{BF}^{+2}$ were clearly observed in the samples having a high Cl/F proportion. When two more equivalents of DBU was added to the sample which has the lowest Cl/F proportion in this series, the strong $(\text{DBU})_3\text{BF}^{+2}$ signal was present in both the ^{19}F and ^{11}B NMR spectrum, besides $(\text{DBU})_2\text{BF}_2^+$ signal (Figure 8).

e. Equilibrium in Ions and Adducts

A 5 mm thick-walled NMR tube, in which 0.15 mmol $(\text{DBU})\cdot\text{BF}_3$ and 0.15 mmol BCl_3 was quenched by 0.18 mmol DBU in CDCl_3 , was sealed under a N_2 atmosphere. At room temperature, the fresh sample gave $(\text{DBU})_2\text{BF}_2^+$ (43%) and $(\text{DBU})\cdot\text{BF}_2\text{Cl}$ as the main peaks in terms of intensity. However, when this sample was put in a 50 °C bath, all ions' peaks dropped down, the $(\text{DBU})\cdot\text{BF}_2\text{Cl}$ and $(\text{DBU})\cdot\text{BFCl}_2$ peaks grew up to become the main peaks, and $(\text{DBU})\cdot\text{BF}_3$ kept almost in the same level as before, as listed in Table 11. This result is in agreement with Equation 16.



In addition, it was found that $(\text{DBU})_2\text{BF}_2^+$ in solution with excess DBU still reacted with Cl^- to form $(\text{DBU})\cdot\text{BF}_2\text{Cl}$ when tetrahaloborate species were not present in the system, at 0 °C.

2) Systems With B - Br Bond

BBr_3 was also expected to react with $(\text{DBU})\cdot\text{BF}_3$ in CDCl_3 to produce the mixed boron trihalide adducts, $(\text{DBU})\cdot\text{BF}_n\text{Br}_{3-n}$ ($n:0\sim3$). The same reaction procedures used in the formation of $(\text{DBU})\cdot\text{BF}_n\text{Cl}_{3-n}$ species were carried out. However, until the proportion of $(\text{DBU})\cdot\text{BF}_3/\text{BBr}_3/\text{DBU}$ was in a ratio of 1:1:3, the separated peaks were observed in the ^{19}F NMR spectrum. The very strong signal of $(\text{DBU})_2\text{BF}_2^+$ shows high resolution. However, some small peaks at $\delta = -114$ ppm, $\delta = -117$ ppm, $\delta = -133$ ppm [$(\text{DBU})_3\text{BF}^{+2}$] and $\delta = -144$ ppm [$(\text{DBU})\cdot\text{BF}_3$]

FIGURE 8
 ^{11}B AND ^{19}F NMR SPECTRA OF $(\text{DBU})_3\text{BF}_2^+$ AND $(\text{DBU})_2\text{BF}_2^+$

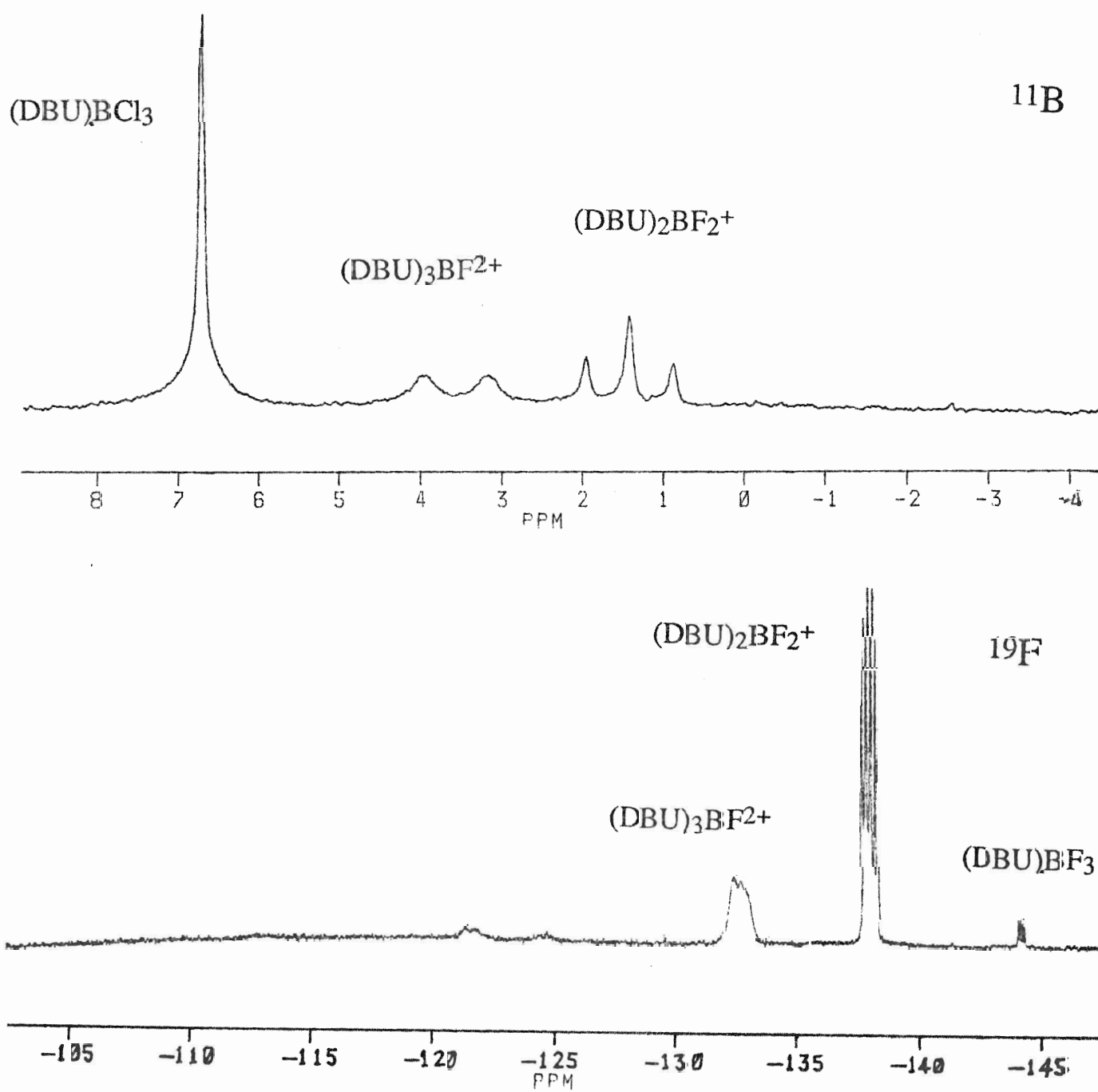


TABLE 11
THE CHANGE OF PEAK AREAS OF ALL SPECIES IN DBU/BF₃/BCl₃
SYSTEM WITH TIME AT 50 °C AND MONITORED BY ¹⁹F NMR

SPECIES	*0 HR.	1 HR.	3 HRS.	6 HRS.	22 HRS.	40 HRS.
BFCl ₃ ⁻	5	8	5	4	2	2
BF ₂ Cl ₂ ⁻	4	4	4	2	2	2
BF ₃ Cl ⁻	2	1	1	1	0	0
(DBU).BFCl ₂	7	10	15	18	27	29
(DBU).BF ₂ Cl	24	27	31	37	43	47
(DBU).BF ₃	9	5	4	5	5	5
(DBU) ₂ BFCl ⁺	7	9	12	9	9	6
(DBU) ₂ BF ₂ ⁺	43	36	29	25	13	8

*Before the sample was put in a 50 °C bath, the redistribution reaction was incompleted.

still were broad. $(\text{DBU})_2\text{BF}_2^+$ did not take part in the rapid redistribution reaction. Up to 1:1:3.8 molar ratio, two broad bands at -114 ppm and -117 pm completely vanished. $(\text{DBU})_3\text{BF}_2^+$ kept the same level, and the amount of $(\text{DBU})_2\text{BF}_2^+$ and $(\text{DBU}).\text{BF}_3$ was more than before. The intensity of all species did not change, even at -30 °C or 50 °C for 5.5 hours.

In a typical partially quenched system, two broad peaks, at $\delta = -117$ ppm and $\delta = -144$ ppm, were usually observed simultaneously. Once the $(\text{DBU}).\text{BF}_3$ peak became a quartet, the peak at -117 ppm disappeared. This is shown in Figure 9. The amount of cations depending on the F/Br proportion was tested, and the result is analogous to changing the F/Cl proportion.

The DBU/ BF_3 / BCl_3 / BBr_3 system was designed for obtaining the new mixed DBU boron trihalide adducts; however, the ^{19}F NMR spectra were almost the same as in the DBU/ BF_3 / BCl_3 system if $\text{BCl}_3 > \text{BBr}_3$, and the ^{19}F NMR spectra tended toward the DBU/ BF_3 / BBr_3 system if $\text{BBr}_3 > \text{BCl}_3$. No new peak was observed in this system.

C. Discussion

1) NMR Parameters

a. Adducts and Cation Species

The ^{19}F NMR chemical shift of the initial adduct, $(\text{DBU}).\text{BF}_3$, is at -144.3 ppm. This shift is more downfield than the shifts of most nitrogen containing BF_3 adducts and the tetramethylurea trifluoroboron adduct^{<40>}. This shift fell into the range of the ester BF_3 adducts^{<48,49>}. ^{19}F and ^{11}B NMR shifts of all mixed adducts $(\text{DBU}).\text{BF}_n\text{Cl}_{3-n}$ move downfield with increasing chlorine substitution, correlating to increasing the ^{11}B - ^{19}F coupling constant, as for other donors^{<16,40>}.

Figure 10 shows that the ^{19}F , ^{11}B chemical shifts and the ^{11}B - ^{19}F coupling constant of the non-chlorine containing species, $(\text{DBU}).\text{BF}_3$, $(\text{DBU})_2\text{BF}_2^+$ and

FIGURE 9
188.2 MHz ^{19}F NMR SPECTRA OF
THE DBU/ BF_3 / BBr_3 SYSTEM

A: DBU: BF_3 : BBr_3 = 8:3:2

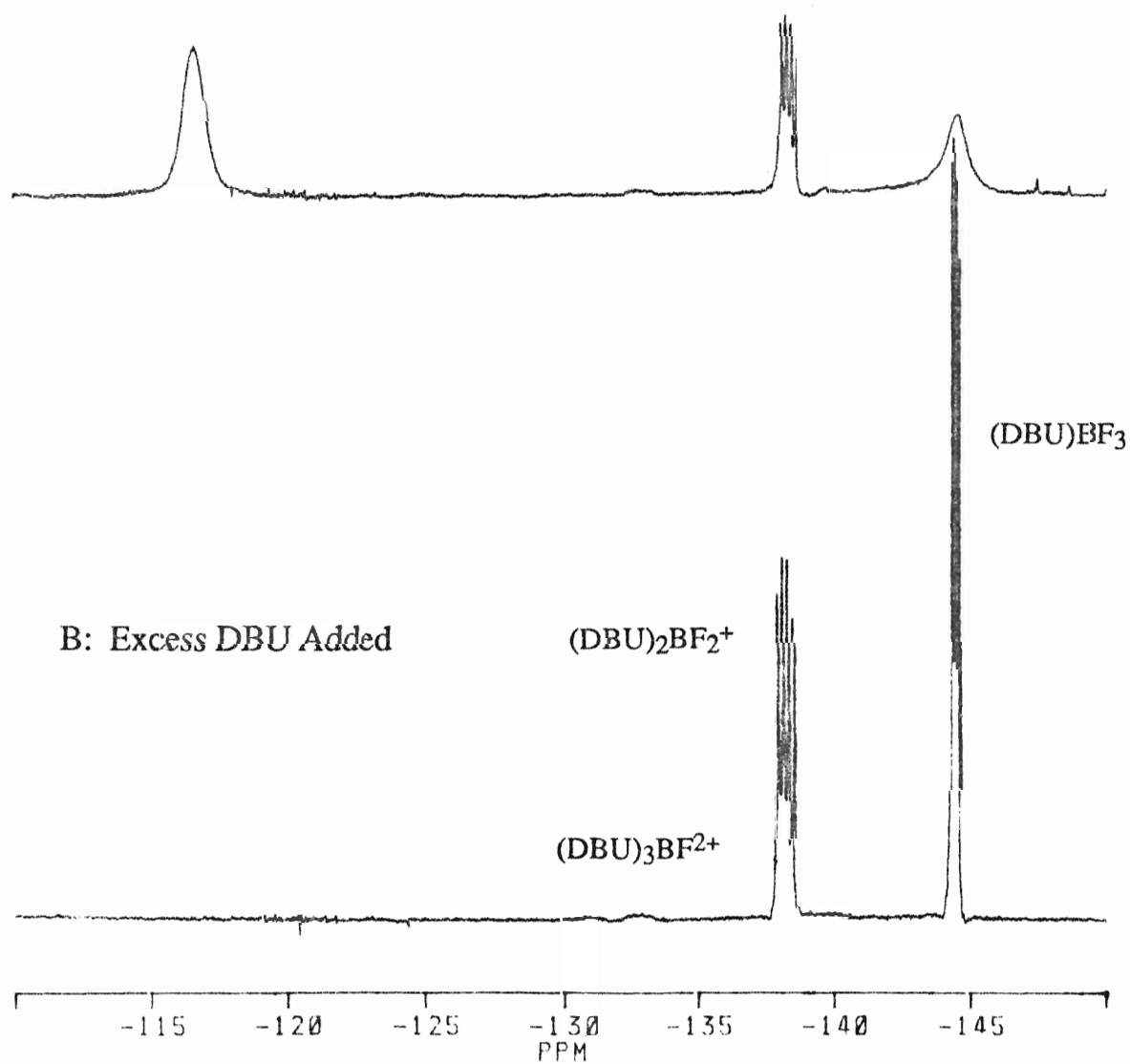
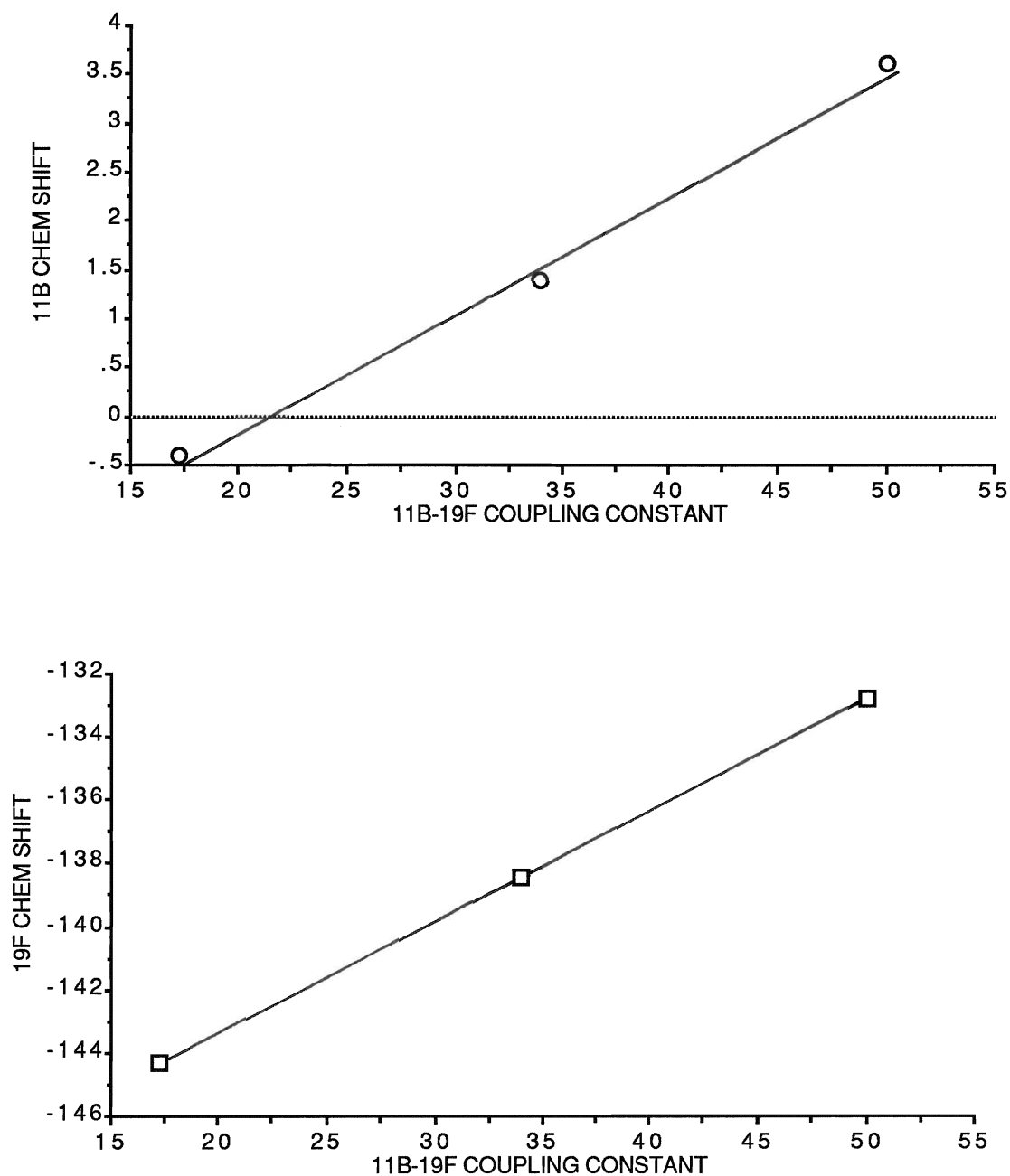


FIGURE 10
LINEAR CORRELATION OF ^{19}F AND ^{11}B NMR PARAMETERS
OF $(\text{DBU})\text{BF}_3$, $(\text{DBU})_2\text{BF}_2^+$ AND $(\text{DBU})_3\text{BF}_2^+$



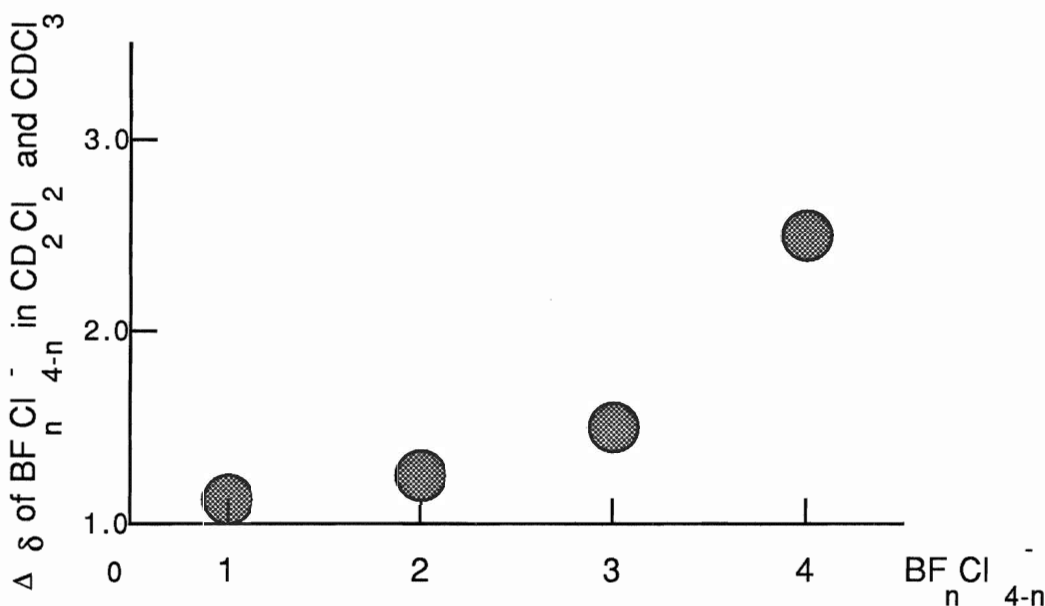
(DBU)₃BF⁺2, have a three-way linear correlation. The calculation was done by using the Statview program in the Macintosh SE computer.

b. Anion Species

BF_nCl_{4-n}⁻ species have been well characterized by both ¹⁹F and ¹¹B NMR in methylene chloride^{<118>}. Referring to this earlier work, the effect of the solvent on the chemical shift is observed. The ¹⁹F chemical shift of BF₄⁻ seems more sensitive to the solvent (Figure 11). The observed isotope pattern of ¹⁰B and ¹¹B for BF₄⁻ shows a difference of 0.052 ppm; this value is slightly smaller than that of an earlier observation (0.06 ppm^{<119>}). The resolution of signals of BF_nCl_{4-n}⁻ species is always in the order of BFCl₃⁻ > BF₂Cl₂⁻ > BF₃Cl⁻. It may be due to BF₃Cl⁻ being more suitable for an association reaction (The mechanism of the association reaction will be described in Chapter 4). In fact, BFCl₃⁻ exhibits a sharp quartet at first and finally vanishes when the chloride replacement reaction is occurring.

FIGURE 11

Δδ OF ¹⁹F NMR OF BF_nCl_{4-n}⁻ SPECIES IN CD₂Cl₂ and CDCl₃



c. ^{10}B Isotopic Pattern of BFCl_3^- in ^{19}F NMR

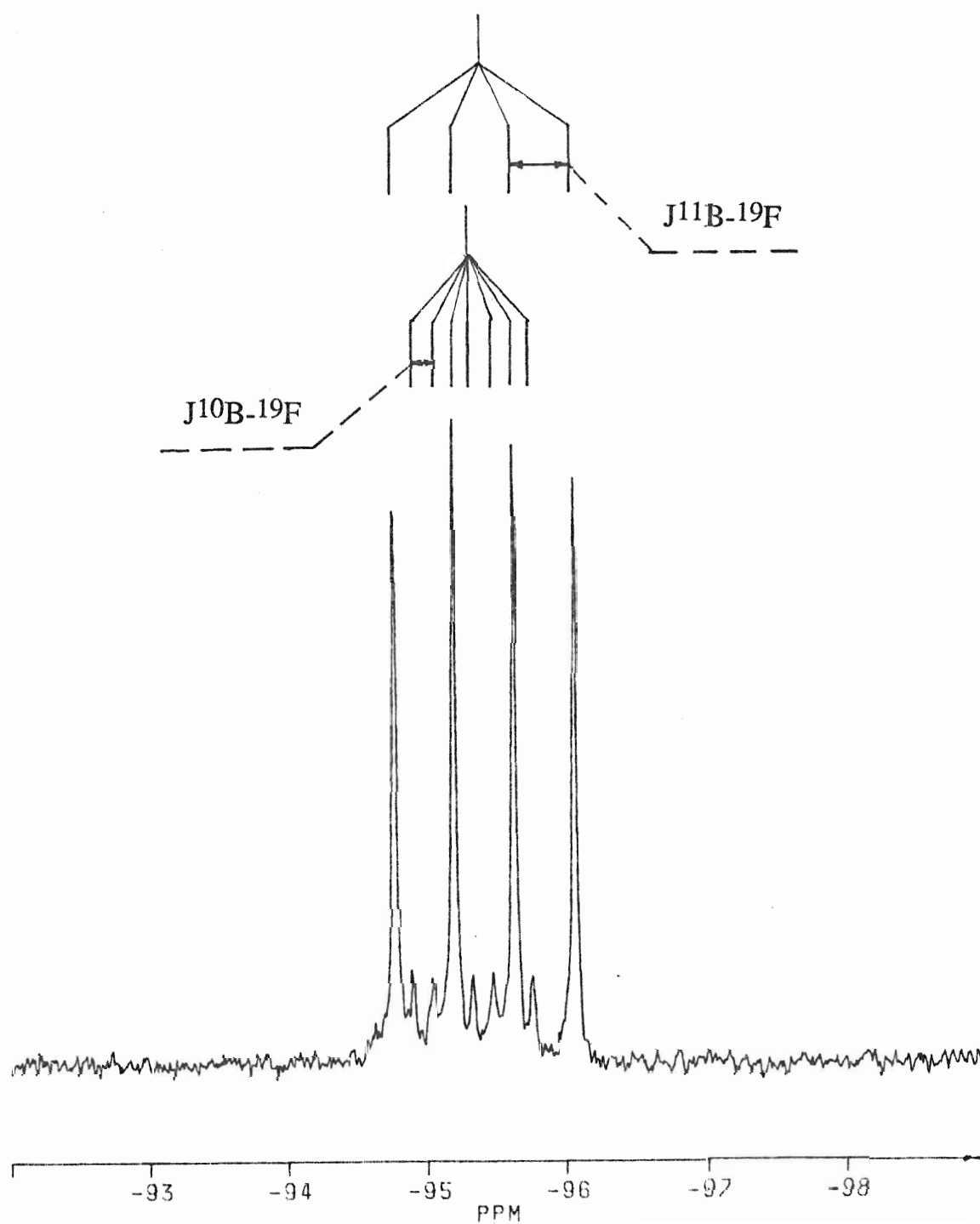
Some small peaks, with an intensity higher than that of the noise level, are always present around the signal of BFCl_3^- in ^{19}F NMR spectra of the DBU/ BF_3/BCl_3 system. In a spectrum from the sample having a 1:1 proportion of Lewis acids and Lewis base (Figure 12), it was found that these small peaks have a regular pattern with almost the same peak height. As is known, the nuclear spin quantum number of ^{10}B is $I = 3$, ^{10}B nucleus can split an NMR signal from a nearby nucleus into a 1:1:1:1:1:1:1 septet. By carefully measuring all of the small lines, it was found that this turns out to be the exact ^{10}B - ^{19}F coupling pattern. Its chemical shift is -95.5 ppm. The isotopic shift of ^{10}B from ^{11}B is 0.092 ppm (17.3 Hz in 188.31 MHz operating frequency), is greater than the isotopic shift in BF_4^- , 0.052 ppm, at the same operating frequency. The coupling constant, $J^{10}\text{B}-^{19}\text{F}$, is 27.2 Hz which is exactly 3.0 times less than $J^{11}\text{B}-^{19}\text{F}$. This is consistent with the fact that the ^{11}B isotope has a magnetogyric ratio γ precisely 3.0 times greater than ^{10}B , according to the dependence of J on γ with isotopic substitution,

$$J^{11}\text{B-X}/J^{10}\text{B-X} = \gamma_{^{11}\text{B}}/\gamma_{^{10}\text{B}} \quad (17)$$

In fact, the determination of $J^{10}\text{B}-^{19}\text{F}$ is not very difficult, in view of the exact relationship between $J^{11}\text{B-X}$ and $J^{10}\text{B-X}$; however, this is the first practical observation of $J^{10}\text{B}-^{19}\text{F}$ in the BFCl_3^- septet at natural abundance.

NMR isotopic effects have been of interest during the last twenty years and the isotopic effects of neighbouring nuclei on the chemical shift of the nucleus have also been recognized^{<120>}. This effect is more significant for the heavy nuclei. For instance, substitution of a deuterium atom for hydrogen causes a chemical shift change of up to 5.2 ppm per substituted atom for ^{59}Co ^{<121>}. The fractional change in mass on substitution seems to have the greatest effect on the isotopic shift. For example, changing from ^{37}Cl to ^{35}Cl , and from ^{81}Br to ^{79}Br produces induced ^{195}Pt shielding changes of 0.167 and 0.028 ppm^{<122>}, respectively. It is thought that substituting ^3H for ^1H will produce the largest fractional change.

FIGURE 12
SPLITTING PATTERN OF F-ON- ^{10}B AND F-ON- ^{11}B
IN ^{19}F NMR SPECTRUM OF BFCl_3^- IN CDCl_3



The large influence of ionic charge on NMR isotopic shifts was shown by Wasylishen and co-workers, very recently^{<123>}. It was found that the isotope effects on the heavy atom chemical shifts are largest for the negatively charged ions and essentially zero for the positively charged ions, and have an intermediate value for neutral species, as predicted by molecular orbital calculations, based on a study of the isoelectronic series of PH_2^- , PH_3 , PH_4^+ and of SnH_3^- , SnH_4 , SnH_3^+ ^{<123><124>}. The largest isotopic shift observed in their work is 5.52 ppm.

The ^{19}F chemical shift affected by ^{10}B was obtained from BF_4^- twenty years ago^{<119>}. Since ^{19}F is not a very heavy nucleus and most of the positive charge is distributed around the boron atom, and also because the mass fraction of ^{11}B to ^{10}B is very small (which is different from PH_2^-), the very small isotopic shift of ^{19}F in $\text{BF}_n\text{Cl}_{4-n}^-$ species is reasonable. The interesting point here is in the difference between the ^{10}B and ^{11}B isotopic shifts' change, from BF_4^- to BFCl_3^- . This difference is increased when the heavier nucleus, Cl^- , replaces the lighter nucleus, F^- . This difference is in the same order (extent) as the isotopic shift caused by ^{10}B and ^{11}B in the ^{19}F spectrum, $0.092 \text{ ppm} - 0.052 \text{ ppm} = 0.040 \text{ ppm}$.

Normally, bond lengths and angles are dependent on isotopic mass because of anharmonic vibrations and centrifugal distortions. Chemical shifts are dependent on bond lengths, and especially, bond angles^{<120>}. The anharmonic vibrations and centrifugal distortion of ^{10}B seem more favourable than those of ^{11}B , due to the smaller mass of the ^{10}B isotope which makes vibration easier. Hence, ^{10}B can make the ^{19}F nucleus more deshielding, which is consistent with all observed results, i.e. the lighter isotope causes more deshielding on the neighbouring nuclei. Since the B-Cl bond is longer and weaker than the B-F bond, the anharmonic vibrations of ^{10}B in the molecule will be more favourable in BFCl_3^- than in BF_4^- . In addition, since BFCl_3^- is an asymmetric ion, the centrifugal distortion of ^{10}B will be also more favourable. Consequently, the isotopic shift of ^{19}F in BFCl_3^- is greater than in BF_4^- , toward low-field.

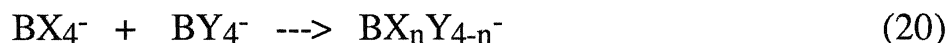
Unfortunately, insufficient resolution of BF_2Cl_2^- and BF_3Cl^- with their smaller coupling constants, $J_{10\text{B}-19\text{F}}$: 18.2 and 8.1 Hz, being greatly overlapped with the great ^{11}B - ^{19}F coupling patterns, prevents the observation of the F-on- ^{10}B septet for a series of $\text{BF}_n\text{Cl}_{4-n}^-$ species. A low viscosity solvent and a high resolution NMR instrument with variable temperature equipment might help with these observations.

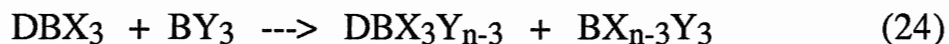
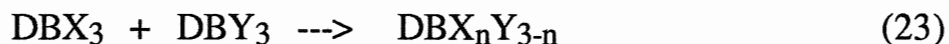
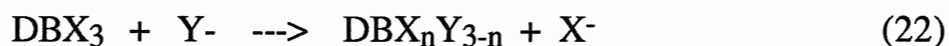
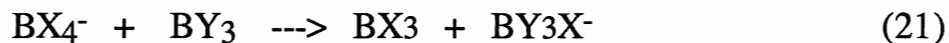
2) Donor Strength Effect on B-X Bond

The B-X bond strength in the order of $\text{B-F} > \text{B-Cl} > \text{B-Br} > \text{B-I}$ is well known (See page 2). Comparing with earlier work^{<52>}, we found that the B-X bond strength is greatly affected, although to different extents, by the coordinated neutral ligands. In most situations with amines or pyridines as donors, $\text{D.BF}_n\text{Br}_{3-n}$ species are stable in excess donor-containing systems at room temperature. However, $(\text{DBU}).\text{BF}_n\text{Br}_{3-n}$ species underwent a rapid halogen exchange reaction under the same conditions. Except for BFBr_3^- , no other B-Br bond containing species was observed. This can be explained by the property of the simple donor-acceptor bond. Since a strong organic base can transfer more electron density to the boron atom site, the ability of the boron atom to attract electrons from the halogen is reduced, and the B-X bonding energy is also then reduced.

3) Redistribution Reaction

Various possible halogen exchange reactions have been proposed as seen in the following equations^{<2>}^{<14>}.





Usually, the mixed tetrahaloborate can be formed by reactions (18), (20) and (21). Its occurring in our DBU/BF₃/BCl₃ is an interesting phenomenon. This is analogous to an earlier work in which the mixed tetrahaloborate also occurred in the TMU.BF₃/TMU.BCl₃/TMU system^{<40>}. In the present DBU/BF₃/BCl₃ system, the approach to an equilibrium distribution of the BF_nCl_{4-n}⁻ species is the opposite to the mixed BF₄⁻/BCl₄⁻ system^{<118>}. The first mixed species to be observed by NMR was BFCl₃⁻, followed by BF₂Cl₂⁻ and BF₃Cl⁻. This difference indicates that the formation process of BF_nCl_{4-n}⁻ in donor present systems is different from that in the BF₄⁻/BCl₄⁻ system.

From ¹⁹F NMR spectra, it is evident that (DBU).BF₃ underwent a rapid exchange reaction with BF₃Cl⁻, as well as the halogen redistribution reaction between (DBU).BF₃ and BCl₃. The B-N bond in this case is very unstable to Cl⁻ attack. On the other hand, for (DBU).BF_nCl_{3-n} and BF_nCl_{3-n} formed from the above redistribution reaction, when the second portion of DBU was added, a competition between the formation of (DBU).BF_nCl_{3-n} from BF_nCl_{3-n} and the formation of fluoroboron cations from (DBU).BF₂Cl and (DBU).BFCl₂ occurred. This has been confirmed by the observation of (DBU)₂BF₂⁺ from ¹⁹F NMR spectra, obtained when Lewis acids > Lewis base in the DBU/BF₃/BCl₃ system, and when the rapid halogen redistribution reactions were still going on in the DBU/BF₃/BBr₃ system. The redistribution reactions in the latter stage is not difficult to understand, according to known reaction process.

The question is in the early stage. We found that the total intensity of positively charged species could not match the total intensity of negatively charged species in ¹⁹F NMR spectra. What are the "missing" cations ?

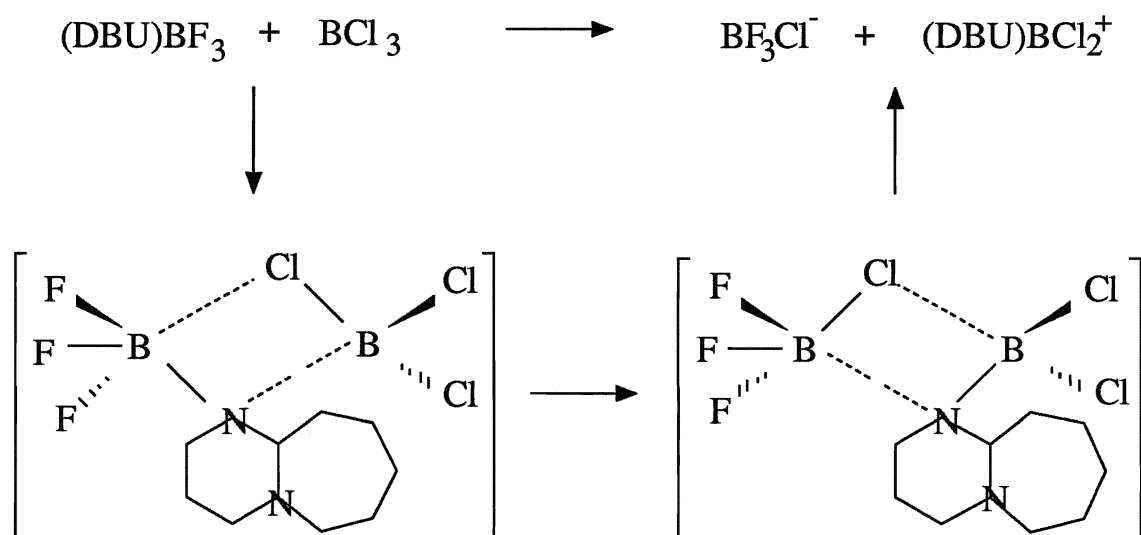
A possible cation is $(\text{DBU})\text{H}^+$, which can balance $\text{BF}_n\text{Cl}_{4-n}^-$ in terms of charge. The hydrolysis of DBU is possible, although DBU has been distilled under a nitrogen atmosphere. Comparing the IR spectrum (appendix 2) of pure DBU and the spectrum from the DBU/ BF_3/BCl_3 system, the N-H⁺ bond is very difficult to identify. In an earlier work^{<40>}, although all materials used were purified under high vacuum condition, the $\text{BF}_n\text{Cl}_{4-n}^-$ species were still observed in the TMU/ BF_3/BCl_3 system. The earlier stage of the distribution reaction in this system was not reported, so it is difficult to tell whether the protonated donor is the significant cation.

$(\text{DBU})\text{BCl}_2^+$ is proposed as another possible cation, according to the following possible reaction mechanism (see Scheme 2). In order to investigate this hypothesis, DBU is added portion by portion to the mixture of $(\text{DBU})\cdot\text{BF}_3$ with BCl_3 , and monitored by ^{11}B NMR. Since the chemical shift of trigonal boron normally is at lower field than that of tetrahedral boron^{<105>}, a new signal at low field would be significant in terms of this hypothesis. However, although the motion of a very broad band from low field (<20 ppm) to high field was observed with increasing amounts of DBU, consistent with increasing the proportion of tetrahedral boron species, no obvious signal at low field was observed when the separated ^{11}B NMR signals were obtained. Whether $(\text{DBU})\text{BCl}_2^+$ is still undergoing the more complicated and rapid further reaction or $(\text{DBU})\text{BCl}_2^+$ is not present is unknown.

Since this problem was getting more and more complicated, we had to stop the investigation, due to limited time resources. In view of the similar NMR pattern having been reported for the TMU/ BF_3/BCl_3 system, we think that the correlation is between DBU and TMU. Since both of them have the ability to offer two lone electron pairs by means of their resonance structures, $^+\text{N}=\text{C}-\text{N}::^-$ and $^+\text{N}=\text{C}-\text{O}::^-$, they may produce a bridging intermediate structure. The second hypothesis seems reasonable, although it has not been proven. Further work may be done using the high resolution instrument equipped with low temperature equipment to slow down

the rapid redistribution reaction at the early stage. But the low temperature may result in very poor resolution, due to the ^{11}B nucleus undergoing a quadrupole relaxation mechanism.

SCHEME 2
THE POSSIBLE FORMATION ROUTE OF $(\text{DBU})\text{BCl}_2^+$



4) Some Properties of $(\text{DBU})_3\text{BF}_2^{2+}$ and $[(\text{DBU})_3\text{BF}_2^{2+}](\text{PF}_6^-)_2$

The ^{19}F NMR spectrum of $(\text{DBU})_3\text{BF}_2^{2+}$ has been observed in CDCl_3 , $\text{CHCl}_3/\text{alcohol}$, water and acetone as solvent.

The ^{19}F chemical shift of $(\text{DBU})_3\text{BF}_2^{2+}$ shows a regular change with increasing polarization of the solvent, from pure CHCl_3 to $\text{CHCl}_3/\text{EtOH}$ in 1:1 and $\text{CHCl}_3/\text{MeOH}$ in 1:1 (Figure 13). The direct connection that comes to mind is hydrogen bonding: $\text{B}-\text{F} \cdots \text{H} \cdots \text{O}-\text{C}$. Fluorine can be deshielded by moving partial electron density to form a hydrogen bond, and then the ^{19}F chemical shift can move toward low field. This seems to be in agreement with the experimental result. However, according to the normal relaxation process, if hydrogen bonding is

present in this system, the molecular tumbling will slow down chemically; hence the line width will increase. Consequently, the resolution of the signal will be worse. But this is just opposite of the experimental observation. The most possible effect on the ^{19}F chemical shift and the line width might be the formation of ion pairs. In less polar solvents, $(\text{DBU})_3\text{BF}_2^+$ tends to form ion pairs with Cl^- to reduce the energy of the system. The ^{19}F chemical shift of the cation will be at higher field, due to the shielding effect of the negative charge of Cl^- on ^{19}F nucleus, and line width will be greater, due to the increased size which reduces the molecular tumbling. In the more polar solvent, $(\text{DBU})_3\text{BF}_2^+$ will be at lower field with better resolution. This explanation is consistent with the experimental results and is also confirmed by the fact of that $(\text{DBU})_3\text{BF}_2^+$ in water gives best resolution.

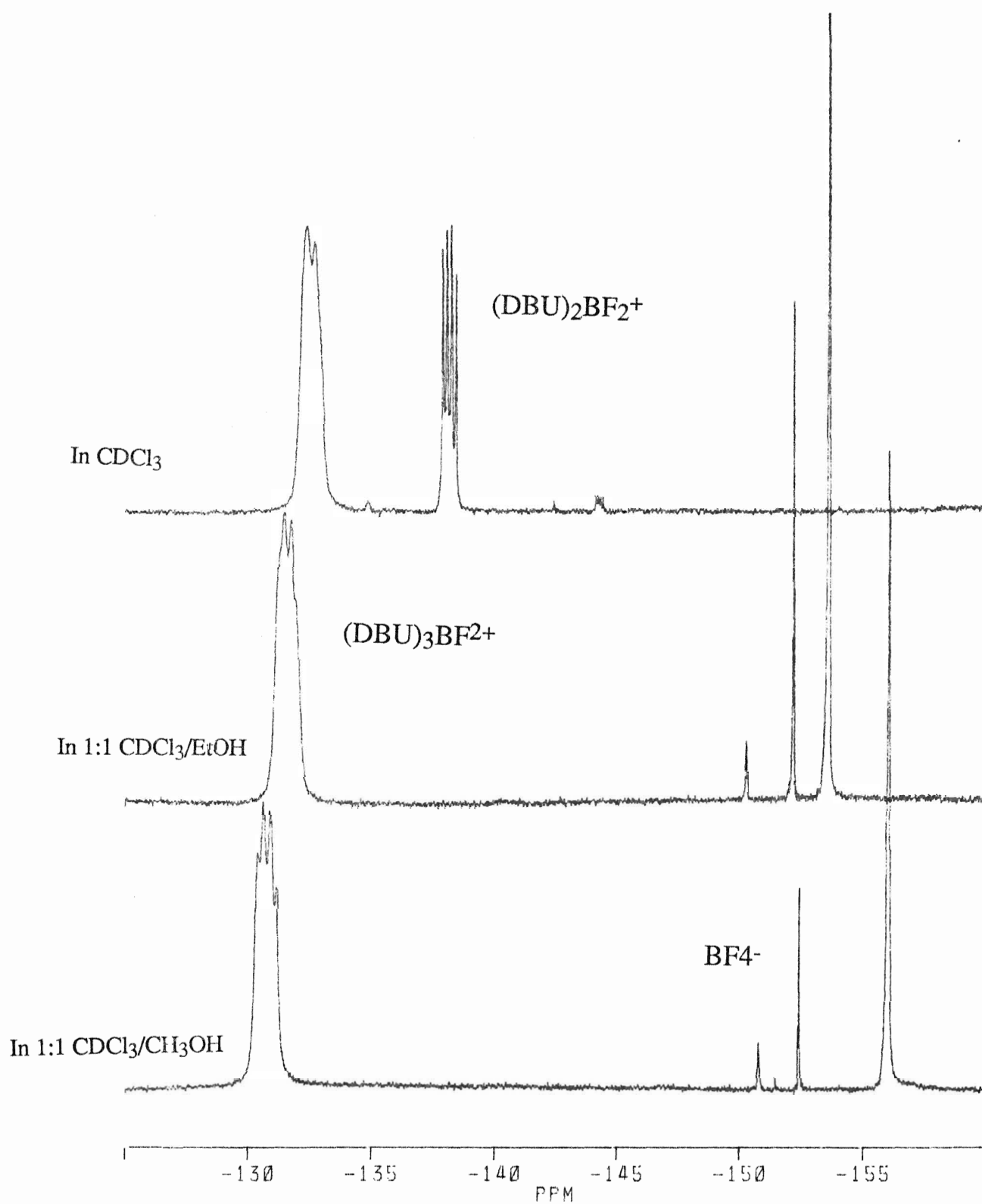
$[(\text{DBU})_3\text{BF}_2^+](\text{PF}_6^-)_2$ is the first $(\text{D}_3\text{BF}_2^+)(\text{X}^-)_2$ salt which has been isolated. Like D_3BH_2^+ ^{<56>} and D_3BBr_2^+ ^{<55>}, $(\text{DBU})_3\text{BF}_2^+$ is very stable to hydrolysis (Figure 13). Its hexafluorophosphate salt can be dissolved in acetone and nitromethane, but not in water, alcohol, chloroform or THF. It is quite resistant to attack by strong organic bases, but decomposes under drastic conditions (Table 12).

TABLE 12
 $[(\text{DBU})_3\text{BF}_2^+](\text{PF}_6^-)_2$ IN ACETONE ACTED
 ON BY *STRONG ORGANIC BASES

REAGENTS	ROOM TEMP.	50 °C, 6 HOURS	50 °C, 24 HOURS
None	no	no	no
Quinuclidine	no	no	slight decomposition
TMG	no	no	decomposition
DBN	no	no	decomposition

*Excess pure bases were used.

FIGURE 13
SELECTIVE SOLVOLYSIS OF $(\text{DBU})_2\text{BF}_2^+$ AND
SOLVENT EFFECT ON ^{19}F NMR SIGNAL OF $(\text{DBU})_3\text{BF}_2^+$



$[(\text{DBU})_3\text{BF}_2^+](\text{PF}_6^-)_2$ was stable in acetone at 50 °C overnight but decomposed in very strong organic bases. The decomposition procedure was monitored by ^{19}F NMR. The decomposition products were observed as NMR signals at $\delta = -137.5$ ppm (broad singlet), $\delta = -143.1$ ppm (quartet, $J = 14.5$ Hz) and $\delta = -146.0$ ppm (quartet, $J = 16.0$ Hz). The expected $(\text{DBU})_n\text{D}_{3-n}\text{BF}_2^+$ peaks were not observed ($n = 1$ or 2). The coupling constant and the chemical shift of these signals suggested that the decomposition products had an O-B-F structure. Alcohols are the possible oxygen donor source.

5) Reactivity of $(\text{DBU})_2\text{BF}_2^+$

The reversibility of $(\text{DBU})_2\text{BF}_2^+$ formation is evident in the $\text{DBU}/\text{BF}_3/\text{BCl}_3$ system (See Table 11), even at 0 °C, but not in the $\text{DBU}/\text{BF}_3/\text{BBr}_3$ system, which is similar to that seen in the earlier report^{<52>}, due to the B-Cl bond being stronger than the B-Br bond. Interestingly, $(\text{DBU})_2\text{BF}_2^+$ reacts not only with Cl^- , but also with $\text{BF}_n\text{Cl}_{4-n}^-$ to form mixed boron trihalide adducts of DBU. The reaction still undergoes the associate mechanism.

$(\text{DBU})_2\text{BF}_2^+$ is unstable. It immediately decomposes in H_2O , methanol and ethanol (Figure 13), which is different than most D_2BF_2^+ ^{<53>} and D_2BH_2^+ ^{<5>}. $(\text{DBU})\cdot\text{BF}_3$ and $(\text{DBU})_3\text{BF}_2^+$ are very stable with respect to hydrolysis, and $(\text{DBU})_2\text{BF}_2^+$ in the middle is very reactive with respect to hydrolysis. The situation can be rationalized as follows. From $(\text{DBU})\cdot\text{BF}_3$, $(\text{DBU})_2\text{BF}_2^+$ to $(\text{DBU})_3\text{BF}_2^+$, the steric hindrance is getting bigger and bigger, tending to destabilize the B-N bond and the molecular or ionic structure; but the positive charge is getting higher and higher, tending to hold the donors more and more tightly. Since $(\text{DBU})\cdot\text{BF}_3$ has the smallest steric factor in this series, the B-N bond is of low energy, and thus the B-N bond is stable. Since $(\text{DBU})_3\text{BF}_2^+$ can hold ligands with a high positive charge and the intermediate structure in the associated

reaction of $(\text{DBU})_3\text{BF}_2^+$ is very unfavourable, ligands can not leave easily. $(\text{DBU})_2\text{BF}_2^+$ may be at the worst point in this balance.

6) Molecular Size Effect on Spin-Lattice Relaxation Time

The spin-lattice relaxation time T_1 of cations and adducts formed from DBU/BF₃/BCl₃ in CDCl₃ is listed in Table 13. The spin-lattice relaxation time depends on the size of compounds. Except (DBU).BFCl₂ and (DBU)₂BFCl⁺ which have larger experimental error caused by the broad peaks in this sample, the T_1 value decreases with increasing size of adducts or ions. This can be directly correlated to the tumbling speed of the molecules or ions in solution. A similar variation has been observed in the pyridine/BF₃/BBr₃ system in CDCl₃ in earlier work done in this laboratory^{<52>}. It was demonstrated that the change in the T_1 value of cations with the viscosity of solvent is much less than that of neutral species. All cationic species have much shorter T_1 values than any neutral species present in the system. For instance, for (pyridine)₂BF₂⁺, $T_1 \sim 0.6$ sec., and for (pyridine).BFBr₂, $T_1 \sim 1.5$ sec., in the same solution. This might result from the formation of ion pairs, which is described in the last section. The effect of ion charge on the T_1 value is difficult to tell from the present data.

TABLE 13
T₁ VALUE OF ¹⁹F OF SPECIES IN DBU/BF₃/BCl₃ SYSTEM

compound	T ₁ /s	Std Dev
(DBU)BF ₃	0.93	0.007
(DBU)BF ₂ Cl	0.60	0.007
(DBU)BFCl ₂	0.61	0.03
(DBU) ₂ BF ₂ ⁺	0.23	0.006
(DBU) ₂ BFCl ⁺	0.14	0.07

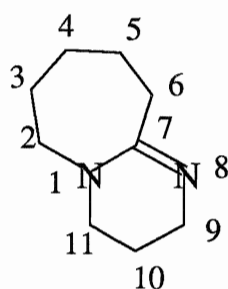
CHAPTER IV

DBN COMPARED TO DBU.

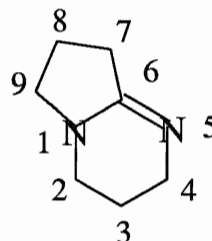
RING SIZE EFFECTS

A. General

A few fully substituted alkyl amidines are commercial available. This chapter is written as a complement to the last chapter and to expand upon the studies from the DBU system to 1,5-Diazabicyclo(4,3,0) non-5-ene (DBN) which is one of the family members of bicycloamidines. The donor containing ring of DBN is the same as in DBU and another one is a five-membered ring, instead of the seven-membered ring in DBU. In view of the multinuclear NMR studies of both of them, the positions of the atoms in both structure are named as following.



IIIa, DBU



IIIb, DBN

As a catalyst, fields of the application of DBN are far fewer than those of DBU¹¹⁶; enlarging on this, the great difference in the catalytic ability with ring size is significant to this work. A comparative study between DBN and DBU in the D/BF₃/BX₃ (X = Cl or Br) system is expected to obtain interesting results pertaining to the correlation of the steric effect with the formation of fluoroboron cations. Since the NMR parameters are very sensitive to slight changes in the local electronic surroundings of the nuclei, these NMR data for DBN and DBU

containing systems are also expected to show the differences between DBN and DBU with respect to their properties.

B. Results

1) ^1H , ^{13}C and ^{15}N NMR of DBU, DBN and Their Boron Trifluoride Adducts

a. ^1H NMR

The ^1H spectra of DBN and $(\text{DBN})\cdot\text{BF}_3$ show first order patterns. Only some multiplets slightly overlap in our 200 MHz spectra. All peaks are identifiable as triplets or quintets (Table 14 and Figure 14). The ^1H spectra of DBU and $(\text{DBU})\cdot\text{BF}_3$ show three groups of overlapped peaks (Appendix 3), but the trend of the chemical shifts' changes from DBU to $(\text{DBU})\cdot\text{BF}_3$, the same as above. In both situations, the free donors' chemical shifts moved to the low field when adducts formed, especially the protons in Position seven for DBN ($\Delta=0.64$ ppm) and the protons in Position six for DBU.

b. ^{13}C NMR

The $^{13}\text{C}\{\text{H}\}$ chemical shifts of DBN, $(\text{DBN})\text{BF}_3$, DBU and $(\text{DBU})\text{BF}_3$ are listed in Table 14 (Spectrum is in Appendix 4). The spectra of free donors were obtained in a 1:1 volume ratio of donor/ CDCl_3 and the spectra of trifluoride adducts were obtained in 1 M solution of CDCl_3 . The ^{13}C NMR peaks of DBN and $(\text{DBN})\cdot\text{BF}_3$ are assigned according to the electronic environment of each carbon. Since carbon in Position six is linked to the nitrogen atom by a double bond, the only signal at very low field (160.2 ppm) is assigned to it.

Complete assignment of all of the ^{13}C peaks for DBU and $(\text{DBU})\cdot\text{BF}_3$ is difficult, due to some protons on the two rings having similar chemical surrounding. Also, there is a great shift change from free donor to adduct that

FIGURE 14
 ^1H NMR SPECTRA OF DBN AND $(\text{DBN})\text{BF}_3$

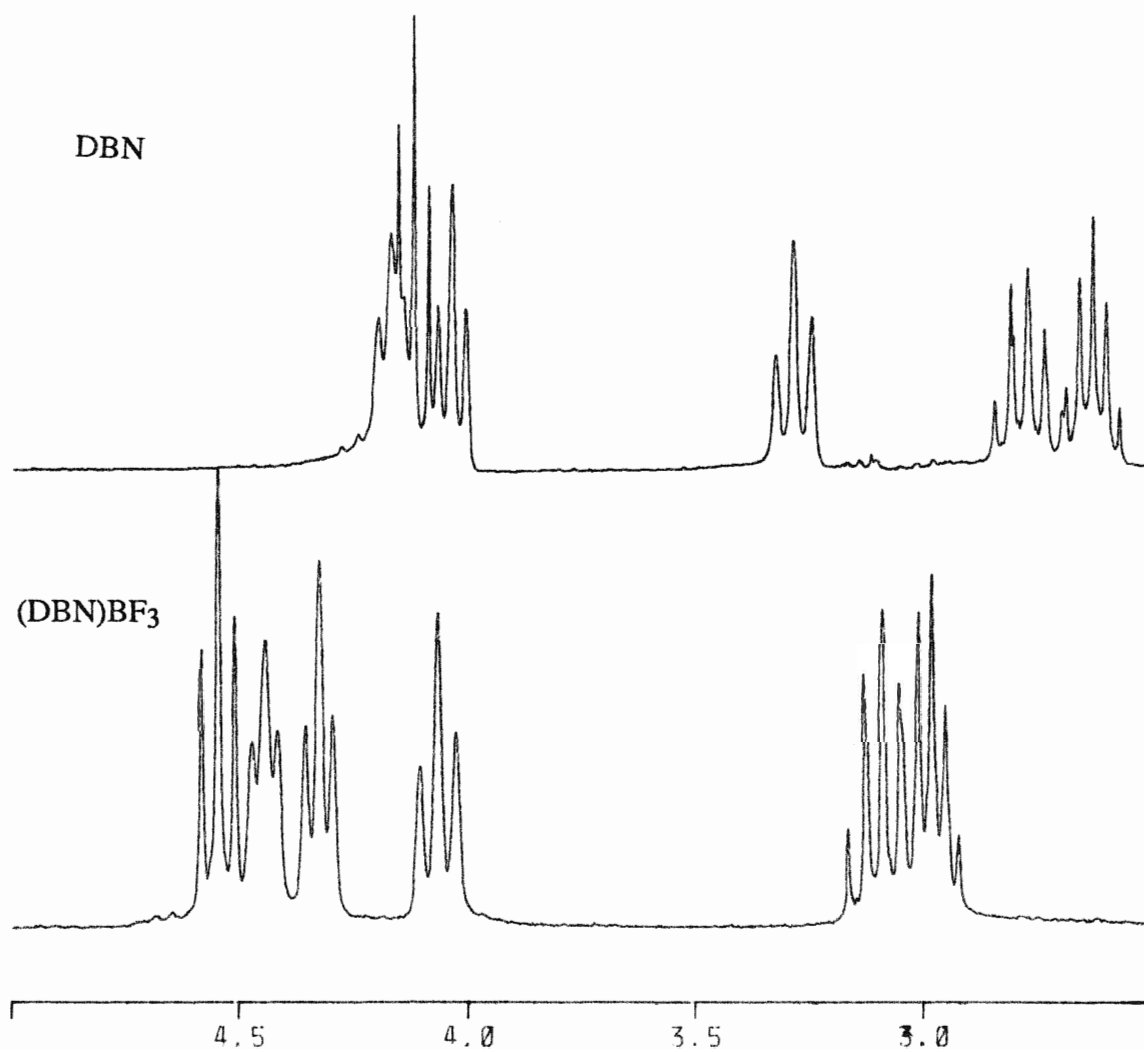


TABLE 14
 ^1H AND ^{13}C NMR CHEMICAL SHIFTS OF DBN AND (DBN)BF₃

POSITION	DBN/(ppm)		(DBN)BF ₃ /(ppm)	
	^1H	^{13}C	^1H	^{13}C
2	3.19	42.7	3.33	40.0
3	1.78	20.5	1.98	19.0
4	3.32	51.1	3.45	52.6
6	-	161.3	-	164.9
7	2.43	31.1	3.07	30.6
8	1.92	19.3	2.09	18.5
9	3.27	43.7	3.55	42.6

TABLE 15
 ^{13}C NMR CHEMICAL SHIFTS OF DBU AND (DBU)BF₃

	DBU/(ppm)	(DBU)BF ₃ /(ppm)
CHEMICAL	22.1, 25.6, 28.1,	20.7, 23.8, 26.7,
SHIFTS	29.4, 36.8, 43.7,	28.7, 30.5, 41.1,
	48.1, 52.6, 161.3 (7)	49.2, 54.0, 168.1 (7)

occurs on the carbon atom linked the double bond, which was clearly observed around 160 ppm.

c. ^{15}N NMR

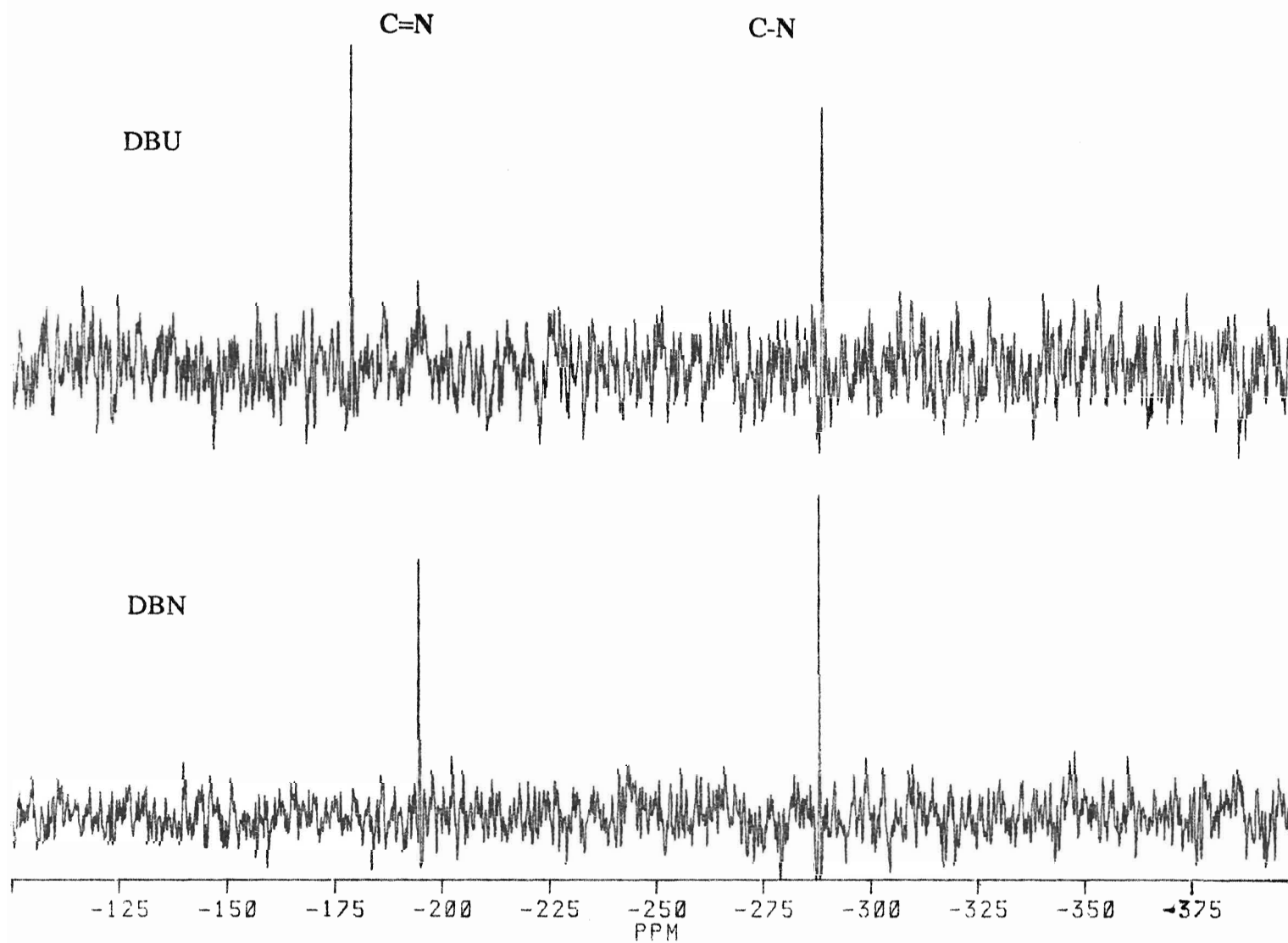
The 20.29 MHz ^{15}N NMR spectra of DBN and DBU were obtained by the INEPT technique (Insensitive Nuclei Enhanced by Polarization Transfer)^{<101>} and are shown in Figure 15. Practically, this method can be utilized to gain high sensitivity in the ^{15}N NMR signal by a polarization transfer from the proton. Two different nitrogen atoms' chemical shifts are assigned according to the respective ^{15}N chemical shift range of the nitrogen atoms of amidines. The NMR data are listed in Table 16. The ^{15}N chemical shift of the amino nitrogen atom is always in the high field^{<125>}. The ^{15}N signals of their adducts were not observed in a 1 M solution of CDCl_3 over night; thus the further study of ^{15}N was discontinued.

TABLE 16
 ^{15}N NMR CHEMICAL SHIFT
OF DBN AND DBU

COMPOUND	CHEMICAL SHIFT /(ppm)	
	C=N	C-N
DBN	-194.6,	-288.0
DBU	-179.1,	-288.8
*NORMAL RANGE	-130~-175,	-300~-325

*Data of the normal range of ^{15}N chemical shifts of amidines are from Reference ^{<125>}.

FIGURE 15
 ^{15}N NMR SPECTRA OF DBN AND DBU



2) Formation of DBN Containing Cations

a. DBN/BF₃/BCl₃ System

The DBN/BF₃/BCl₃ system shows similar ¹⁹F and ¹¹B NMR patterns to those of the DBU/BF₃/BCl₃ system. The ¹⁹F and ¹¹B NMR spectra of the DBN/BF₃/BCl₃ system are shown in Figures 16 and 17. All species of the tetrahaloborate, trifluorochloroboron adducts of DBN and DBN fluoroboron cations are present, although the order and the range of chemical shifts of some adducts and cations are different in the DBU/BF₃/BCl₃ system. The ¹⁹F and ¹¹B NMR parameters of the DBN/BF₃/BCl₃ system are listed in Table 17. In order to compare the change in the NMR parameters between DBN and DBU containing systems, the ¹⁹F and ¹¹B NMR parameters of DBU/BF₃/BCl₃ systems are listed again in brackets in Table 17.

TABLE 17
*¹⁹F AND ¹¹B NMR PARAMETERS FOR
DBN/BF₃/BCl₃ AND DBU/BF₃/BCl₃ SYSTEMS

SPECIES	CHEMICAL SHIFTS (ppm)		J ¹⁹ F- ¹¹ B(Hz)
	¹⁹ F	¹¹ B	
(DBN).BF ₃	-149.9(-144.3)	-0.6(-0.4)	17.4(17.3)
(DBN).BF ₂ Cl	-129.2(-124.6)	3.0(2.9)	34.1(36.3)
(DBN).BFCl ₂	-118.1(-112.8)	6.0(5.8)	62.6(62.7)
(DBN).BCl ₃	-	6.5	-
(DBN) ₂ BF ₂ ⁺	-149.4(-138.4)	0.7(1.4)	31.6(34.0)
(DBN) ₂ BFCI ⁺	-131.6(-121.6)	~4.5(~5.4)	-
(DBN) ₃ BF ₂ ⁺	-143.4(-132.8)	2.2(3.6)	47.8(50.1)
** (DBN)(DBU)BF ₂ ⁺	-143.9	0.9	32.8
** (DBN)(DBU)BFCI ⁺	~-126	-	-

FIGURE 16
188.3 MHz ^{19}F NMR SPECTRUM OF A TYPICAL
DBN/ BF_3/BCl_3 SYSTEM(mole ratio 2:1:1)

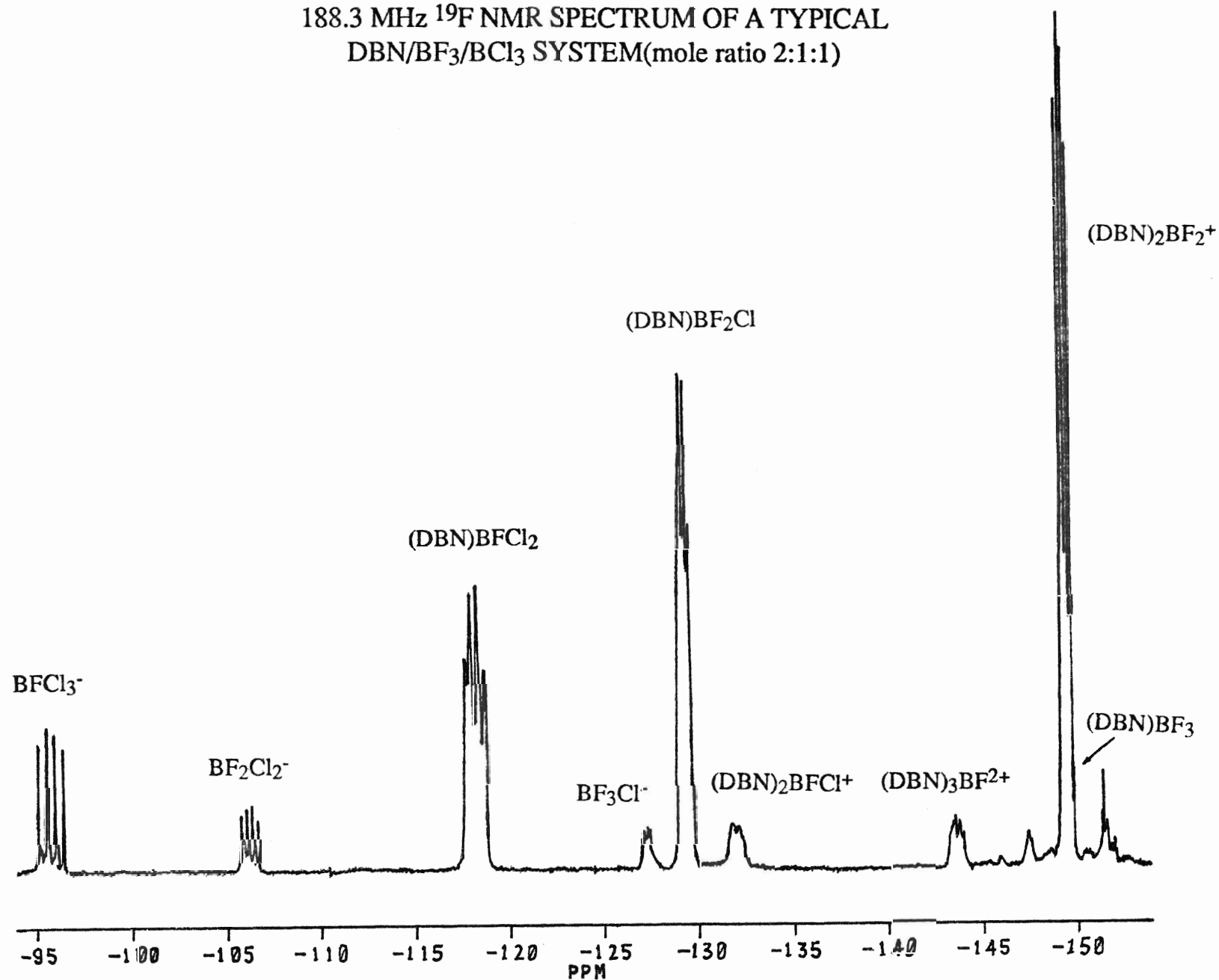
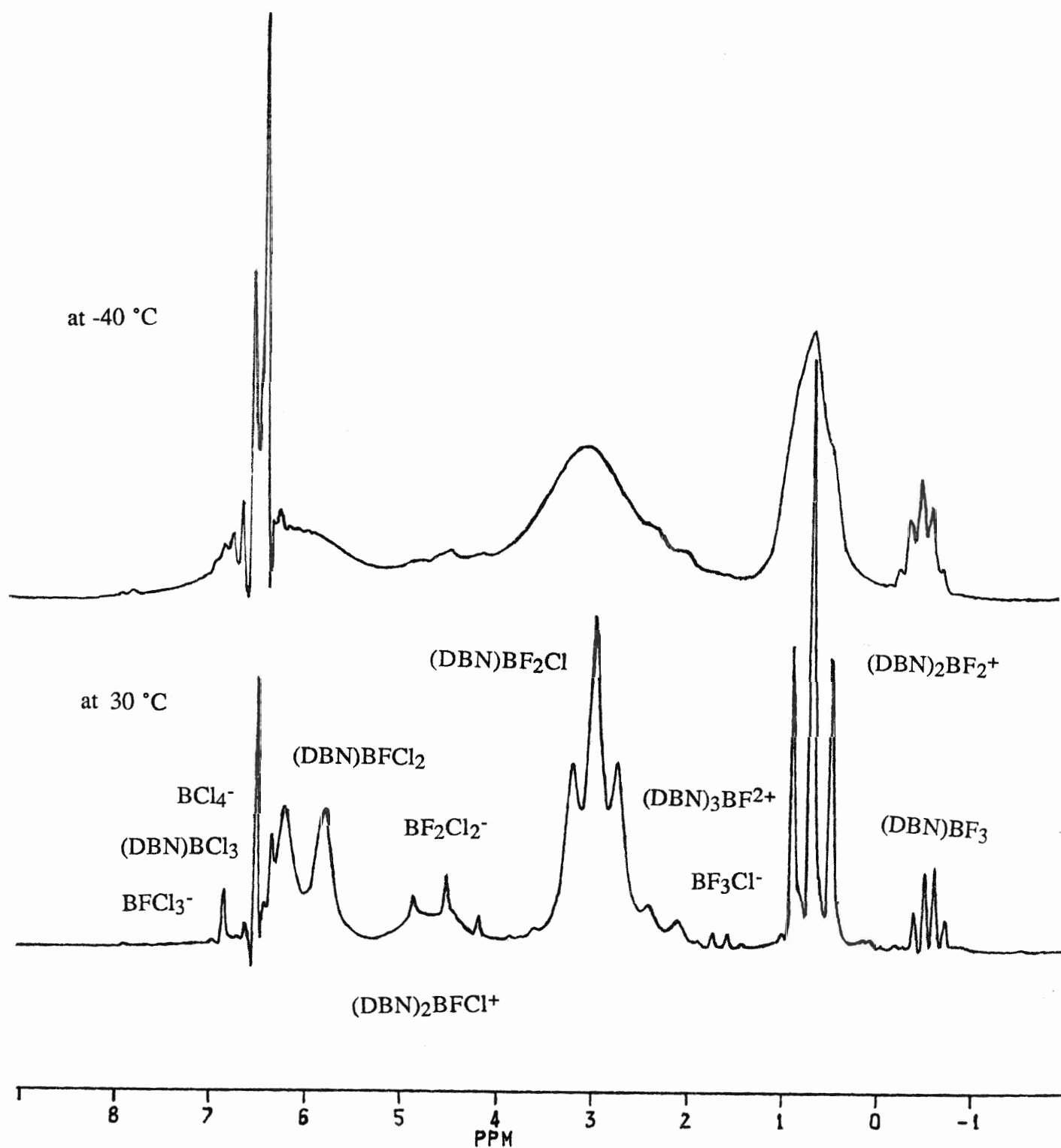


FIGURE 17
160.4 MHz ^{11}B NMR SPECTRA OF DBN/ BF_3/BCl_3 SYSTEM
AT AMBIENT AND LOW TEMPERATURE



* $\text{BF}_n\text{Cl}_{4-n}^-$ species are the same as in DBU/ BF_3/BCl_3 system.

**Ligand-mixed cations will be described in Chapter VII.

The difference in the ^{19}F chemical shifts between $(\text{DBN})\cdot\text{BF}_3$ and $(\text{DBN})_2\text{BF}_2^+$ is 0.5 ppm. These two signals overlap each other at the 188.3 MHz operating frequency. The difference in the ^{19}F chemical shifts between $(\text{DBN})\cdot\text{BF}_3$ and $(\text{DBN})_3\text{BF}^{+2}$ is 6.1 ppm. Both differences are much smaller than in the analogous DBU system, 5.9 ppm and 11.5 ppm, respectively.

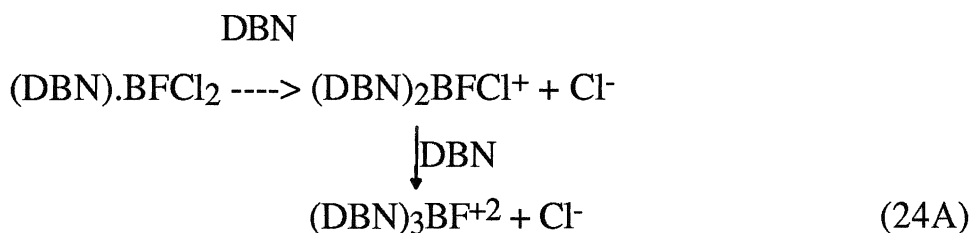
The chemical shifts of the one-chlorine containing species, BF_3Cl^- , $(\text{DBN})\cdot\text{BF}_2\text{Cl}$ and $(\text{DBN})_2\text{BFCl}^+$ are in a range analogous to the DBU containing system in ^{19}F NMR spectra, but the order is the opposite.

$(\text{DBU})_2\text{BFCl}^+$, $(\text{DBU})\cdot\text{BF}_2\text{Cl}$, BF_3Cl^- , $(\text{DBN})\cdot\text{BF}_2\text{Cl}$, $(\text{DBN})_2\text{BFCl}^+$

Low field ————— High field

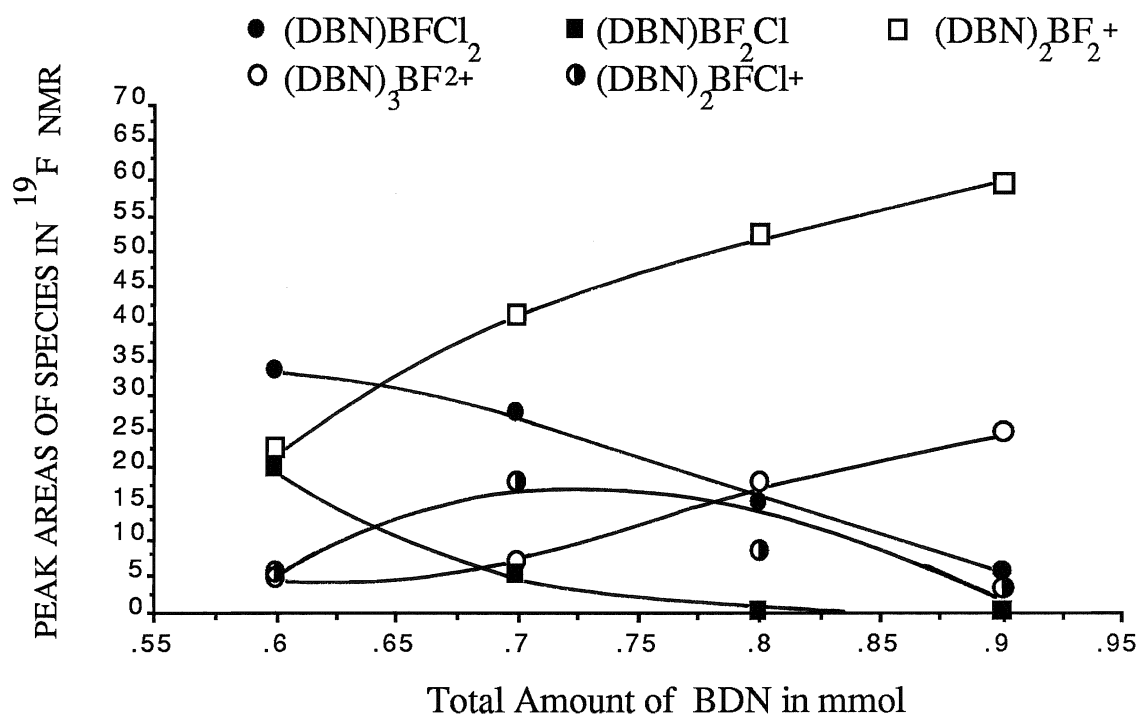
In a series of experiments searching for the $(\text{DBN})_3\text{BF}^{+2}$ cation, three different Cl/F ratios, 0.5:1, 1:1 and 2:1, in the DBN/ BF_3/BCl_3 system were prepared in CDCl_3 . $(\text{DBN})_3\text{BF}^{+2}$ as a poor quartet was clearly observed under 1:1 and 2:1 ratio conditions. Its intensity in the ^{19}F NMR is 25% and 29%, respectively. It was not clearly observed under 0.5:1 ratio of Cl/F.

$(\text{DBN})_2\text{BFCl}^+$, which shows a broad ^{19}F NMR signal in CDCl_3 , was more easily observed than $(\text{DBU})_2\text{BFCl}^+$. As an intermediate product during the formation of $(\text{DBN})_3\text{BF}^{+2}$, it increased first and then decreased when the second donor was added gradually (Figure 18), which is consistent with Equation 24A.



All cations were confirmed by FABMS: for the $(\text{DBN})_2\text{BF}_2^+$ cation, peaks at m/z 297, $[(\text{DBN})_2\text{BF}_2^+]$ and at m/z 173, $[(\text{DBN})\text{BF}_2^+]$ were observed in both

FIGURE 18
 THE CHANGE OF PEAK AREAS OF ADDUCTS AND CATIONS
 WITH INCREASING DBN FOR DBN/BF₃/BCl₃ SYSTEM
 (BF₃: BCl₃ = 0.2 mmol : 0.2 mmol)



solution and as a PF_6^- salt; for $(\text{DBN})_2\text{BFCI}^+$, peaks at m/z 313, $[(\text{DBN})_2\text{BFCI}^+]$ and at m/z 189, $[(\text{DBN})\text{BFCI}^+]$ were observed in solution. $(\text{DBN})_3\text{BF}^{+2}$ was detected by the isotope pattern of $[(\text{DBN})_3\text{BF}(\text{PF}_6)]^+$ at m/z 547 for the pure solid sample. (The details see Chapter VIII).

b. DBN/ BF_3 / BBr_3 System

In the DBN/ BF_3 / BBr_3 system, Br/F ratios of in 1:1, 1:1.5 and 1:2 ratios were prepared. When excess DBN was added to the mixed $(\text{DBN})\cdot\text{BF}_3$ and BBr_3 at -63°C in CDCl_3 , only BFBr_3^- was observed, at -79.6 ppm, with a coupling constant of 113.3 Hz in a ^{19}F NMR spectrum. A very broad band moved to high field as the amount of DBN increased, which indicates the boron trihalide adducts increased gradually. However, when the rapid exchange reaction was fully quenched, only $(\text{DBN})\cdot\text{BF}_3$ and a little BF_4^- remained. This system can not be analogous to the DBU/ BF_3 / BBr_3 system. Mixed boron trihalide adducts, $(\text{DBN})\cdot\text{BF}_n\text{Br}_{3-n}$, were not formed by the redistribution reaction.

c. Low Temperature ^{11}B NMR

The low temperature ^{11}B NMR spectra have been obtained for both the DBN/ BF_3 / BCl_3 system and the DBU/ BF_3 / BCl_3 system using a instrument (500 MHz for proton) with a 160.4 MHz operating frequency. At -39.5°C , most signals became very broad, and only $\text{D}\cdot\text{BCl}_3$ remained sharp. Several new sharp peaks appeared around 6.3 to 6.9 ppm. The number and the shape are different for the different systems. The low temperature ^{11}B spectrum of the DBN/ BF_3 / BCl_3 system is shown in Figure 17a.

d. DBN/ BF_3 / BCl_3 /DBU System

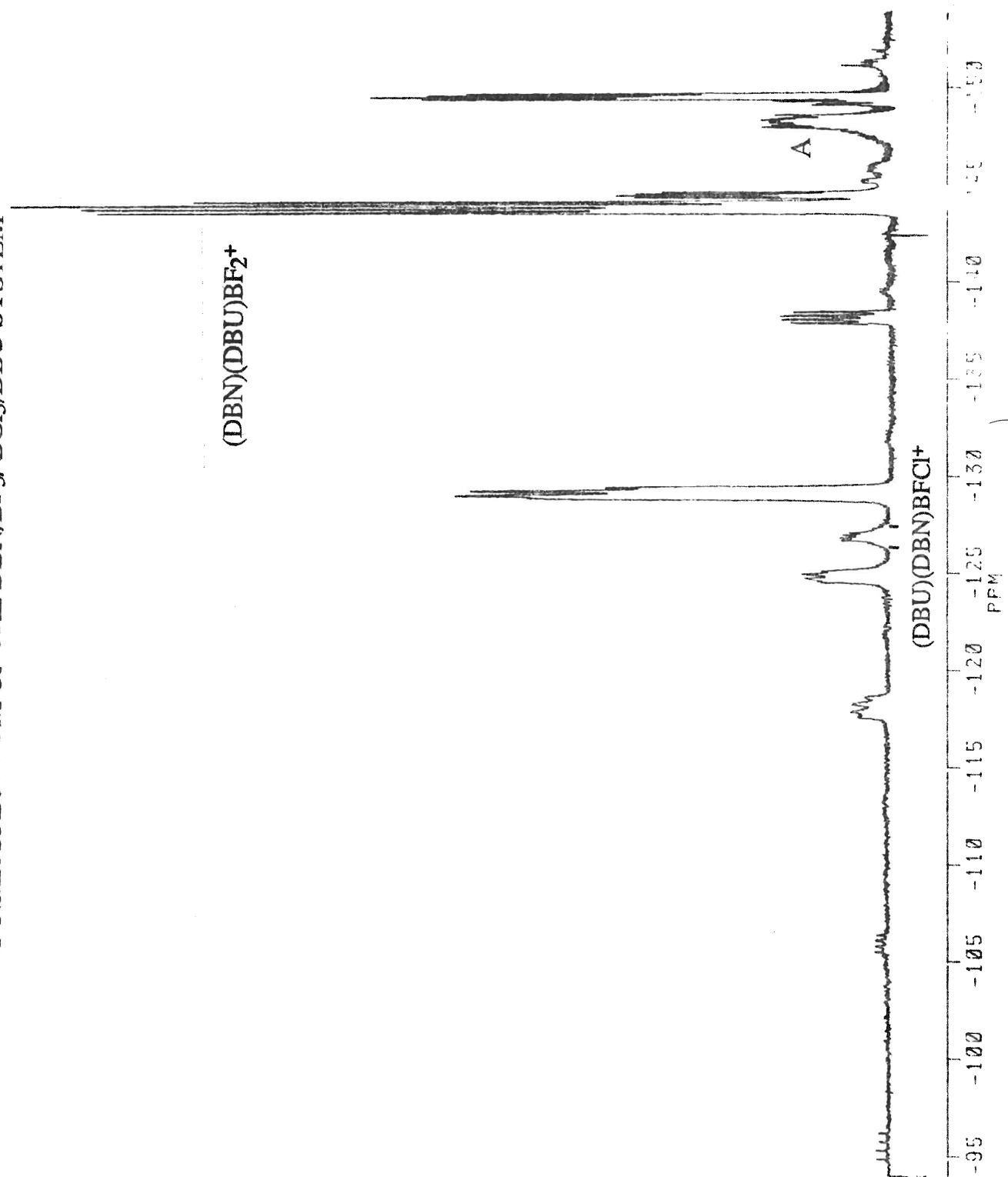
Ligand-mixed fluoroboron cations will be discussed mainly in Chapter VII. As related to the DBU and the DBN system, the determination of some species is described as follows. DBU, as the second donor, was added to a solution of

(DBN).BF₃ and BCl₃ in CDCl₃ in a 1:0.8 molar ratio (Figure 19). Table 18 lists the change of the percentage of peak areas in the ¹⁹F NMR spectra. The substitution of chlorine from (DBN).BF₂Cl by DBU is in agreement with the main change in peak areas among all species. (DBN)(DBU)BFCI⁺ should have formed from (DBN).BFCl₂ when DBU was added, but it was not distinguished at the beginning because no evident new peak was present in the expected range in the ¹⁹F spectra.

TABLE 18
THE CHANGE OF THE INTENSITY OF SPECIES IN
THE DBN/BF₃/BCl₃/DBU SYSTEM WITH
INCREASING DBU MONITORED BY ¹⁹F NMR
(Initially, the system is in (DBN).BF₃:BCl₃ = 0.1 mmol:0.08 mmol)

Species	<u>Amount of DBU in mmol</u>						
	0.10	0.15	0.20	0.25	0.30	0.35	0.40
BFCl ₃ ⁻	3.9	2.3	3.4	1.7	0.3	~0	0
BF ₂ Cl ₂ ⁻	8.1	5.0	4.1	2.1	0.6	0	0
[BF ₃ Cl ⁻ and (DBN)(DBU)BFCI ⁺]	8.7	7.1	4.7	3.7	2.6	1.8	~0
(DBN).BFCl ₂	9.0	8.2	7.2	5.2	3.3	1.9	0
(DBN).BF ₂ Cl	40.3	40.3	35.2	30.1	24.2	15.2	7.9
[(DBN) ₂ BF ₂ ⁺ and (DBN)BF ₃]	11.8	12.8	12.8	13.8	14.8	15.8	15.4
(DBU).BF ₂ Cl	3.2	5.2	5.8	5.7	5.6	4.0	2.4
(DBU) ₂ BF ₂ ⁺	2.0	2.3	2.5	3.1	3.6	4.3	5.1
(DBN)(DBU)BF ₂ ⁺	5.2	9.2	14.0	20.6	29.8	38.9	52.6
(DBU).BF ₃	1.1	2.1	2.9	4.4	5.8	7.8	9.3
A	3.8	5.2	7.3	9.6	9.7	10.3	7.2

FIGURE 19
 ^{19}F NMR SPECTRUM OF THE DBN/BF₃/BCl₃/DBU SYSTEM



Finally, it was found that (DBN)(DBU)BFCl⁺, as a "broad singlet", overlapped with BF₃Cl⁻, according to the chemical shift order of one chlorine containing species described in section a. Its intensity seems invariant under our experimental conditions. The mixed-ligand doubly charged cation, (DBN)(DBU)₂BF₂²⁺, was not detected in this experiment. A remarkable and unidentified broad peak "A" at $\delta = -148.1$ ppm in the ¹⁹F NMR spectra increased with increasing free DBU, but finally decreased. Some unidentified small peaks might be from impurities. The ¹¹B spectrum does not give more information, except for the confirmation of the (DBN)(DBU)BF₂⁺ cation.

C. Discussion

1) Donor Ability

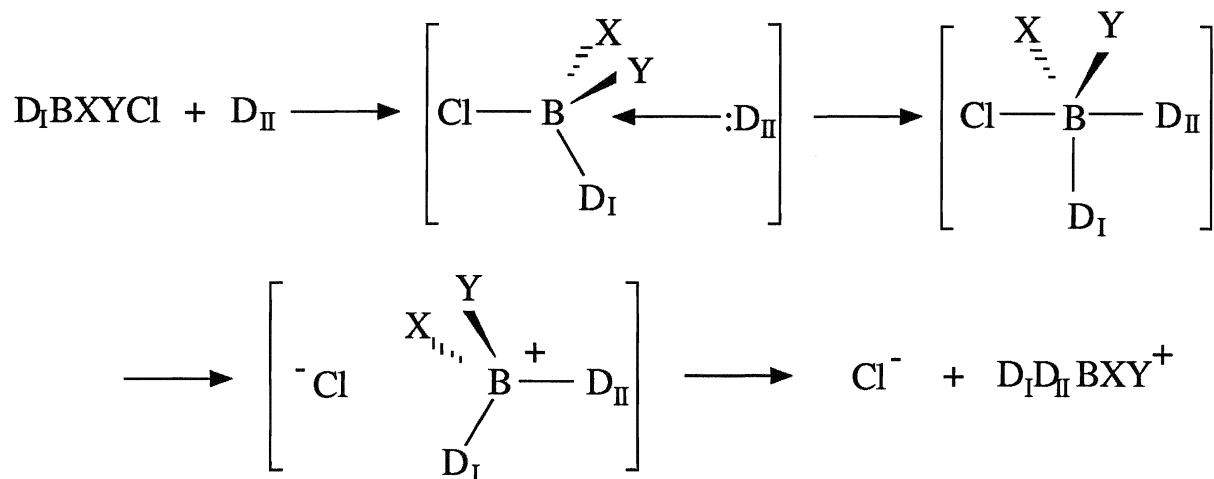
Amidine's resonance structure was well known (see page 9). In this work, ¹⁵N NMR spectra of both DBU and DBN show that the two nitrogen atoms' chemical shift differences were smaller than the common range of amidines, N(1) - 130 ppm ~ -175 ppm and N(2) -300 ppm ~ -325 ppm [N(1): imino nitrogen and N(2): amino nitrogen]. A possible reason is proposed as follows. Since the two nitrogen atoms in DBU and DBN are fixed by two rings, the intramolecular rotation between nitrogen and carbon is forbidden. Thus the lone electron pair on the amino nitrogen atom can easily delocalize toward the imino nitrogen atom and join the resonance in the system. DBN has more efficient resonance, since its five-membered ring has the better planarity and the orientation of a lone electron pair on the amino nitrogen is more suitable for contribution to the resonance system. In fact, the ¹⁵N chemical shift difference between the two nitrogen atoms in DBN is 16 ppm closer than in DBU, which is mainly caused by the ¹⁵N shift of N(1) moving to higher field. When a lone electron pair from the imino nitrogen donates to a Lewis

acid, the electron density can be moved to the donor site through the resonance system, more effectively.

The ^1H and ^{13}C NMR studies confirmed that the donor ability of DBU and DBN is contributed mainly by their resonance systems, since the most significant change in both ^1H and ^{13}C chemical shifts on the complex atoms are near the $\text{N}=\text{CR}-\text{N}$ region. The chemical shifts of the atoms in other regions show less change. For instance, the ^1H and ^{13}C chemical shift of atoms in position (4) for DBN only has a little change on the complex atoms, although this position is one neighbour of the donor atom.

2) Reactivity of $\text{D.BF}_n\text{Cl}_{3-n}$ and Associate Reaction Mechanism

$(\text{DBN}).\text{BF}_2\text{Cl}$ and $(\text{DBU}).\text{BF}_2\text{Cl}$ have the similar reactivities in the chloride replacement reaction. The entering amidine ligand replaces chloride almost immediately. However, $(\text{DBN}).\text{BFCl}_2$ reacts with DBN much faster than $(\text{DBU}).\text{BFCl}_2$ reacts with DBU. Since the chloride replacement reaction for mixed boron trihalide adducts is dependent on the size of the coordinated ligands and the concentration of the entering group, an associative reaction mechanism ($\text{S}_{\text{N}}2$) was suggested. The mechanism can be demonstrated by the reaction between DI.BXYCl and DII :



SCHEME 3

When both X and Y are fluorides, the intermediate structure is stable whether DI is DBU or DBN, as small fluorides do not exhibit a large steric effect with D. But when X is fluoride and Y is chloride, DI's size becomes significant, due to an increased steric hindrance making the intermediate product unfavourable. Consequently, chloride replacement in (DBU).BFCI₂ is more difficult than from (DBN).BFCI₂.

This associative reaction mechanism also seems to be present with chloride replacement from in BF_nCl_{4-n}⁻ species and D₂BFCI⁺ formed from a neutral ligand, because the size of the coordinated ligands and entering ligands evidently influence these reactions.

3) Why (DBN).BF₂Br and (DBN).BFBr₂ are Unfavourable

Most nitrogen donor containing organic bases can form mixed boron trihalide adducts, D.BF_nBr_{3-n}. Although the separated (DBU).BF_nBr_{3-n} species were not observed at ambient temperature, the formation of (DBU)₂BF₂⁺ and (DBU)₃BF₂⁺ indicated that (DBU).BF₂Br and (DBU).BFBr₂ were present. The "forbidden" redistribution reaction in the DBN/BF₃/BBr₃ system is unusual. As is known, (amine).BF₂I and (amine).BFI₂ were not favourable when (amine).BF₃ reacted with BI₃^{<16>}. This could initially be explained by a "Symbiosis Principle", based on hard and soft acids and bases (See page 7). In fact, there are no absolutely "hard" or "soft" bases and acids. The terms hard and soft are relative and qualitative. Normally, F and N are "hard" bases and Br is "soft" base. DBN may be a much "harder" base than some amines, making bromide, in turn, relatively much weaker. In general, for a hard base, the donor atom is of high electronegativity and low polarizability. "The electronegativity" of nitrogen seems increased by the efficient resonance structure in DBN. Then the bromide tends to flock together and DBN tends to flock together with fluoride. From an energy viewpoint, the slight

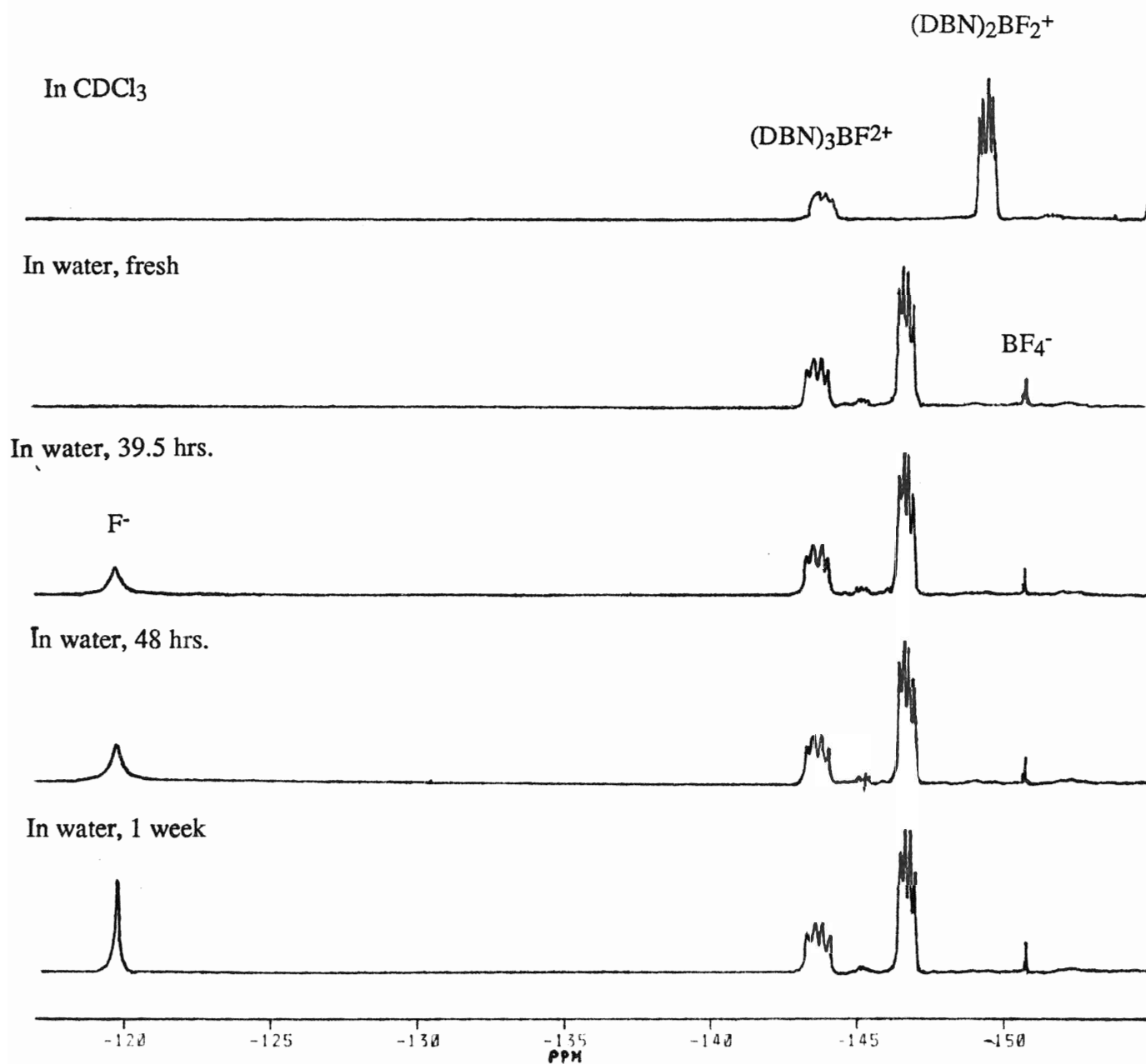
difference in the free energy ΔG can cause the remarkable difference in the equilibrium constant K .

4) The Comparison of DBN and BDU Fluoroboron Cations

Both $(\text{DBN})_2\text{BF}_2^+$ and $(\text{DBN})_3\text{BF}_2^+$ were isolated as PF_6^- salts. $(\text{DBN})_3\text{BF}_2^+$ has properties similar to $(\text{DBU})_3\text{BF}_2^+$, but $(\text{DBN})_2\text{BF}_2^+$ is very different from $(\text{DBU})_2\text{BF}_2^+$. It is stable in water up to 85 °C, but decomposes in boiling water. Figure 20 shows $(\text{DBN})_3\text{BF}_2^+$ and $(\text{DBN})_2\text{BF}_2^+$ in chloroform and in water. The cations seem to undergo a very slow decomposition in water at room temperature. The new peak at $\delta = -119.9$ ppm is free fluoride, which was confirmed by dissolving Na^+F^- in water. In the ^{11}B spectrum, a broad band at $\delta \sim 19$ ppm was observed which was produced by the decomposition of chloroboron compounds during water extraction (Appendix 5). This signal is like that of $\text{B}(\text{OH})_3$ ^{<105>}.

Better resolution of $(\text{DBN})_3\text{BF}_2^+$ was also obtained in polar solution, which is consistent with a suggestion of ion pairs in solution (see page 63). Since $(\text{DBN})_3\text{BF}_2^+$ shows a better resolution than $(\text{DBU})_3\text{BF}_2^+$ in the same solvent, the size of ions can be reasonably thought of as being the major factor. A T_1 study of pure $[(\text{DBN})_3\text{BF}_2^+](\text{PF}_6^-)_2$ and $[(\text{DBU})_3\text{BF}_2^+](\text{PF}_6^-)_2$ in acetone confirmed this result. The T_1 value is 0.59 sec. for $(\text{DBN})_3\text{BF}_2^+$ and 0.47 sec. for $(\text{DBU})_3\text{BF}_2^+$.

FIGURE 20
 ^{19}F NMR SEQUENCE OF $(\text{DBN})_2\text{BF}_2^+$ AND $(\text{DBN})_3\text{BF}_2^+$
IN CDCl_3 AND WATER

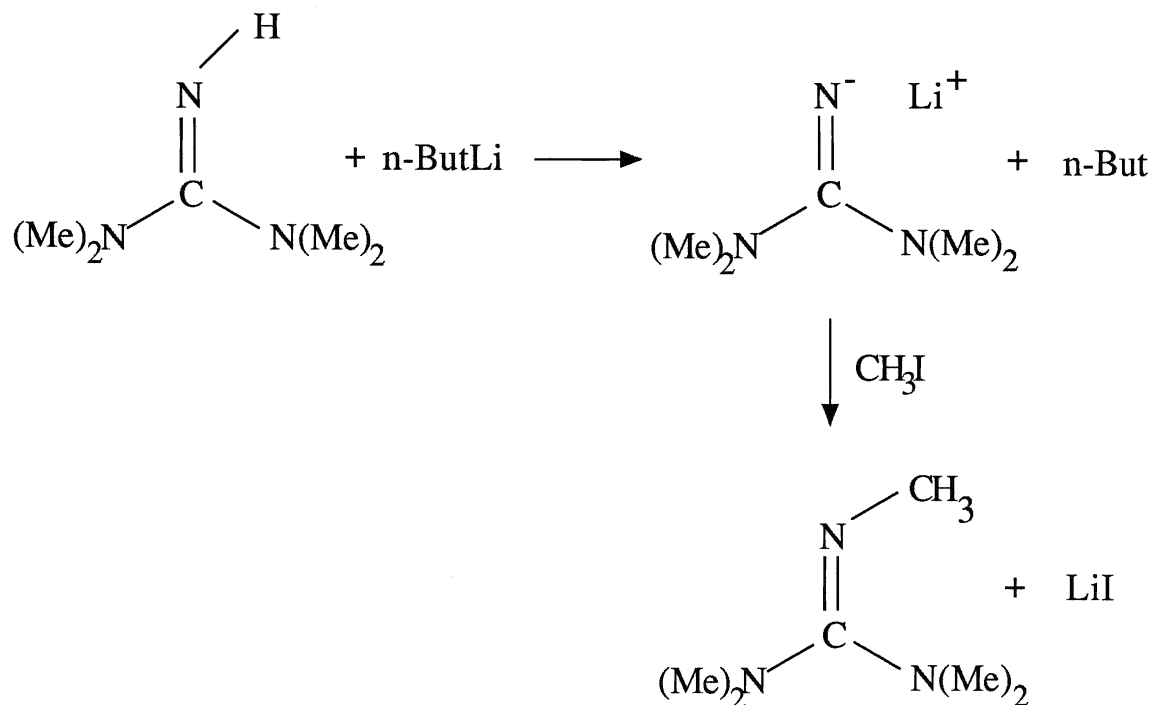


CHAPTER V

SYSTEMS WITH LOW-STERICALLY-HINDERED GUANIDINES

A. Introduction

As described in Chapter I, pentamethylguanidine(PMG) is one of the strongest guanidine bases. It also has the smallest steric hindrance among all acyclic pentaalkylguanidines. Since any intramolecular inversion and rotation can not cause isomeric changes in this molecule and since this molecule does not have a weak bond such as the N-H bond, PMG is expected to be one of the suitable donor ligands and the most basic guanidine ligand in our tetrahedral fluoroboron cation system. Up to now, PMG is still not commercially available. Ten years ago, an attempt was made to synthesize it in this laboratory^{<126>}, using a classical method^{<84>}, but a very low yield made future studies difficult. A new synthetic procedure was proposed by Dr. Holland in Scheme 4.



SCHEME 4

A series of experiments was designed for synthesizing PMG for the present work, which was described in Chapter II.

Relating to PMG, tetramethylguanidine(TMKG) was introduced into the fluoroboron cation systems. Since interest in the stability of ligands is directly responsible for the initiation of the studies of boron complexes, more attention was paid initially to the possibility of forming TMKG containing fluoroboron cations, and the strength of the N-H bond contained in TMKG.

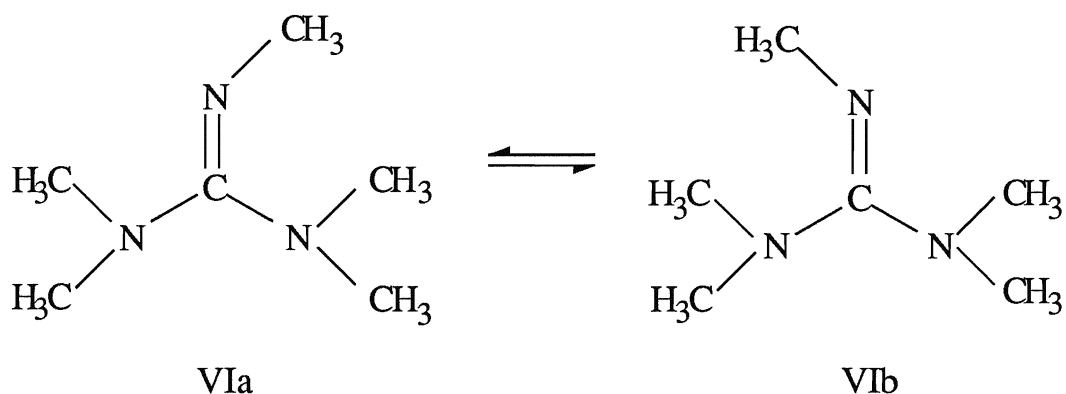
B. Results and Discussion

1) Synthesis of Pentamethylguanidine

a. The Thermodynamic Study of PMG

Although the ^1H NMR(Figure 2b) and mass spectrometry data (Figure 2a) supported the presence of PMG, we have not obtained any other confirmation. The thermodynamic properties of PMG are expected to help in the final determination.

Since the intramolecular exchange between structure VIa and VIb is slow for PMG at room temperature, a 1:2:2 ^1H NMR pattern is observed. With rising temperature, the intramolecular exchange between VIa and VIb will be accelerated and the two equally separated signals in ^1H NMR should become close to each other and finally become one singlet. Conversely, by lowering the temperature far enough, the two methyl groups on one amino nitrogen may be induced to cause the two split ^1H NMR signals, based on the different chemical surrounding. Unfortunately, the temperature controlled system equipment is not available in Brock, and thus only a brief study was carried out.



An NMR tube containing PMG was heated to 90 °C and then immediately put into the probe of a Bruker WC-80 NMR instrument. The two higher intensity signals are lowered equally and the lower signal maintained the same height. This indicates that the two signals caused by two -N(CH₃)₂ groups tend to move toward each other and increase their line width. When the temperature cooled to room temperature, the spectrum showed a 1:2:2 pattern again. This result is consistent with structure VI of PMG.

The low temperature experiment was performed in the Bruker AC-200 NMR instrument by running one scan, after the sample was cooled to -90 °C. All three of the signals became a bit broader, but no splitting was observed. This is probably due to the increased viscosity of the solution at low temperature.

b. The Properties of Lithioguanidine, Li[N=C(NMe₂)₂]

Lithioguanidine is the intermediate product of the synthesis of PMG. It does not dissolve in the non-polar solvent hexane, or in the less polar solvent ether/hexane in a 5:1 ratio, but does dissolve in the polar solvent THF/hexane in a 5:1 ratio, due to its ionic property. Lithioguanidine is very sensitive to air and is hydrolysed to LiOH and H[N=C(NMe₂)₂]^{<91>}. However, our observation does not seem to agree with the literature. LiOH is white in colour, but our decomposition products are yellow to red-brown. Its colour is in agreement with Li₃N (CRC handbook). Although the bonding situation is not very clear, noting the presence of

this hexamer itself is important in the understanding of the question that arose in the synthetic process of pentamethylguanidine.

c. The Major Effect on the Synthesis of PMG

When CH_3I is added to lithioguanidine, HMG^+ was produced in all of the experiments as a major product, instead of PMG. Hexamethylguanidine, HMG^+ , is a well known stable organic ion. This reaction at room temperature is exothermic, which indicates HMG^+ 's stability. This reaction is not a simple stepwise reaction, because amounts of PMG did not increase with decreasing amounts of CH_3I . The possible reaction mechanism is: 1) When one Li-N bond was broken by CH_3^+ or I^- , the other two Li-N bonds will still strong enough, and the hexamer core of lithium was not broken, as no Li^+I^- precipitate occurred in the first five minutes at 20°C or in the first 10 minutes at 0°C . When the second methyl group attacked the imino nitrogen, the whole hexameric structure was disturbed, and the HMG^+ formed then combined with free I^- entered the solid phase. 2) One imino nitrogen was simultaneously attacked by two methyl groups from different directions, due to there being three Li-N bonds for each imino nitrogen atom in the same chemical environment.

Further study suggested that this reaction does not to be seem kinetically controlled, but rather, appears to be a thermodynamically controlled reaction. We have tried to control the formation of HMG^+ by reducing the concentration, reducing the speed of CH_3I addition and reducing the reaction temperature. The formation of HMG^+ depends on the temperature. It was not produced at -40°C . However, under this condition, no reaction was evident. Once the temperature was raised over 0°C , HMG^+ was gradually produced.

2) N-H Bond Effect on $\text{TMG}/\text{BF}_3/\text{BCl}_3$ System

a. NMR Patterns of the $\text{TMG}/\text{BF}_3/\text{BCl}_3$ System and $(\text{TMG})_2\text{BF}_2^+$

In the ^{19}F NMR spectrum of a fully quenched TMG/BF₃/BCl₃ system, only (TMG).BF₃ and (TMG)₂BF₂⁺ give rise to quartets. Two other unidentified broad peaks are located at $\delta = -143$ ppm and $\delta = -170$ ppm, which are shown in Figure 21. The mixed (TMG).BF_nCl_{3-n} species have been observed in partially quenched systems with poorer resolution in ^{19}F NMR spectrum. The ^{19}F and ^{11}B NMR parameters of all species present are listed in Table 19.

(TMG)₂BF₂⁺ was identified by comparing its coupling constant in both ^{19}F and ^{11}B (1:2:1) spectra, and confirmed by FABMS where it was found to have m/z at 279.

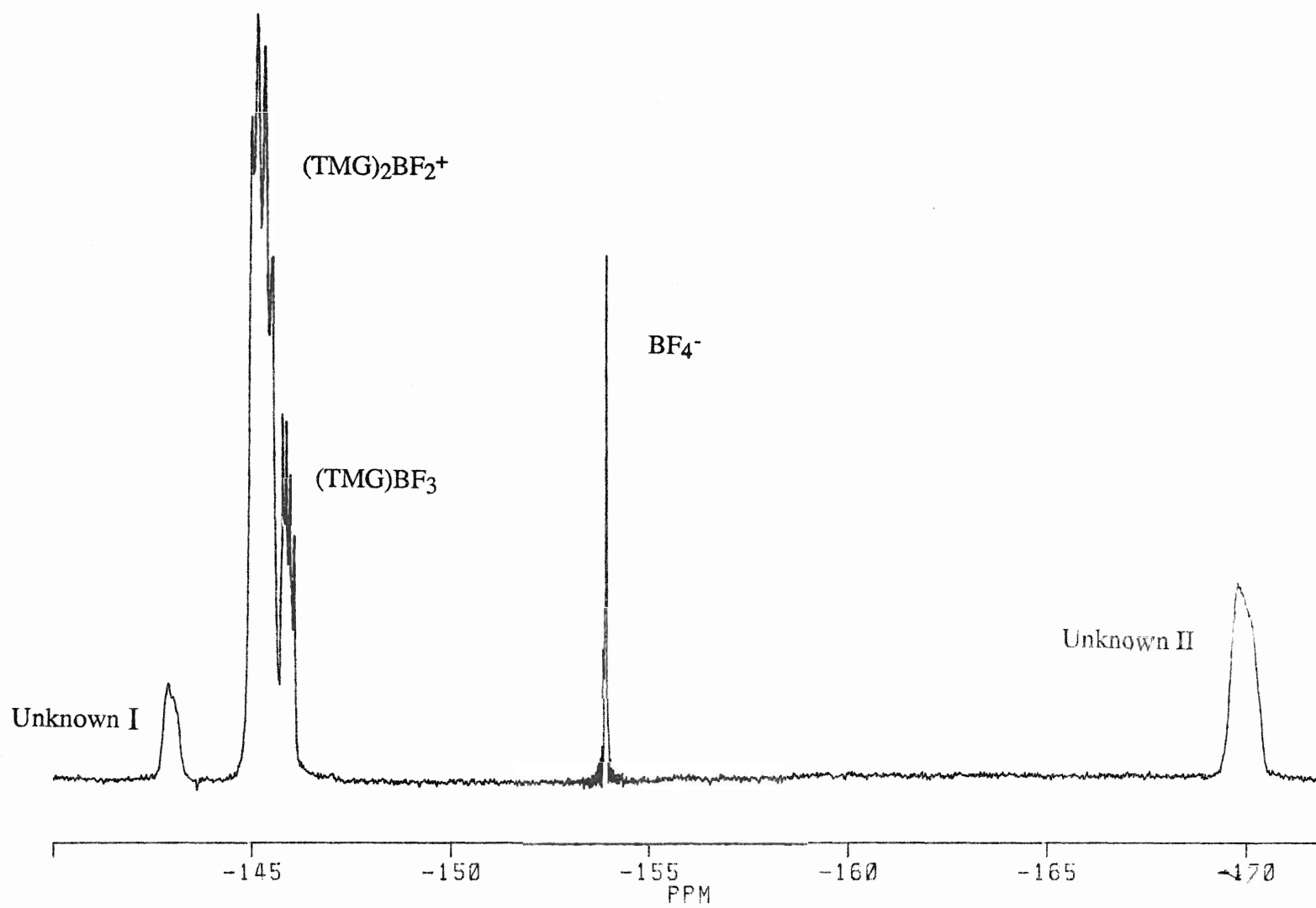
b. N-H bond effect

TMG has almost the same strength as a base, as do DBU and DBN, as well as very small steric hindrance. Its resonance structure, N=C(N)₂, can be thought of as being analogous to these amidine bases, but their NMR patterns in the D/BF₃/BCl₃ systems (D: TMG, DBU or DBN) are quite different. The main reason for this is that TMG has a N-H bond. When mixed (TMG).BF_nCl_{3-n} species are formed, not only can chloride be replaced by the second portion of entering base to form

TABLE 19
 ^{19}F AND ^{11}B PARAMETERS OF TMG/BF₃/BCl₃ SYSTEM

SPECIES	CHEM. SHIFT		$J^{11}\text{B}-^{19}\text{F}$ /Hz
	^{19}F /ppm	^{11}B /ppm	
(TMG).BF ₃	-145.8	-0.8	17.5
(TMG) ₂ BF ₂ ⁺	-145.2	-0.3	31.5
(TMG).BF ₂ Cl	-129.2	-	-
(TMG).BFCl ₂	-116.7	-	-
Unknown I	-143.0	-	-
Unknown II	-169.8	-	-

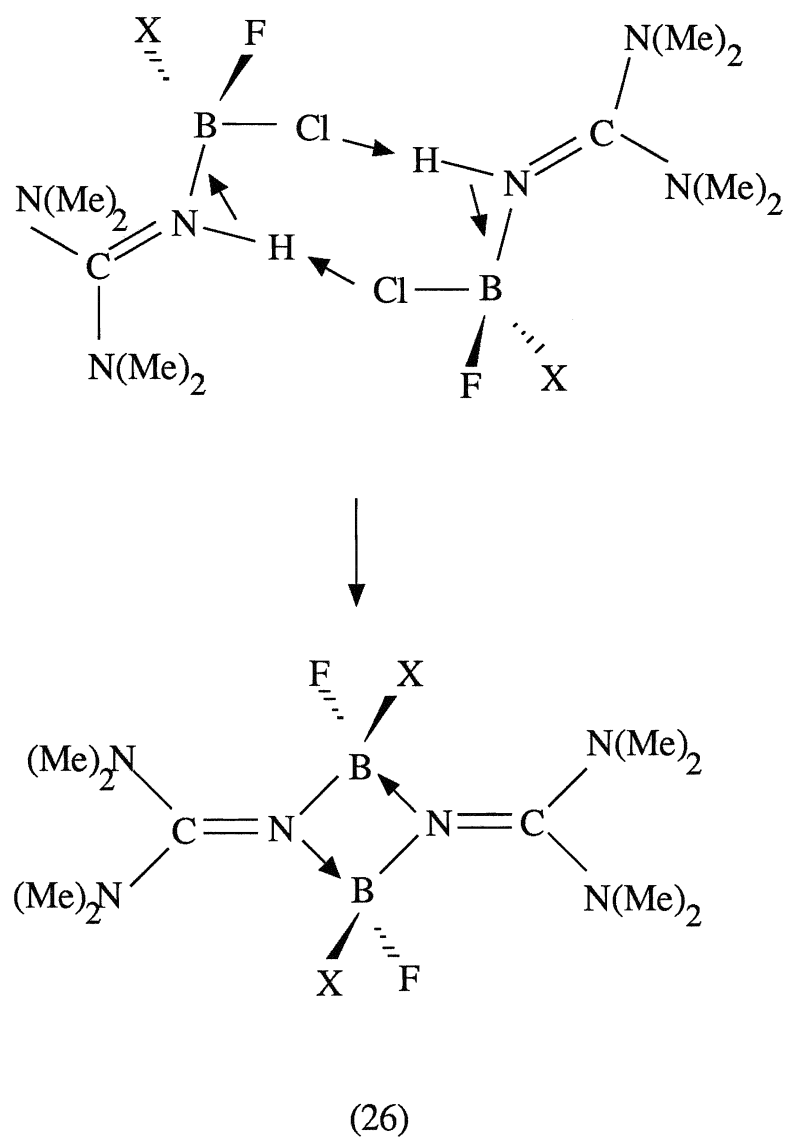
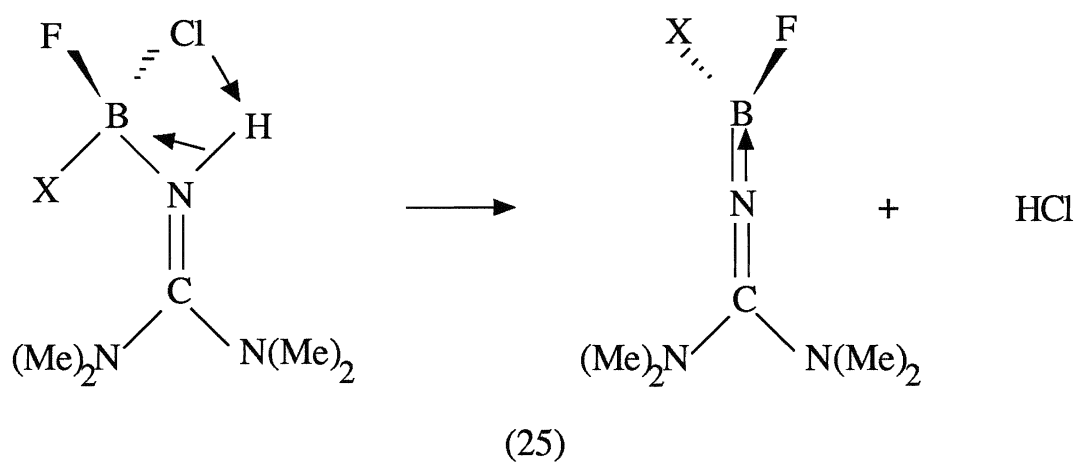
FIGURE 21
 ^{19}F NMR SPECTRUM OF THE TMG/ BF_3/BCl_3 SYSTEM



the fluoroboron cation, but HCl can also be lost by an intramolecular interaction or intermolecular interaction, due to the weak N-H bond being easily broken when B-Cl bond containing compounds are present^{<5>}. Which interaction is more favourable has not yet been proven. Possible reactions and the assignment of the ^{19}F NMR signals are proposed. If the reaction proceeded according to Equation 25, the products would be two tricoordinated boron compounds. If the reaction went according to Equation 26, we should obtain three signals, because when X is Cl, with two possible isomers, it can cause two ^{19}F NMR signals. Since only two unknown signals were observed in the ^{19}F NMR spectra, the former reaction seems more possible. However, the very broad peaks for these two signals indicate a very slow motion for the molecules, which seems to fix the model of the dimers which have much greater size than the monomers, according to the quadruple relaxation mechanism. More possibly, since the Cl-B bond can not be stable in this system, the two signals in the ^{19}F NMR spectra are for one monomer and for one dimer, respectively, with X as F. The signal at higher field might be that of the dimer, due to the lower resolution. The ^{11}B NMR spectra in 60.4 MHz operating frequency did not clarify the situation.

All species decomposed in water immediately. Free fluoride gives the most significant peak in the ^{19}F NMR spectrum at $\delta = -119$ ppm with a percentage of more than 83%, which is different than the DBU and the DBN containing systems. This means that all B-F bonds in various TMG containing fluoroboron compounds are easier to cleave.

The fully explanation for the behaviour of the TMG/ BF_3/BCl_3 system depends on the availability of the related pentaalkylguanidine when applied to the D/ BF_3/BCl_3 system.



CHAPTER VI

 ^{19}F CHEMICAL SHIFT OF D.BF_3 AND D_2BF_2^+ FORMED FROM
 $\text{N}=\text{C}-(\text{X})_2$ ($\text{X}=\text{N},\text{S}$) AND $\text{N}=\text{CR}-\text{X}$ ($\text{X}=\text{N},\text{O},\text{S}$) CONTAINING BASES

A. Introduction

In the former chapters, we have studied the singly charged and doubly charged fluoroboron cations formed from $\text{N}=\text{CR}-\text{N}$ and $\text{N}=\text{C}(\text{N})_2$ containing bases, based on the classical donor-acceptor theory. Many experimental observations and results have been satisfactorily explained by means of this theory. However, it was found that explaining the relationship between the ^{19}F NMR chemical shift and the ligands' properties for these compounds, just according to the base strength and the steric factors which contributed to the shielding effect of the ^{19}F nucleus, was not sufficient, although effects based on the properties of bases are important.

In this chapter, some other factors will be considered, in order to build a more complete model with which to search for the possible relationship between the ^{19}F chemical shifts and the ligands' properties. The tetrahedral boron trihalide adduct (D.BF_3) and the difluoroboron cation (D_2BF_2^+) were chosen for this study, because both of these types of compounds have an sp^3 hybridized boron atom and $\text{N}-\text{B}-\text{F}$ as the basic functional group. D_3BF_2^+ has the same properties, but the steric effect is too exaggerated.

As is well known, a chemical shift is due to a shielding difference between two nuclei of the same species in different environments. Normally, ligand electron-donating ability was thought to influence the chemical shifts of the related nuclei, whether they be transition metals or main group elements. But atoms that do not have d orbitals, yet have the same hybridized orbitals such as all sp^3 or all sp^2 , will simplify the effect of the electronic configuration and the molecular geometry.

For considered model compounds, an analysis of all of the data which has been collected up to the present shows that the ^{19}F chemical shifts are greatly affected by the properties of ligands. For the same type of ligand, the one which is the stronger base and which exhibits smaller steric hindrance has the better electron-donating ability. It causes the ^{19}F chemical shift to move toward the higher magnetic field, due to the greater shielding effect of the fluorine nucleus. But for different types of ligands, ^{19}F chemical shifts depend on the basicity and the steric effect to a lesser extent, and greatly depend on the structure of the ligands. For instance, the ^{19}F chemical shift of $(\text{amidine})_2\text{BF}_2^+$ is to lower field than that of $(\text{amine})_2\text{BF}_2^+$ and similar to $(\text{pyridine})_2\text{BF}_2^+$. On the other hand, most D.BF_3 or D_2BF_2^+ species with a ligand having the $\text{N}=\text{C}-\text{N}$ structure are found in a small range ($-144 \text{ ppm} \sim -150 \text{ ppm}$ for D.BF_3). These values include some unpublished data^{<50>} which is listed in Table 20.

TABLE 20
 ^{19}F CHEMICAL SHIFT OF SOME $\text{N}=\text{C}-\text{X}$ ($\text{X}=\text{N}, \text{C}$)
 -CONTAINING D.BF_3 AND D_2BF_2^+

LIGAND	DBF_3	D_2BF_2^+
$\text{MeC}(\text{NMe}_2)=\text{NMe}$	-146.9	-144.0
$\text{PhC}(\text{NMe}_2)=\text{NMe}$	-147.6	-145.4

In order to expand the range of the observations, some $\text{N}=\text{CR}-\text{X}$ ($\text{X} = \text{O}$ or S) containing compounds were chosen as bases, including 2-methyl-2-oxazoline, 2-ethyl-2-oxazoline ($\text{N}=\text{CR}-\text{O}$), 2-methyl-2-thiazoline ($\text{N}=\text{CR}-\text{S}$) and 2-methyl(thio)-2-thiazoline [$(\text{N}=\text{C}-(\text{S})_2)$], to be studied in $\text{D/BF}_3/\text{Cl}_3$ system.

Few studies in coordination chemistry have been reported in which these bases are considered as ligands. A similar compound has been reported as a bridging ligand in a multinuclear cluster^{<127>}. Since the time in which to conduct

experimental work for this thesis was limited, we could not go into many details about the investigation of fluoroboron cations formed with these ligands.

B. Results

Trifluoroboron adducts and difluoroboron cations of these oxazolines and thiazolines have been formed by the same methods as were used for the amidine containing compounds. The ^{19}F and ^{11}B NMR parameters of these compounds and related mixed fluorochloroboron adducts are listed in Tables 21 and 22.

TABLE 21
 ^{19}F CHEMICAL SHIFTS OF THE SPECIES IN
 $\text{N}=\text{C}-\text{X}$ ($\text{X}=\text{O}, \text{S}$) CONTAINING $\text{D}/\text{BF}_3/\text{BCl}_3$ SYSTEMS

D	D.BF ₃	D ₂ BF ₂ ⁺	D.BF ₂ Cl	D.BFCl ₂
MOZ	-149.5	-151.9	-130.7	-122.8
EOZ	-149.1	-151.2	-130.3	-122.5
MTZ	-147.0	-145.9	-128.2	-118.9
MTTZ	-147.1	-145.3	-127.1	-117.1

TABLE 22
 COUPLING CONSTANT, $J^{19\text{F}-11\text{B}}$, OF THE SPECIES IN
 $\text{N}=\text{C}-\text{X}$ ($\text{X}=\text{O}, \text{S}$) CONTAINING $\text{D}/\text{BF}_3/\text{BCl}_3$ SYSTEM

D	D.BF ₃	D ₂ BF ₂ ⁺	D.BF ₂ Cl	D.BFCl ₂
MOZ	11.0	25.8	37.9	63.3
EOZ	11.3	26.3	37.9	63.0
MTZ	12.7	29.8	39.5	65.1
MTTZ	13.8	30.4	40.0	65.9

In the typical ^{19}F NMR spectra of the $\text{MOZ}/\text{BF}_3/\text{BCl}_3$ system (which are shown in Figure 22), $(\text{MOZ})\cdot\text{BF}_n\text{Cl}_{3-n}$ and $(\text{MOZ})_2\text{BF}_2^+$ species were present, but no $\text{BF}_n\text{Cl}_{4-n}^-$ species were found. All of signals show high resolution. EOZ and MTZ containing systems show similar ^{19}F NMR patterns as in the $\text{MOZ}/\text{BF}_3/\text{BCl}_3$ system, but the $\text{MTTZ}/\text{BF}_3/\text{BCl}_3$ system gave a little different ^{19}F NMR pattern (Figure 23). In Figure 23, as well as $(\text{MTTZ})\cdot\text{BF}_n\text{Cl}_{3-n}$ and $(\text{MTTZ})_2\text{BF}_2^+$ species, BFCl_3^- and BF_2Cl_2^- species were observed in ^{19}F NMR spectrum, although these species seem not to be as favourable as in the $\text{DBU}/\text{BF}_3/\text{BCl}_3$ and $\text{DBN}/\text{BF}_3/\text{BCl}_3$ systems. All of $\text{D}\cdot\text{BF}_3$ ($\text{D} = \text{MOZ}, \text{EOZ}, \text{MTZ}$ and MTTZ) are located at $\delta = -147 \sim -149$ ppm, and D_2BF_2^+ have the a little different δ locations, depending on D being oxazolines or thiazolines, in the ^{19}F NMR spectra. Multiplets in the ^{11}B NMR spectra always overlapped each other at the 60.4 MHz operating frequency.

Both thiazolines and oxazolines have a similar reactivity, and all of them have a less reactivity than DBU and DBN in the $\text{D}/\text{BF}_3/\text{BCl}_3$ systems. Both oxazolines and thiazolines can replace chloride in $\text{D}\cdot\text{BF}_2\text{Cl}$ to form D_2BF_2^+ , but the reaction is slow. D_3BF_2^+ has not been observed from these systems yet.

C. Discussion

Comparing ^{19}F chemical shift data for all of the $\text{C}=\text{N}$ containing $\text{D}\cdot\text{BF}_3$ adducts, it is found that the values are close, from $(3,5\text{-Me}_2\text{Py})\cdot\text{BF}_3$, at $\delta = -152.2$ ppm, to $(\text{DBU})\cdot\text{BF}_3$, at $\delta = -144.3$ ppm; all are at lower field than $(\text{amine})\text{BF}_3$. As is known, the major anisotropic effects in organic molecules are associated with π -electrons reacting with the applied field, particularly the π -electrons of the carbon-carbon and the carbon-oxygen bonds, such as ^1H being very deshielded in compounds $\text{H}-\text{C}(\text{R})=\text{O}$. In the considered systems, with the core structure $\text{F}-\text{B}-\text{N}=\text{C}-\text{X}$, although the fluorine atom does not directly bond to the π system, the anisotropy effect on the ^{19}F shift is still present, due to the anisotropy effect not

FIGURE 22
 ^{19}F NMR SPECTRA OF THE $\text{MOZ}/\text{BF}_3/\text{BCl}_3$ SYSTEM

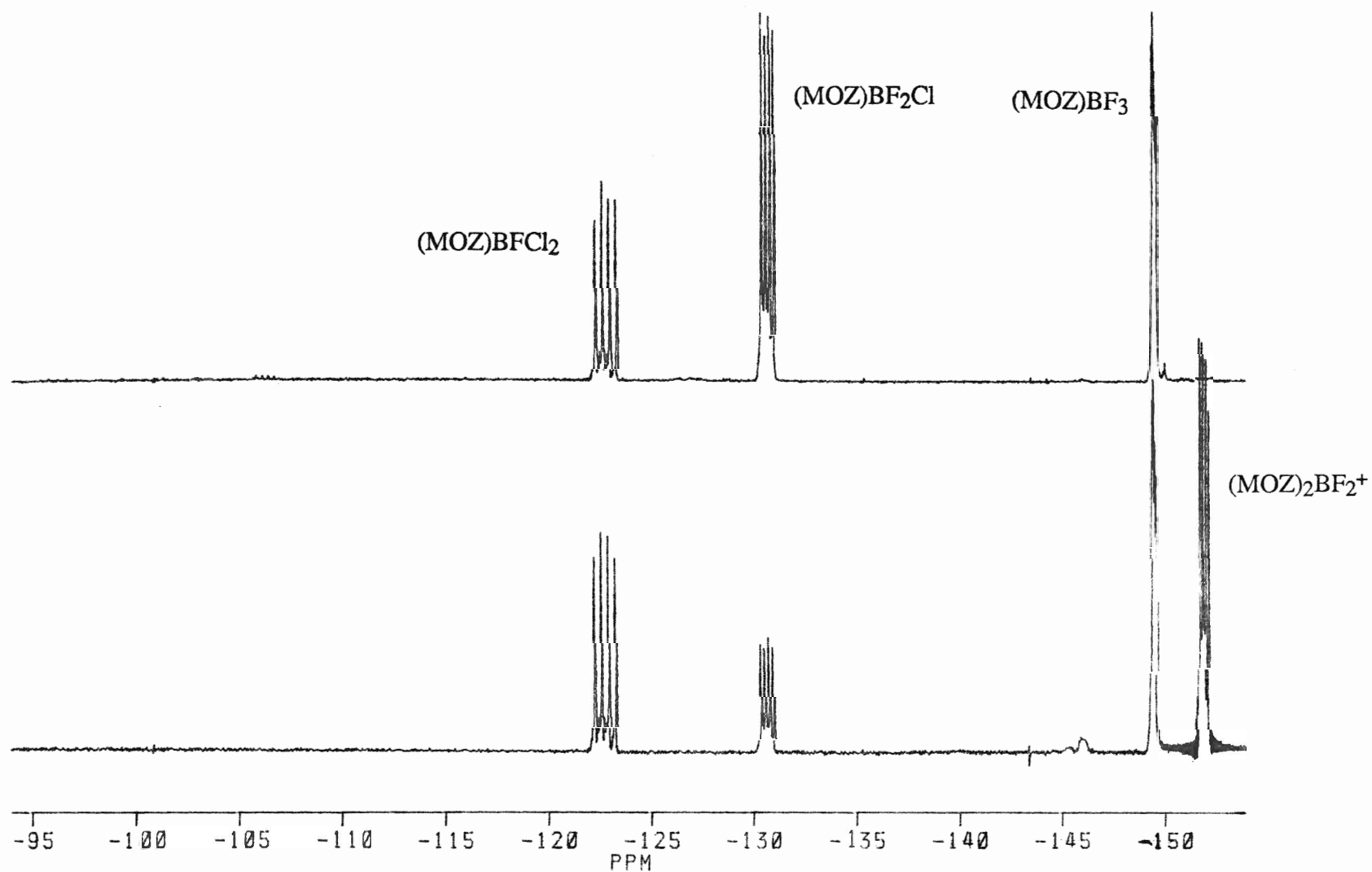
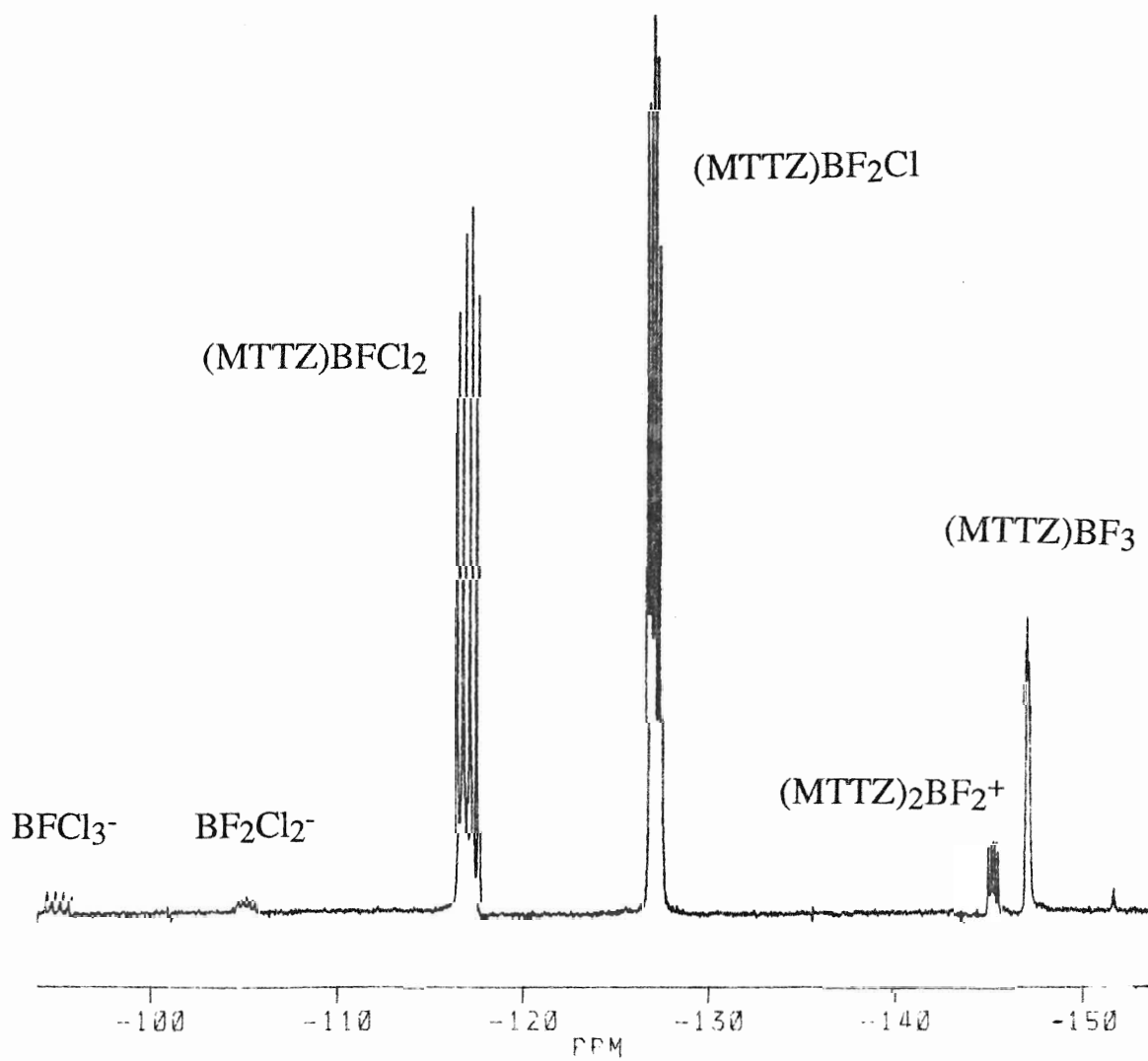
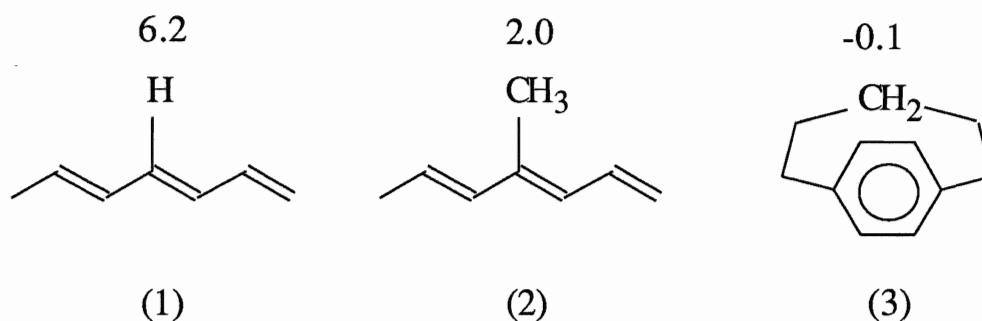


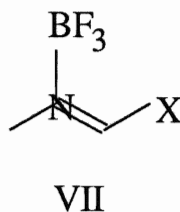
FIGURE 23
 ^{19}F NMR SPECTRUM OF THE MTTZ/ BF_3/BCl_3 SYSTEM



being dependent on the direct bonding^{<102>}. But the question is that π -electron systems do not always produce the deshielding effect. For a nucleus, in a certain region, the shift is to lower field, and in another region, the shift is to higher field. A known sequence for ^1H shifts is as follows:



The situation in our present system (Structure VII) seems more like Compound (2), than (1) or (3). The paramagnetic [equivalent to deshielding, as in (1)] factor has a more favorable effect than that of the diamagnetic [equivalent to shielding, as in (3)] factors on VII. Although the ^1H shift of the protons on the terminal methyl group in Compound (2) show only a small change to downfield due to neighbouring anisotropic effects, these effects might be significant for ^{19}F shifts of Structure VII containing compounds, due to the higher sensitivity of ^{19}F shift, relative to the ^1H shift to the chemical surrounding of respective nuclei.



CHAPTER VII

MIXED-LIGAND DIFLUOROBORON CATIONS

A. Introduction

This chapter is based on the study of the boron trihalide adducts and the homo-ligand fluoroboron cations from the last four chapters. Mixed-ligand difluoroboron cations do not show any big differences from homo-ligand difluoroboron cations, but by writing separate chapters for each, the presentation of this thesis can be made better. The ligand substitution reaction of difluoroboron cations is a new procedure.

B. Results

1) DD'BF₂⁺ Formed From D.BF₂Cl

Most of the DD'BF₂⁺ cations in this work were prepared by the same method that was used in the preparation of D₂BF₂⁺, that is, by D' replacing Cl⁻ in the mixed boron trihalide adducts, D.BF₂Cl (which are listed in Table 23).

As a typical example, (DBU)(quinuclidine)BF₂⁺ formation was monitored by ¹⁹F NMR as is shown in Figure 24. For the DBU/BF₃/BCl₃ system in a 2:1:1 molar ratio (DBU: 0.2 mmol), all ion species and neutral adduct species are present as usual. When 0.02 mmol to 0.10 mmol of quinuclidine was introduced as the second entering group into this system, anions and neutral adducts reacted with quinuclidine easily. The absolute intensity of bis(DBU)difluoroboron cation also dropped down, as referred to the internal C₆F₆ standard. The formation process of (DBU)(Q)BF₂⁺ is shown in Figure 25. This replacement reaction took place almost quantitatively. Similar trends were also obtained from the DBN/BF₃/BCl₃/DBU system (see Chapter IV) and the DBN/BF₃/BCl₃/Q system.

FIGURE 24
QUINUCLIDINE TITRATION OF (DBU)BF₃/BCl₃
IN 0.1 mmol:0.1 mmol MONITORED BY ¹⁹F NMR

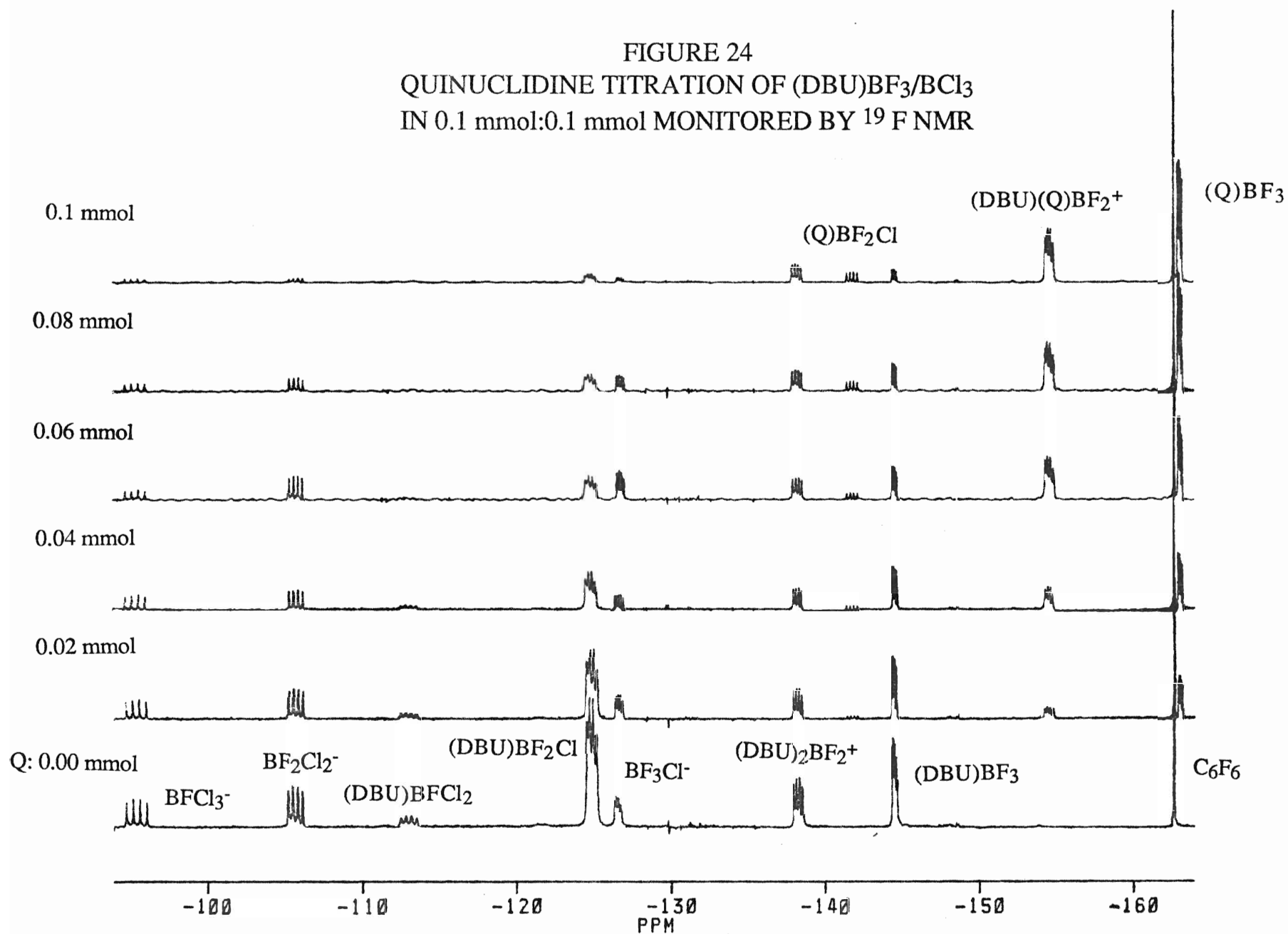


FIGURE 25
FORMATION OF (DBU)(QUINUCLIDINE)BF₂⁺ FROM
(DBU)BF₃ / BCl₃ BY ADDING QUINUCLIDINE

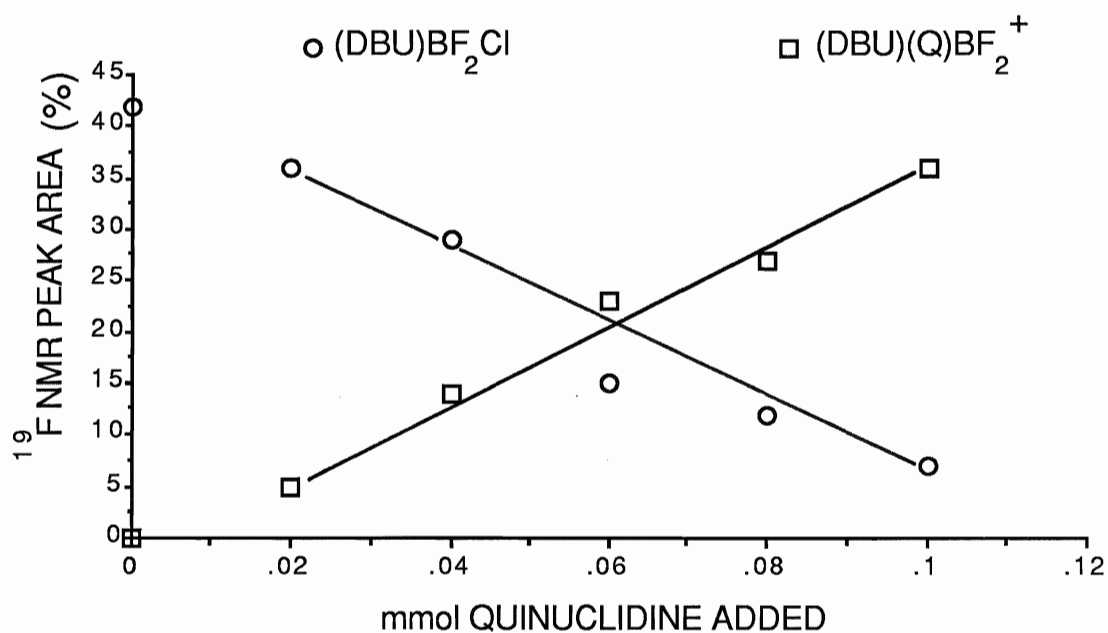


TABLE 23
 ^{19}F AND ^{11}B NMR PARAMETERS OF
 MIXED-LIGAND DIFLUOROBORON CATIONS

CATIONS	CHEM. SHIFT		$J^{11}\text{B}-^{19}\text{F}$ /Hz
	$^{19}\text{F}/\text{ppm}$	$^{11}\text{B}/\text{ppm}$	
(DBU)(DBN) BF_2^+	-143.9	0.9	32.8
(DBU)(Q) BF_2^+	-154.6	1.2	31.3
(DBU)(MOZ) BF_2^+	-145.3	-	25.9
(DBU)(EOZ) BF_2^+	-144.9	-	24.7
(DBN)(Q) BF_2^+	-158.6	1.5	30.8
(DBN)(MOZ) BF_2^+	-150.4	-	25.5
(DBN)(EOZ) BF_2^+	-149.8	-	24.0
(MTZ)(MOZ) BF_2^+	-149.1	-	27.5
(MTZ)(EOZ) BF_2^+	-148.5	-	28.2

However, this reaction does not always occur with every donor, D'. Neither concentrated nor diluted pyridine and methyl-substituted pyridines could form $\text{PyD}'\text{BF}_2^+$ with (DBU). BF_2Cl or (DBN). BF_2Cl . For quantitative work, DBU/ $\text{BF}_3/\text{BCl}_3/\text{Py}$ in the 2:1:1:X system (X: 0-1), $(\text{Py})\text{BF}_3$ is more favourable than any of the others. The change in the proportion of peak areas in the ^{19}F NMR spectra with increasing amount of pyridine is listed in Table 24.

Oxazolines and thiazolines did not replace Cl^- from (DBN) BF_2Cl , but DBN and DBU can replace Cl^- from (Oxazoline) BF_2Cl and (Thiazoline) BF_2Cl to give mixed-ligand difluoroboron cations.

TABLE 24
 PYRIDINE TITRATION OF DBU/BF₃/BCl₃ SYSTEM
 MONITORED BY ¹⁹F NMR AND SHOWN IN PEAK AREAS
 [DBU:BF₃:BCl₃ = 0.2 mmol : 0.1 mmol : 0.1 mmol]

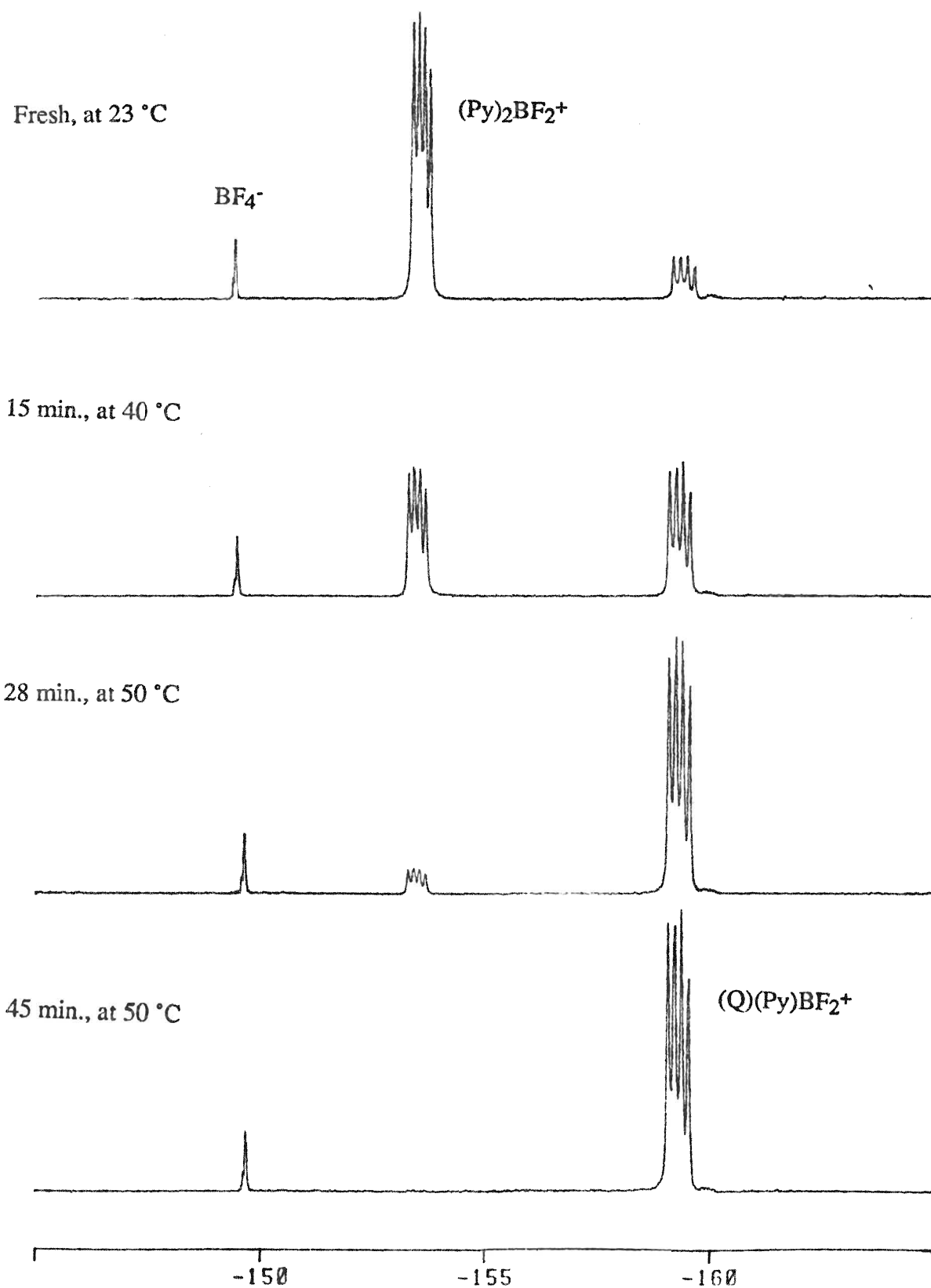
Species	<u>Pyridine in mmol</u>					
	0	0.02	0.04	0.06	0.08	0.10
BFCl ₃ ⁻	8	8	7	4	3	1
BF ₂ Cl ₂ ⁻	14	14	11	6	3	1
BF ₃ Cl ⁻	8	11	8	4	2	2
(DBU).BFCl ₂	7	4	4	3	3	4
(DBU).BF ₂ Cl	40	30	26	22	17	13
(DBU).BF ₃	13	14	13	10	8	9
(DBU) ₂ BFCl ⁺	2	1	0	0	0	0
(DBU) ₂ BF ₂ ⁺	9	8	7	7	6	5
Py.BF ₂ Cl	0	2	3	5	6	7
Py.BF ₃	0	8	21	37	48	58

2) DD'BF₂⁺ Formed From D₂BF₂⁺

(Quinuclidine)(pyridine)BF₂⁺ was formed by a ligand replacing reaction starting with (Py)₂BF₂⁺PF₆⁻ and quinuclidine, and was also isolated as the first DD'BF₂⁺X⁻ type compound. The reaction process was monitored using ¹⁹F NMR and is shown in Figure 26. No further substitution was evident in this reaction. (FABMS data will be discussed in Chapter VIII). However, when starting with (Q)₂BF₂⁺ and 4-methylpyridine, no reaction occurred. DBN, and TMG could not replace quinuclidine in (Q)₂BF₂⁺, even under drastic conditions.

FIGURE 26
THE FORMATION OF (Q)(Py)BF₂⁺ FROM LIGAND SUBSTITUTION
REACTION IN ACETONE MONITORED BY ¹⁹F NMR

[Mole ratio of (Py)₂BF₂⁺PF₆⁻ / Q = 1: 5]



The much stronger Lewis bases DBN, DBU and TMG react with $(\text{Py})_2\text{BF}_2^+\text{PF}_6^-$ immediately and give a series of fluoroboron containing products in the solution phase, as well as some precipitate which is very air sensitive. Several quartets are present in the ^{19}F NMR spectra. By comparing the reaction taking place in acetone with the reaction taking place in nitromethane, D_2BF_2^+ ($\text{D} = \text{DBN}, \text{DBU}$ and TMG) was tentatively identified in these systems. Their ^{19}F - ^{11}B coupling constants are comparable to the known values measured in CDCl_3 . $(\text{DBN})_2\text{BF}_2^+$ was also confirmed by FABMS, which yielded a peak, m/z at 297. The reactivity of various donors with Py_2BF_2^+ is in the order of $\text{DBN} > \text{DBU} > \text{TMG} \gg \text{Quinuclidine}$.

C. Discussion

1) Basicity Effect on Cation Formation From DBF_2Cl

Since DBU and DBN have high electron delocalization capabilities, the positive charge on the boron atom can be greatly reduced and thus the B-Cl bond becomes very weak. The stronger Lewis base quinuclidine can easily replace Cl^- to form $(\text{Q})(\text{D})\text{BF}_2^+$, but the weaker Lewis base pyridine can not. As is known, quinuclidine has a very difficult time replacing chloride in $(\text{amine})\text{BF}_2\text{Cl}$, the B-Cl bond weakening in DBU and DBN-containing $\text{D.BF}_2\text{Cl}$ being evident. However, the B-Cl bond may not be weak enough for pyridine to attack. It is necessary to point out that the replacement of bromide by D' in $\text{D.BF}_2\text{Br}$ depends on the steric hindrance of the second entering ligand $\text{D}'^{<51>}$, which is not consistent with the previous case of chlorine replacement in $\text{D.BF}_2\text{Cl}$. This may be explained according to the difference in the bond strength between B-Cl and B-Br. Since the B-Br bond is much weaker than the B-Cl bond, breaking the B-Br bond is relatively easy. The base strength is not very important in the case of the B-Br bond, but the steric hindrance becomes significant. However, the B-Cl bond is relatively strong (even

weakened by DBU or DBN), and a stronger base is required to break B-Cl bond; thus the base strength becomes significant. The requirement of base strength in the second portion ligands is also proven by the unique procedure used to form (guanidine)(oxazolin)BF₂⁺ and (guanidine)(thiazoline)BF₂⁺. The DBU/pyridine/BF₃/BCl₃ system shows an unexpected result. When pyridine was added (from 0 to 0.04 mmol), BF_nCl_{4-n}⁻ species did not change much, which means that pyridine is less able to replace Cl in BF_nCl_{4-n}⁻ to form Py.BF_nCl_{3-n} than the strong Lewis bases. The most significant change in this system is the increase of Py.BF₃ and the decrease of (DBU).BF₂Cl. No direct and simple relationship between the different species was correlated. The redistribution reaction seems to occur at the same time as the replacement reaction.

2) Correlation between NMR parameters and ligand on DD'BF₂⁺

"Pairwise" interaction parameters have been successfully used to confirm the identity of haloboranes, tetrahaloborates and haloboron cations. In a simpler model, the ¹⁹F chemical shift and the ¹¹B-¹⁹F coupling constant of D₂BF₂⁺, DD'BF₂⁺ and D'₂BF₂⁺ can be correlated as a linear relationship when D and D' are the same type of compound. The Statview program in the Macintosh SE was used for this calculation. The exact linear correlation for (DBU)₂BF₂⁺, (DBU)(DBN)BF₂⁺ and (DBN)₂BF₂⁺ has been obtained and is shown in Figure 27. Both the correlation coefficient and R-squared are equal to 1.000. This linear relationship is also suitable for correlating the NMR parameters of amine and pyridine containing systems, respectively. Oxazoline and thiazoline mixed difluoroboron cations are also satisfied by the linear correlation to a large extent. The correlation coefficient and R-squared of some related species are listed in Table 24. However, this linear correlation is not suitable to the different type of compounds, such as amidine as D and amine as D', or amine as D and pyridine as D'. "Pairwise" interaction parameters are more useful in these situations^{<52>}. In

fact, even in these complicated situations, we can still find some indications of $\text{DD}'\text{BF}_2^+$, due to the ^{19}F chemical shift or the ^{11}B - ^{19}F coupling constant often being close to one parameter of D_2BF_2^+ or $\text{D}'_2\text{BF}_2^+$.

FIGURE 27
LINEAR CORRELATION OF ^{19}F CHEM. SHIFT WITH
 $J^{11}\text{B}$ - ^{19}F OF AMIDINE DIFLUOROBORON CATIONS

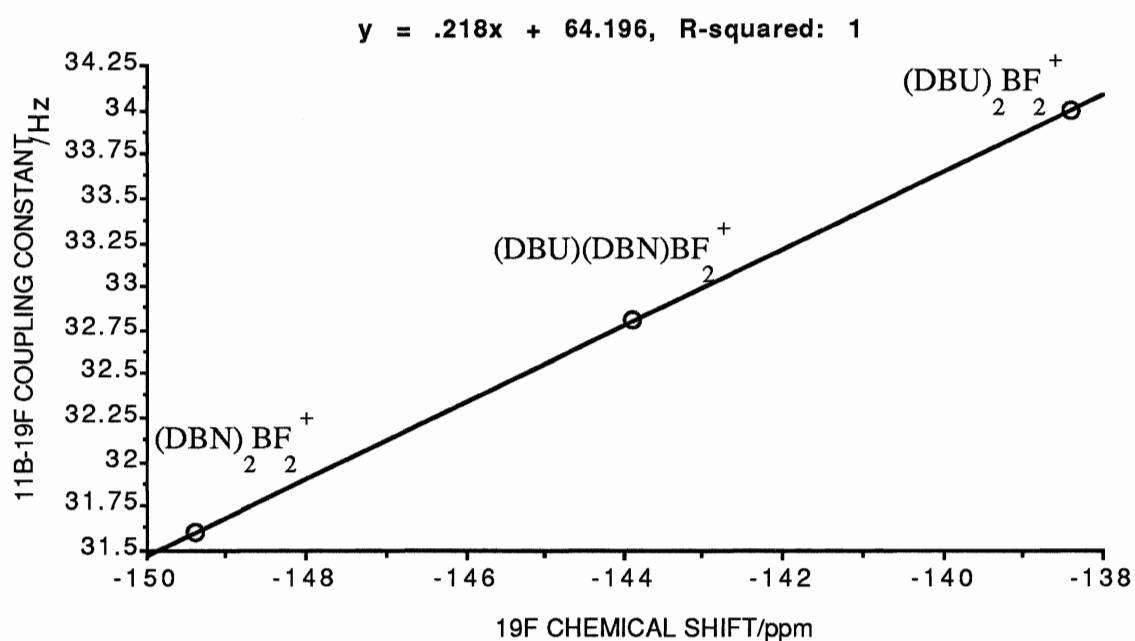


TABLE 24
THE LINEAR CORRELATION OF ^{19}F NMR CHEMICAL SHIFT AND
 $J^{19}\text{F}$ - ^{11}B OF D_2BF_2^+ , $\text{DD}'\text{BF}_2^+$ AND $\text{D}'_2\text{BF}_2^+$ (D: oxazoline and D': thiazoline)

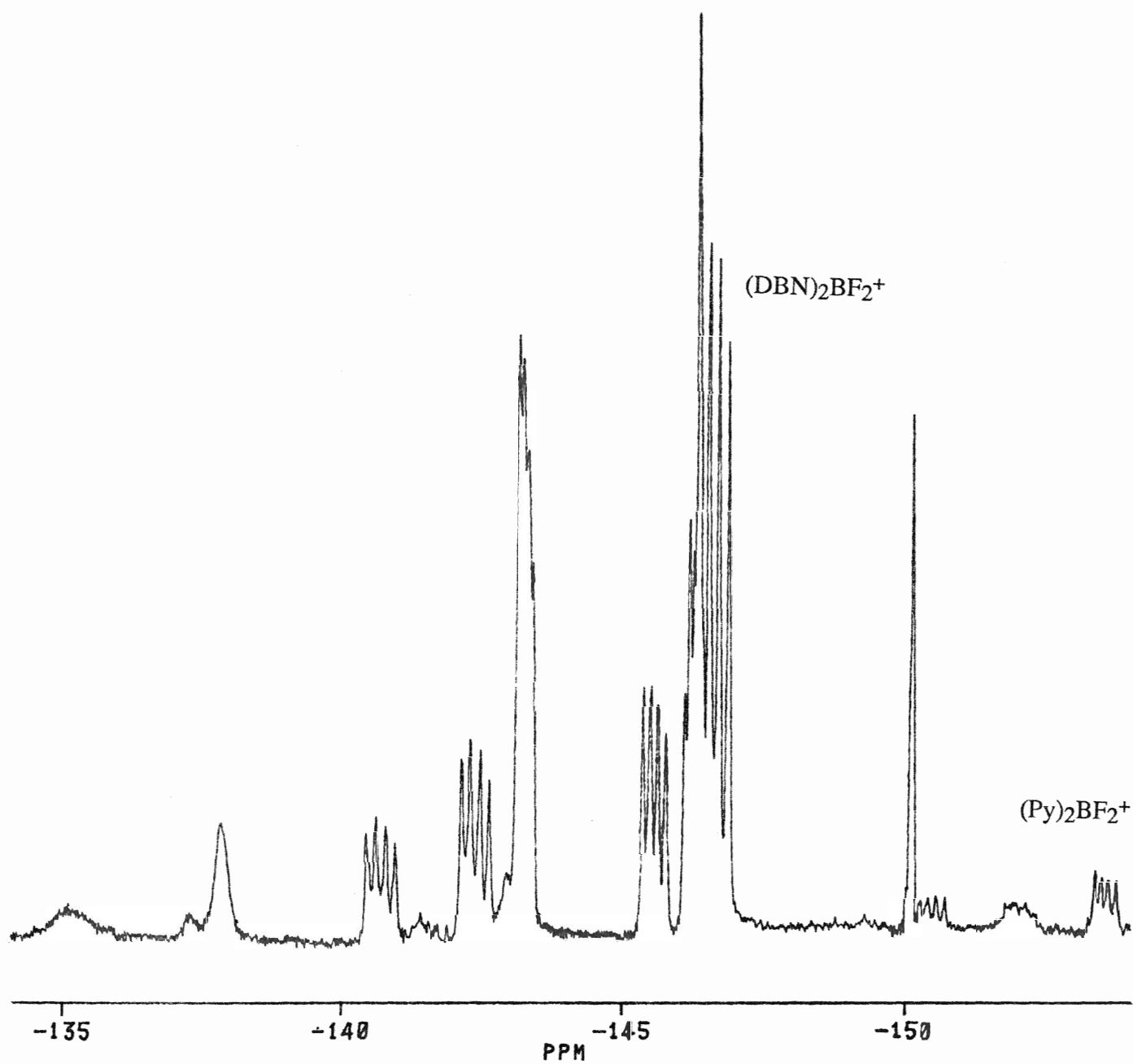
D	D'	CORRELATION	R-SQUARED
MOZ	MTZ	0.996	0.993
EOZ	MTZ	0.994	0.987

3) Effects on Ligand Substitution Reaction of Difluoroboron Cations

The ligand substitution reaction of fluoroboron cations is thermodynamically dependent. Quinuclidine reacts with Py_2BF_2^+ very slowly at room temperature and the reaction is certainly accelerated with increasing temperature.

The reactivity of Lewis bases with difluoroboron cations is strongly dependent on the base strength of both of the ligands in the difluoroboron cations and the entering ligands. The weak base did not replace the strong base in the difluoroboron cations. The strong base quinuclidine, can only replace one pyridine from $\text{Py}_2\text{BF}_2^+\text{PF}_6^-$, with no further substitution occurring. The reaction mechanism can be thought as a typical associative reaction. But much stronger bases such as DBU and DBN can replace two pyridines in Py_2BF_2^+ . The intermediate products, $(\text{DBU})(\text{Py})\text{BF}_2^+$ and $(\text{DBN})(\text{Py})\text{BF}_2^+$ might be also present. These very strong bases make the substitution reaction very complicated, due to the fact that the solvent taking part in the reaction, such as DBN reacting with $(\text{Py})_2\text{BF}_2^+\text{PF}_6^-$ in acetone as shown in Figure 28. Higher resolution quartets from higher field to lower field are: $\delta = -153.6$ ppm ($J = 23.3$ Hz), $\delta = -150.5$ ppm ($J = 27.6$ Hz), $\delta = -146.6$ ppm ($J = 31.5$), $\delta = -146.2$ ppm ($J = 15.2$ Hz), $\delta = -145.6$ ppm ($J = 25.0$ Hz), $\delta = -143.3$ ppm ($J = 14.1$ Hz), $\delta = -142.4$ ppm ($J = 31.1$ Hz) and $\delta = -140.7$ ppm ($J = 31.0$ Hz). These NMR patterns have not yet been fully identified.

FIGURE 28
THE COMPLICATED ^{19}F NMR PATTERN FORMED FROM
DBN ADDED TO $(\text{Py})_2\text{BF}_2^+\text{PF}_6^-$ IN ACETONE



CHAPTER VIII

FAST ATOM BOMBARDMENT MASS SPECTROMETRY

STUDIES OF FLUOROBORON CATIONS

A. General

Fast atom bombardment mass spectrometry (FABMS) was initially introduced into our research work as a secondary technique for confirming the presence of fluoroboron cations. In previous work^{<51,52>}, it was found that positive ion FABMS was a complementary technique to NMR for detecting the formation of fluoroboron cations, since it can be applied directly to the solution and is sensitive to the cations with almost negligible interference from the solvent and neutral adducts present.

In the present work, more information about fluoroboron cations has been obtained from the FAB spectra. The value of being able to apply FAB directly to the solution is proven by comparing the FAB spectrum of ions from the solution sample with the FAB spectrum of the solid sample in matrix.

D_3BF^{+2} type cations were detected in their ion cluster forms, $[(D_3BF^{+2})(X^-)]^+$, as well as the detection of the fluoroboron cations (+1). The stability of the fluoroboron cations in the gas phase and the fragmentation process of these cations will be discussed in this chapter.

The ligand substitution reaction of the difluoroboron cations in the gas-phase will be investigated in order to complement the similar reaction in the condensed-phase. The gas-phase ligand substitution reaction itself in the FAB-MS ion source is also an interesting topic to study.

B. Results and Discussion

1) Singly Charged Difluoroboron Cations

a. Mass Spectra

Whether for the solution sample or for the solid sample, 3-nitrobenzyl alcohol as matrix were always used to support and dissolve the sample. $(\text{DBU})_2\text{BF}_2^+$ (Figure 29), $(\text{DBN})_2\text{BF}_2^+$ and $(\text{TMG})_2\text{BF}_2^+$ (Appendix 6) have been detected in the mother solution which contains mixed boron trihalide adducts. The D_2BF_2^+ isotope pattern was present in the parent peak. The cluster $[(\text{D}_2\text{BF}_2^+)_2\text{X}^-]^+$ was not observed, even for the solid sample $[(\text{DBN})_2\text{BF}_2^+](\text{PF}_6^-)_2$ dissolved in NBA (Figure 30). DBF_2^+ as the major fragment peak is present, resulting from the loss of one donor molecule from the difluoroboron cations (Equation 27).



Most ligand mixed difluoroboron cations were directly obtained from the mother solution, except $(\text{Q})(\text{Py})\text{BF}_2^+$ which is in the form of the pure solid salt, $(\text{Q})(\text{Py})\text{BF}_2^+\text{PF}_6^-$ (Figure 31). As well as the parent peak of $\text{DD}'\text{BF}_2^+$, two fragment peaks, DBF_2^+ and $\text{D}'\text{BF}_2^+$, are always present with differing intensities.

DH^+ is another peak which is typically found in these systems. It is always higher in intensity in the complicated solution sample with excess donor present, than in the pure solid sample. (This is described in the section 4 in detail).

b. The Value of the Application of FAB to Complicated Solution Systems

The applications of FABMS directly to the complicated solution systems have been preliminarily explored in a recent study^{<52>}. However, in which extent, the FAB spectra of the solution systems being in agreement with the FAB spectra of the solid salts dissolved in NBA has not yet been fully established, due to the fact that few difluoroboron cation salts had been isolated at that time.

In this work, by comparing the FAB spectra of the solid salt, $[(\text{DBN})_2\text{BF}_2^+](\text{PF}_6^-)$, with the cation, $(\text{DBN})_2\text{BF}_2^+$ (which is in a mixture with neutral adducts in CDCl_3), it was found that the qualitative results agree well. Both

FIGURE 29
FAB SPECTRUM OF $(\text{DBU})_2\text{BF}_2^+$ IN SOLUTION

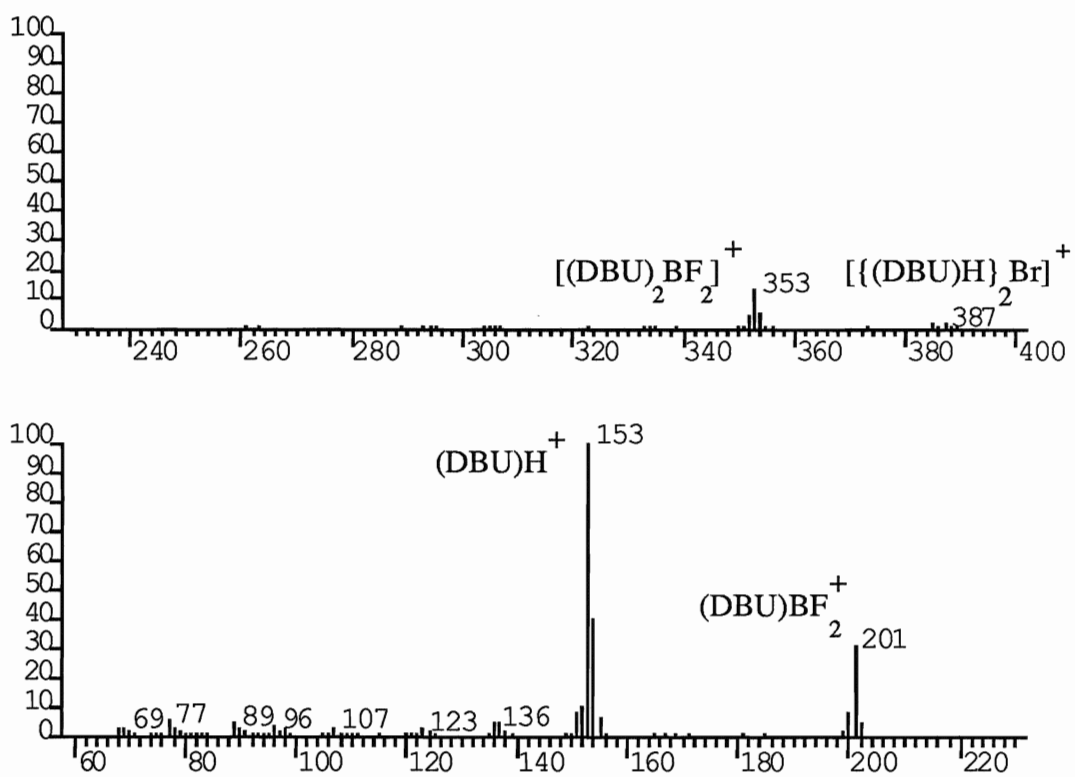


FIGURE 30
FAB SPECTRUM OF $[(\text{DBN})_2\text{BF}_2]^+(\text{PF}_6)^-$

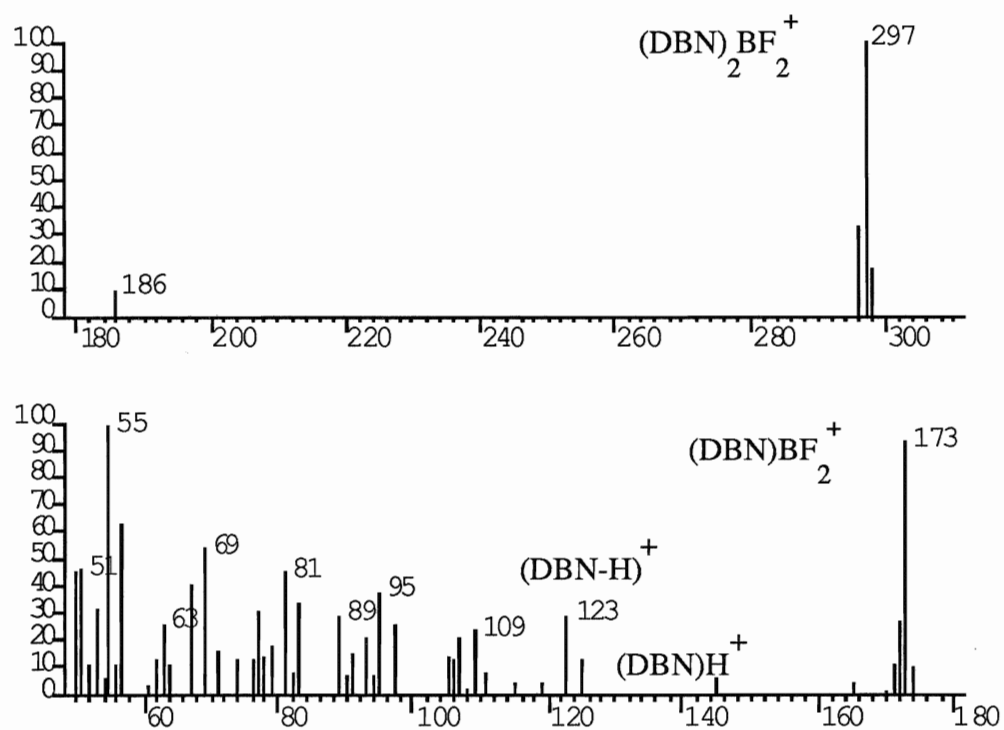
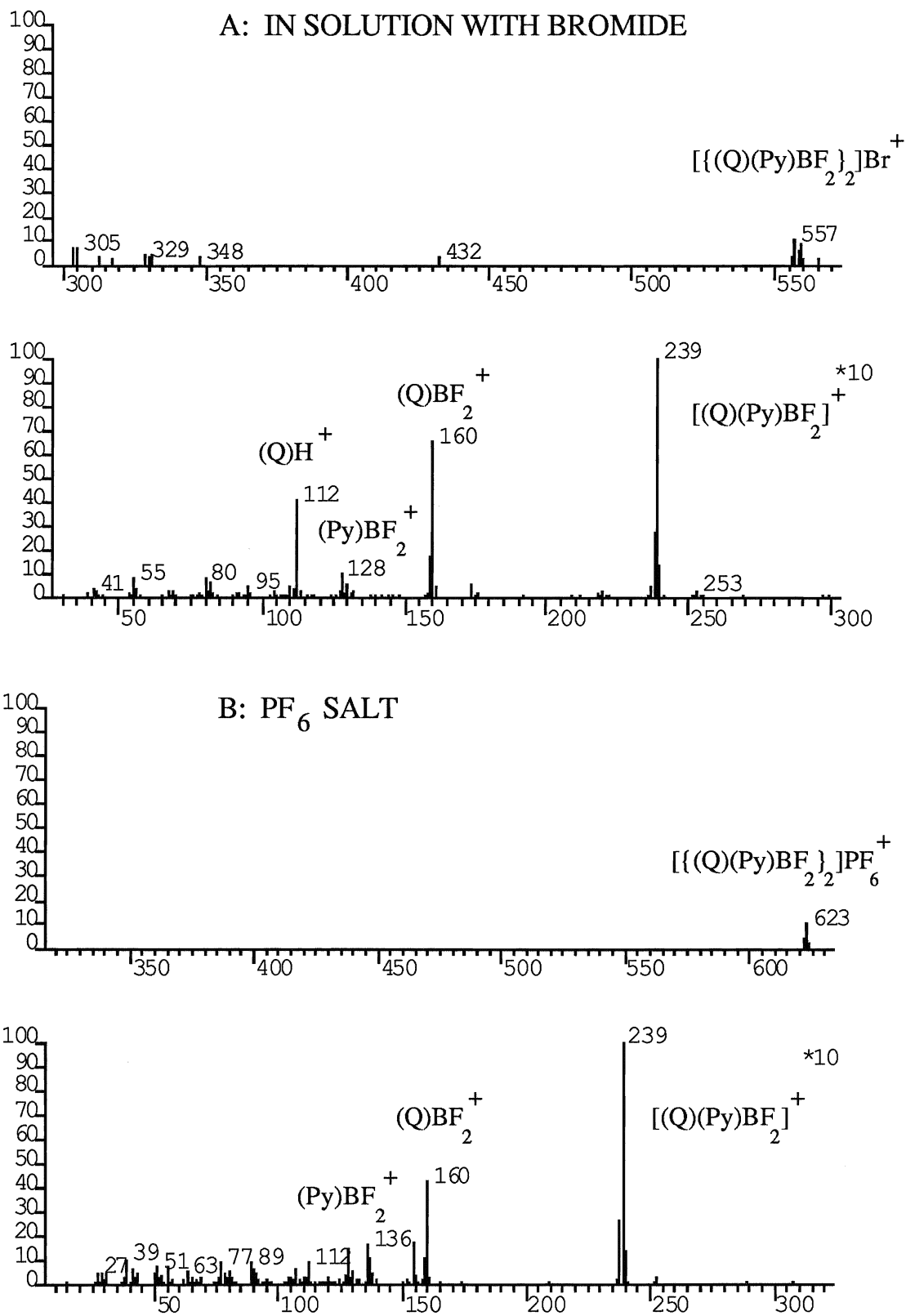
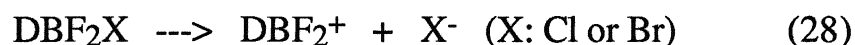


FIGURE 31
FAB SPECTRA OF (QUINUCLIDINE)(PYRIDINE)BF₂⁺
IN SOLUTION AND IN THE SOLID STATE



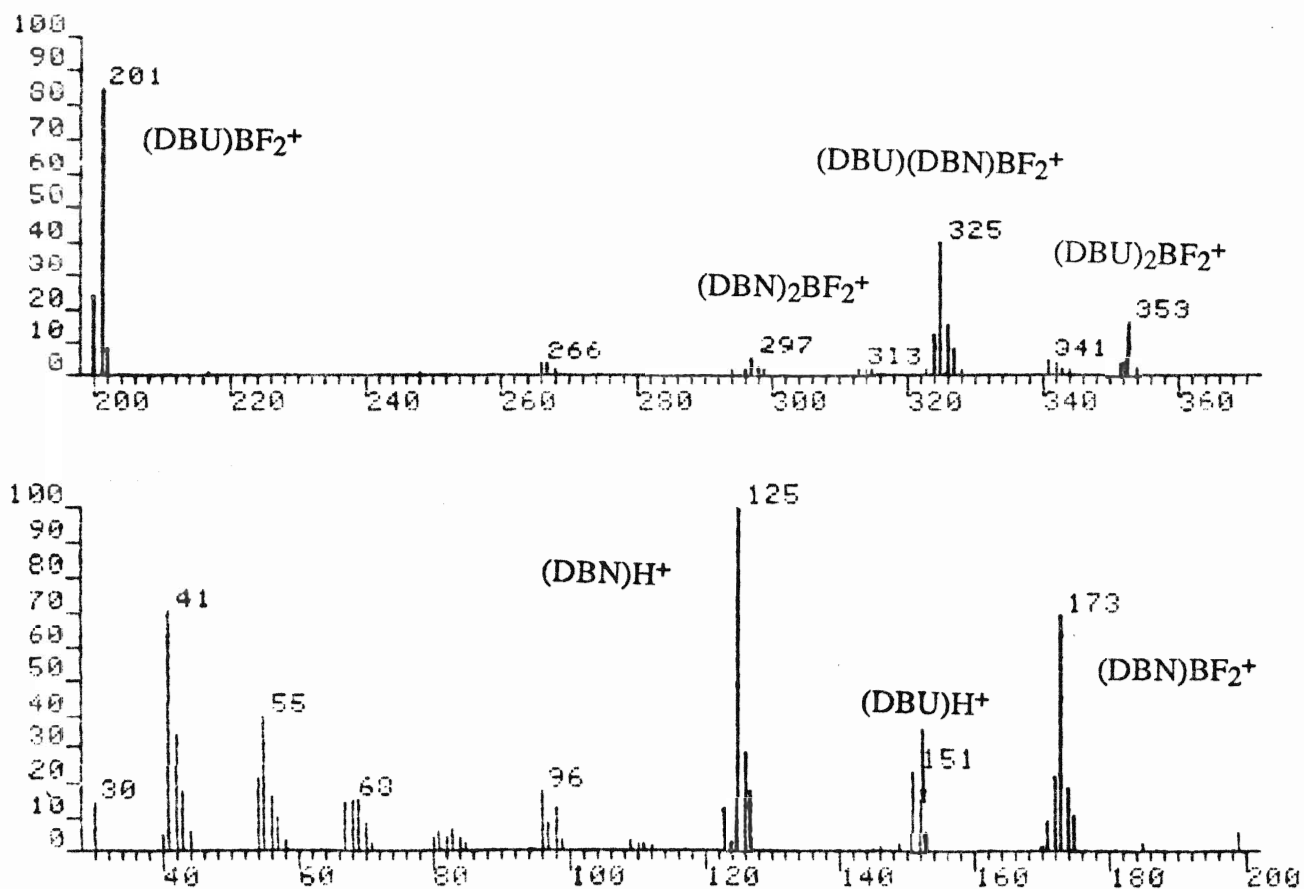
of them have the characteristic parent peak, $D_2BF_2^+$, the fragment peak, DBF_2^+ , and the protonated base peak, DH^+ . However, the quantitative results are not in agreement. The pure solid salt gives a much higher intensity for $D_2BF_2^+$, which indicates that the fragment peak, DBF_2^+ , does not just arise as a result of $D_2BF_2^+$ losing one ligand. Since DBX_2^+ could be generated from DBX_3 when X is Cl or Br, but not F in FABMS^{<52>}, the adduct DBF_2Cl is a possible source of the DBF_2^+ formed (Equation 28). This ionic cleavage of B-X is also consistent with earlier observations of $(Q)_2BF_2^+$ in both the solid state and in solution. In a series of FAB spectra from the DBU/ BF_3 / BCl_3 /Py system (Py: pyridine and some methyl substituted pyridines), ligand-mixed difluoroboron cations were not formed (based on NMR studies), but peaks, m/z at 201, $(DBU)BF_2^+$, were always present, which indicates the possible fragmentation of $(DBU).BF_2Cl$.



A clearer picture was obtained after the first mixed-ligand difluoroboron cation was isolated as the hexafluorophosphate salt, $[(\text{quinuclidine})(\text{pyridine})BF_2^+](PF_6^-)$. Comparing the FAB spectrum of this cation in solution with the spectrum of the solid state, we observed the very similar FABMS patterns. Both of the spectra give ion cluster peaks, $[(Q)(Py)BF]X^+$ (X is Br and PF_6^- , respectively), parent peaks, $(Q)(Py)BF_2^+$, and the fragment peaks, $(Q)BF_2^+$ and $(Py)BF_2^+$, in semiquantitative agreement. In both situations, the intensity of $(Q)BF_2^+$ is consistently higher than that of $(Py)BF_2^+$, which builds a "solid" base for studying the N-B bond strength of fluoroboron cations in the gas phase of the solution system. Although fragment peaks, DBF_2^+ , may arise as a result of the dissociation of $D.BF_2X$, $D_2BF_2^+$ seems to be nearly independent of the presence of the mixed boron trihalide adducts.

In the DBN/ BF_3 / BCl_3 /DBU system (see Figure 19 and Table 18), $(DBU)(DBN)BF_2^+$, $(DBU)_2BF_2^+$ and $(DBN)_2BF_2^+$ were observed in the FAB spectrum (Figure 32), as well as in the ^{19}F NMR spectrum. But the intensity of signals does not match the relative amounts, in the NMR spectrum.

FIGURE 32
FAB SPECTRUM of THE DBN/BF₃/BCl₃/DBU SYSTEM



(DBU)(DBN)BF₂⁺: (DBU)₂BF₂⁺ is 2.4 : 1 in the FAB spectrum and 10 : 1 in the NMR spectrum.

c. The Effect of Cation Size on the Formation of Ion Clusters

It was reported that the anion and cation sizes had some influence on the formation and the stability of larger clusters^{<128>}. The stronger ion-cluster intensity signals are directly related to the size of the cation. For group IB and IIB elements, the oligomeric species can always be observed in the positive ion FAB spectra and normally have the higher order^{<129>}. For difluoroboron cations, the cluster, [(DD'BF₂⁺)_n(X⁻)_{n-1}]⁺, has only been observed when n = 1 and 2. This phenomenon has been observed in previous work, but not followed up. Similarly, for (quinuclidine)(2-Etpyridine)BF₂⁺ and (quinuclidine)(4-Phpyridine)BF₂⁺, only n=1 was observed, but for (quinuclidine)(pyridine)BF₂⁺ and (quinuclidine)(picoline)BF₂⁺, n=2 was observed. Since the donor molecules used in this work are larger than the substituted pyridines, we could not observe the n=2 cluster, whether the anion was Cl⁻, Br⁻ or PF₆⁻, or whether the cation was in solution or in its solid salt. Of course, a more sensitive instrument may detect very small amount of ion clusters.

d. The Stability of N-B Bonds in a Gas Phase

For the DBN/BF₃/BCl₃/Q system (Appendix 7), (DBN)(Q)BF₂⁺ and (DBN)(Q)BFCI⁺ are identified as cations present in the ¹⁹F NMR spectrum. In the FAB spectrum, the parent peak at m/z 284 is (DBN)(Q)BF₂⁺. The intensity of (DBN)BF₂⁺ is 8.5 times greater than the intensity of (Q)BF₂⁺; normally, for (Q)(Py)BF₂⁺ (Py: pyridine or substituted pyridines)^{<52>}, the intensity of (Q)BF₂⁺ is higher than that of (Py)BF₂⁺, which is consistent with the ligand base strength. From the chemical structure of these ligands, the steric effect of ligands does not seem to be predominant, because the crowded space can weaken both N-B bonds in DD'BF₂⁺. Once difluoroboron cations are formed, the stability of the N-B bond

seems to only depend on the strength of the bonding. Obviously, the basicity of ligands plays an important role in the stability of the B-N bond in the nitrogen donor containing fluoroboron cations. The order of the basicity is DBN > quinuclidine > pyridine, and the relative intensities for DBF_2^+ are $(\text{DBN})\text{BF}_2^+ > (\text{Q})\text{BF}_2^+$ and $(\text{Q})\text{BF}_2^+ > (\text{Py})\text{BF}_2^+$.

2) Doubly Charged Fluoroboron Cations, D_3BF_2^+

a. Background

Multiply charged cations in transition metal complexes can normally be observed in FABMS spectra by formal reduction or by clustering with anions; sometimes several simultaneous processes are required^{<130>}. In some cases, a sequential loss of the ligand occurred accompanied by a change in the formal oxidation state of metals over a wide range^{<131>}. Doubly charged intact cations were observed directly in only a very few situations^{<132>}.

Since boron only has a +3 valent state in general, its high reduction potential prevents B^{3+} being reduced to a lower valence, which is different than the situation for transition metal ions. FABMS studies of doubly charged fluoroboron cations may give some interesting information about the bonding situation or about a reduction mechanism in the gas phase.

b. Mass Spectra

Tris(DBU) and tris(DBN)monofluoroboron hexafluorophosphate salts dissolved in NBA were studied by FABMS (Figures 33 and 34). Both of them show the identified ion cluster as parent peaks, and fragment peaks as listed in Table 26. The ion cluster peaks were not observed in solution sample when using FABMS, although some fragment peaks were the same as in the solid salts(Figure 35). For the solid salts, $[\text{D}_3\text{BF}_2^+](\text{PF}_6^-)_2$, the spectra within the range of the experimental

FIGURE 33
FAB SPECTRUM OF $[(\text{DBN})_3\text{BF}^{2+}](\text{PF}_6^-)_2$

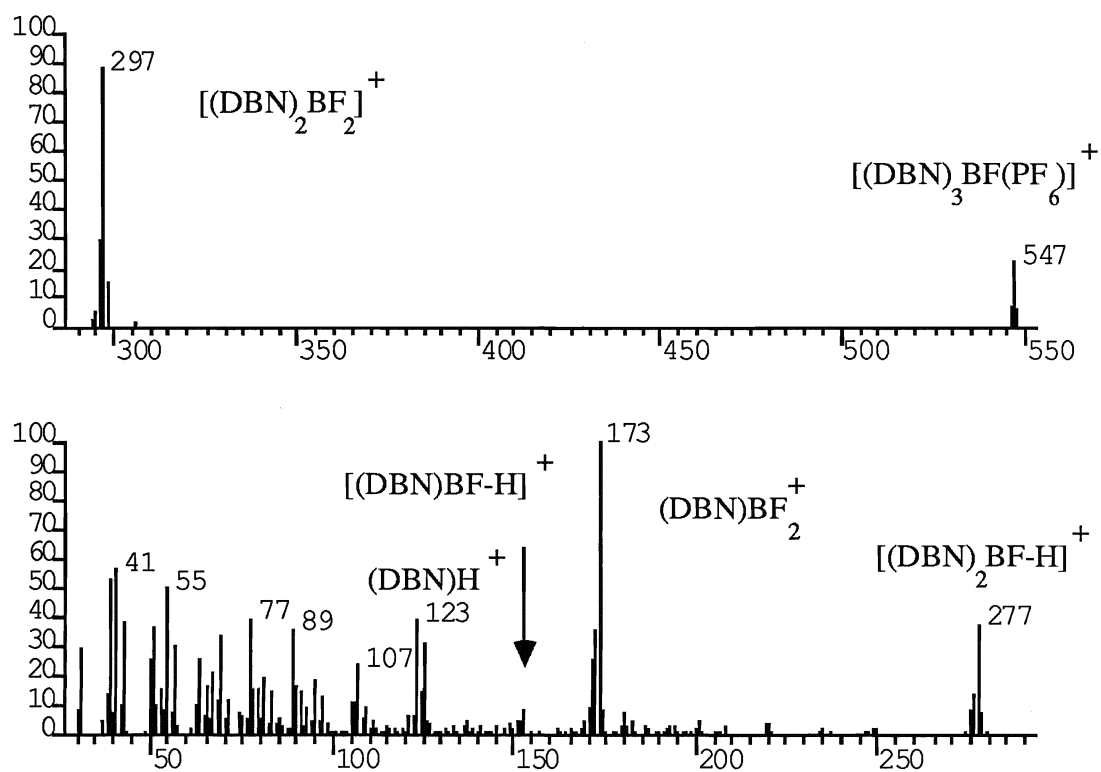


FIGURE 34
FAB SPECTRUM OF $[(\text{DBU})_3\text{BF}^{2+}](\text{PF}_6^-)_2$

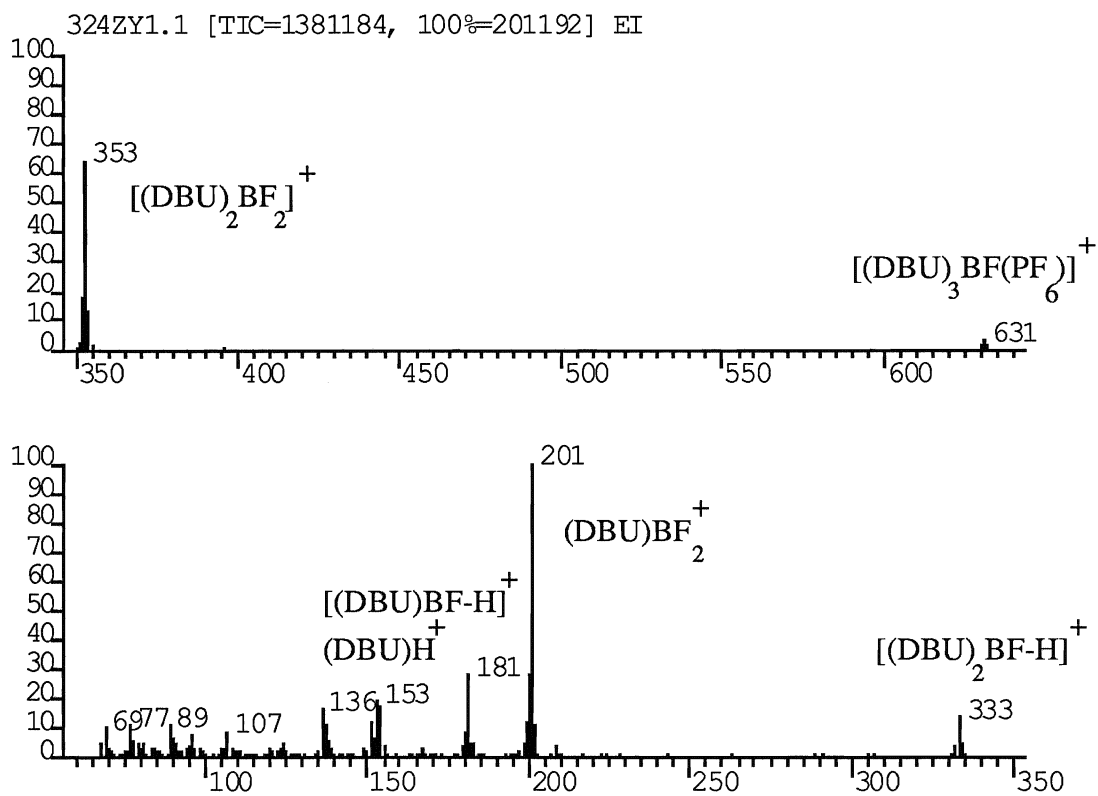
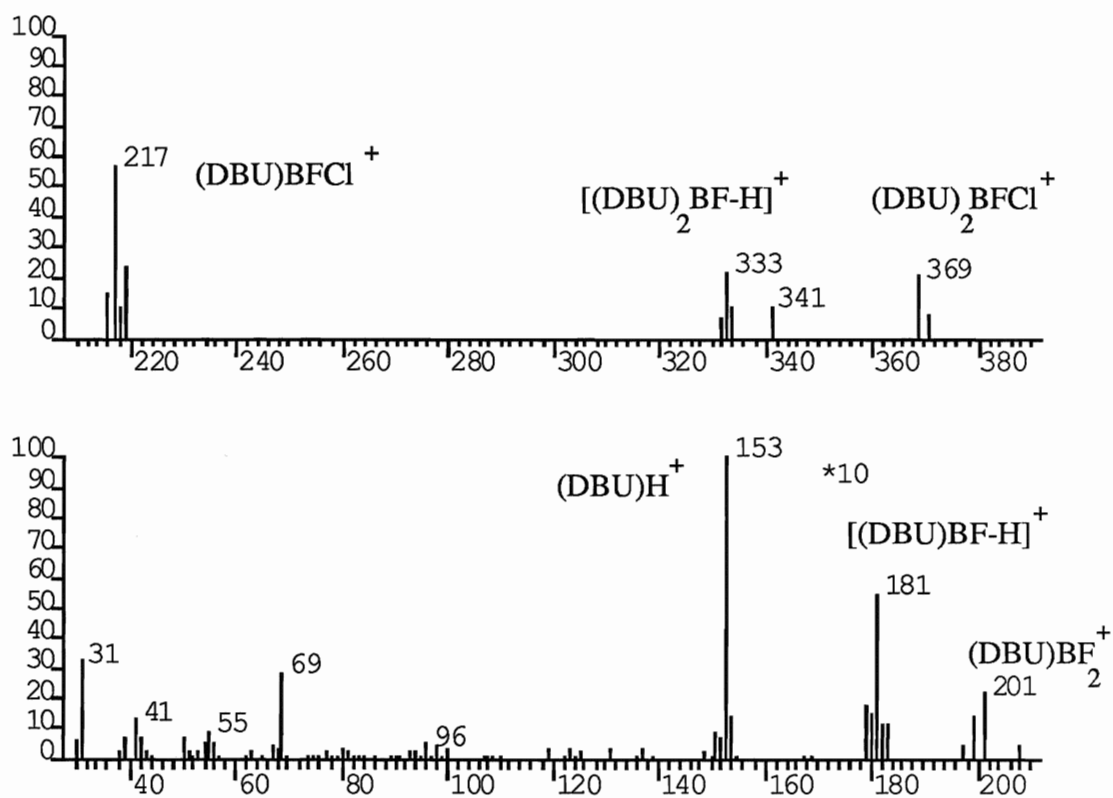


FIGURE 35
FAB SPECTRUM OF DBU/BF₃/BCl₃ SYSTEM WITH HIGH Cl/F RATIO



error can be repeated to a certain extent (Table 26). This makes a semiquantitative study of the stability of doubly charged cations in the gas phase possible.

TABLE 26
MAJOR ION PEAKS AND THEIR INTENSITY
OF [(DBN)₃BF²⁺](PF₆⁻)₂ AND [(DBU)₃BF²⁺](PF₆⁻)₂

IONS	DBN(*Intensity)	DBU(*Intensity)
[(D ₃ BF)(PF ₆)] ⁺	547(22, 14)	631(0.9, 1.1)
(D ₂ BF-H) ⁺	277(38, 25)	333(10, 14)
(DBF-H) ⁺	153(8.5, 12)	181(29, 29)
(D ₂ BF ₂) ⁺	297(88, 81)	353(56, 64)
(DBF ₂) ⁺	173(100, 100)	201(100, 100)
(DH) ⁺	125(31, 28)	153(15, 19)

* Each sample was run twice.

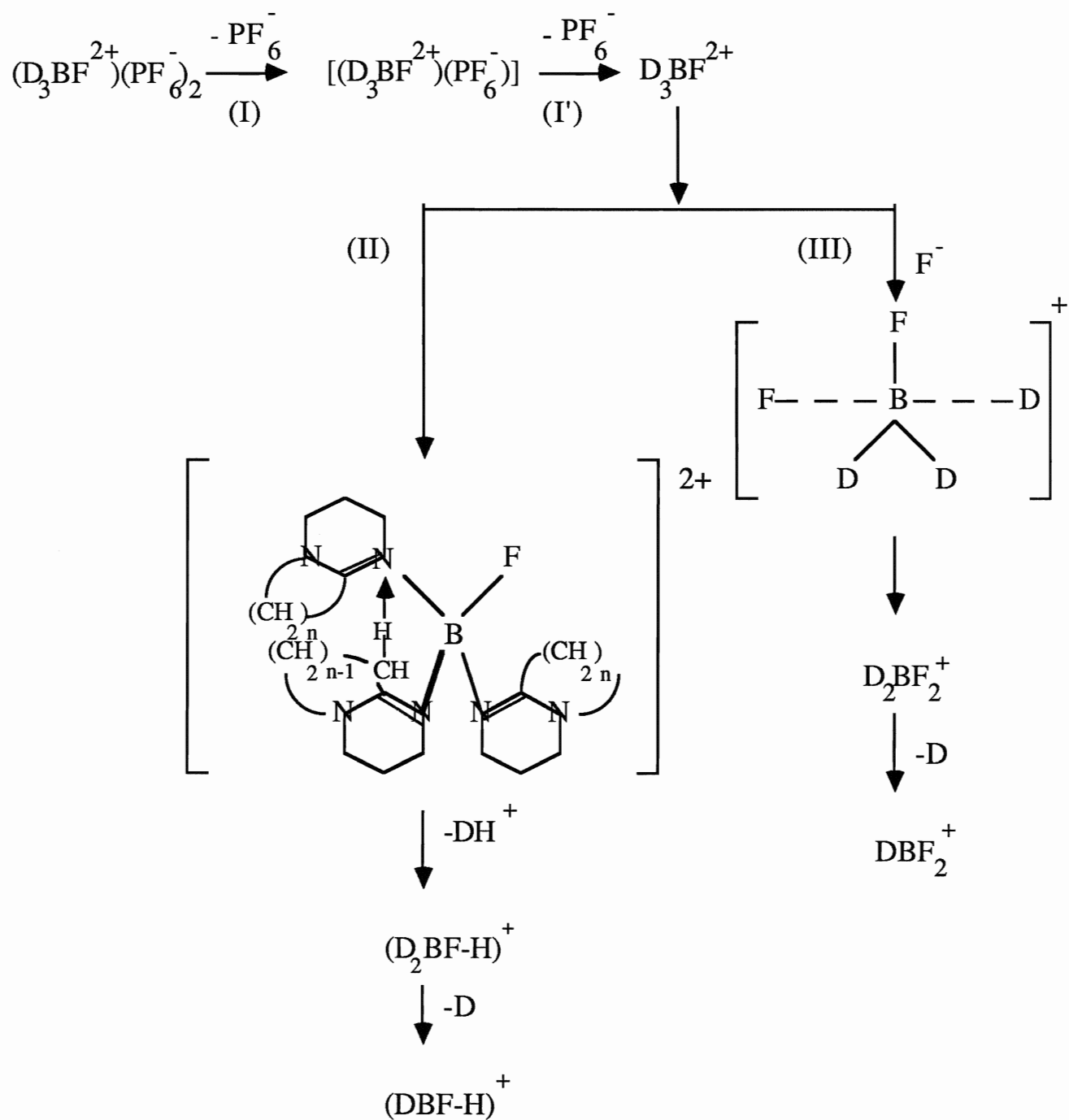
c. Mechanism of the Ionization

The interpretation of the FABMS spectra of tris(DBU) and tris(DBN) monofluoroboron hexafluorophosphate salts indicates that the ionization to monopositive ions occurs the three different ways. The ionization processes for D₃BF²⁺ are shown in Scheme 5.

Firstly, [(D₃BF)²⁺(PF₆)⁻]⁺ is formed directly from its neutral salt by losing one PF₆⁻ by the action of a neutral atom beam or the matrix. In a less probable situation, D₃BF²⁺ combining with one PF₆⁻ forms the ionic aggregate, [(D₃BF)²⁺(PF₆)⁻]⁺ as the highest monopositive ion.

Secondly, D₃BF²⁺, by losing one protonated donor molecule, DH⁺, forms [D₂BF-H]⁺ and its second fragment, [DBF-H]⁺, by the cleavage of another N-B bond. The mechanism for the formation of these fragments is proposed, based on

SCHEME 5
THE POSSIBLE IONIZATION MECHANISMS OF
 $(D_3BF^{2+})(PF_6^-)_2$ IN FAB/MS ION SOURCE



their structural features. Since the proton on the carbon neighbouring the imino nitrogen is more reactive than the others, this proton has the potential to leave. When these bicycloamidines acted as donor molecules offering electrons to boron atoms, this proton will be much more reactive, due to partial electron density moving to the acceptor site and due to the less powerful attractive force which is operating on this proton. It can attack the imino nitrogen atom of another neighbouring ligand and make this N-B bond weaker than other the N-B bonds; DH^+ is then lost. The second fragment results from the normal cleavage of the covalent bond.

Thirdly, D_3BF^{2+} reacting with fluoride produces the difluoroboron cation (+1). Fluoride can be formed as a result of the generation of PF_6^- by the neutral atom beam ($\text{PF}_6^- \rightarrow \text{PF}_5 + \text{F}^-$). The reaction may undergo an associative or a dissociative intermediate step.

d. Stability of Ions in the Gas-Phase

The calculated results of the peak intensity percentage of the boron containing species is listed in Table 27.

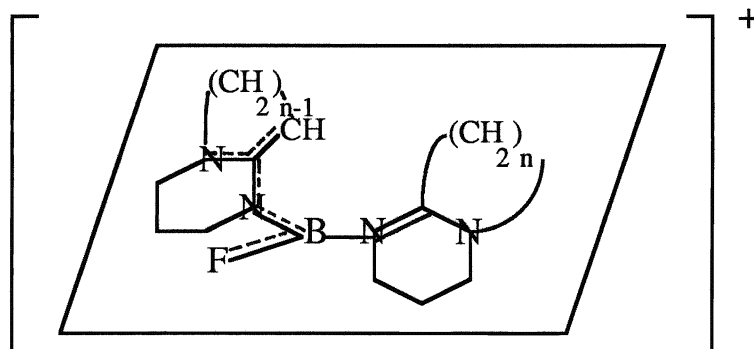
TABLE 27
THE ION INTENSITY PERCENTAGE OF BORON
CONTAINING SPECIES OF THE $(\text{D}_3\text{BF})(\text{PF}_6)_2$ TYPE IN FABMS

D	$(\text{D}_3\text{BFX})^+$	$(\text{D}_2\text{BF-H})^+$	$(\text{D.BF-H})^+$	$(\text{D}_2\text{BF}_2)^+$	$(\text{D.BF}_2)^+$
DBN	8.5, 6.0	15, 11	3.5, 5, 2	34, 35	39, 43
DBU	1.1, 0.5	5.1, 6.7	15, 14	28, 31	51, 48

The stronger ion intensity associated with $[(\text{DBN})_3\text{BF}(\text{PF}_6)]^+$ as compared with $[(\text{DBU})_3\text{BF}(\text{PF}_6)]^+$ probably relates to the smaller size of $(\text{DBN})_3\text{BF}^{2+}$, since

the attraction of 2+ and 1- ions is inversely proportional to the distance between the positive and the negative centre.

The ratio of $(D_2BF-H)^+/(DBF-H)^+$ is 3:1 for $D=DBN$ and 1:3 for $D=DBU$, which means that the B-N bond in $(DBN)_3BF^{2+}$ is more stable than in $(DBU)_3BF^{2+}$, in the gas phase. Since the basicity of DBN is similar to the basicity of DBU, the ring size is one of the possible factors affecting the stability of D_3BF^{2+} . The more crowded ion system has the higher energy, which makes the dissociation of the ion easier. Another possible factor is the electronic effect. In Chapter IV, we discussed that DBN has a more favourable electron resonance structure. We suppose that electrons, in $[(DBN)_2BF-H]^+$, are in a highly delocalized state and form a large π system containing six atoms (Structure VIII), i.e. a six centre eight electron system $[(N)(C)C-N-B-F]$. Another DBN ligand can be either perpendicular to this π system or rotate along the N-B bond. In this structural pattern, the large positive charge on the boron atom is distributed efficiently by the ligands. It is very difficult to distinguish which is the most important factor in the stability of $[(DBN)_2BF-H]^+$, but π bonding as the agent responsible for the stability of the sp^2 hybridization system is most likely.



Structure VIII

e. Doubly charged Intact Cations

The doubly charged intact cation, $(\text{DBN})_3\text{BF}^{2+}$, is probably observed, but at a very low intensity, m/z at 201 (2.9%, 5.3%). This ion should be identified by using the isotopic cluster occurring with half integral mass separation in the expected mass/charge range; however, its isotopic peaks are too low to detect with our MS-30 mass spectrometer. The ^{10}B isotope peak has been observed in one scan with m/z at 200.5. The occurrence of the doubly charged ion, $[\text{RuL}_3]^{2+}$, in the FAB spectra has been thought to relate to the presence of the matrix^{<136a>}, 3-nitrobenzyl alcohol, and not to depend on the dissociation of $[(\text{RuL}_3)^{2+}](\text{X}^-)_2$. The formation process for $[\text{D}_3\text{BF}]^{2+}$ is not completely understood.

3) Singly Charged Monofluoroboron Cations

D_2BFCl^+ and $\text{DD}'\text{BFCl}^+$ types of cations are detected by FABMS in this work. The parent ion peaks, D_2BFCl^+ or $\text{DD}'\text{BFCl}^+$ are normally present. The fragment peaks DBFCl^+ from D_2BFCl^+ , and DBFCl^+ and $\text{D}'\text{BFCl}^+$ from $\text{DD}'\text{BFCl}^+$ are identified. The characteristic isotopic patterns of chlorine, ^{35}Cl and ^{37}Cl in a 3:1 ratio, confirm the composition of these cations. $(\text{DBN})_2\text{BFCl}^+$ and $(\text{DBN})(\text{Q})\text{BFCl}^+$ are two examples. For the former, $(\text{DBN})\text{BFCl}^+$ is a characteristic fragment ion and for the latter, both $(\text{DBN})\text{BFCl}^+$ and $(\text{Q})\text{BFCl}^+$ are characteristic fragment ions, as well as parent ions. The "BMASROS" research was consistent with the isotopic patterns we actually measured.

Since the formation of D_2BFCl^+ is difficult to control under our experimental conditions, D_3BF^{2+} is present together with D_2BFCl^+ . We know that D_3BF^{2+} can react through a rearrangement reaction, with one fluoride replacing one donor molecule in the FABMS ion source. D_2BFCl^+ also can be formed by chloride replacing the donor molecule in D_3BF^{2+} in the FABMS ion source when the system contains a lot of free chloride. Therefore we are not sure that we are detecting D_2BFCl^+ itself from solution by FABMS. For instance, in a

DBU/BF₃/BCl₃ system with Cl >> F, both (DBU)₃BF²⁺ and (DBU)₂BFC⁺ were observed in a ¹⁹F NMR spectrum, and in the FAB spectrum, (DBU)₂BFC⁺ is present, but we can not simply say whether or not this ion peak is formed by a rearrangement reaction in the FABMS ion source.

4) DH⁺X⁻

The DH⁺ ion peak is always present in the FAB spectra of the fluoroboron cation systems, either in the complicated solution systems or in the pure solid salts. However, the intensity of DH⁺ is much higher for the solution samples than for the pure solid samples, because the excess donor molecules in solution contributes to DH⁺ formation, by protonation from the matrix in the FABMS ion source. The protonating ability of the organic bases in the FABMS ion source is proportional to the basic strength. In our systems, it was found that the intensity of DH⁺ is in the order (amidine)H⁺ > (quinuclidine)H⁺ > (pyridine)H⁺. The peak of (Pyridine)H⁺ is always present at a very low level.

The isolated DH⁺X⁻ compounds, (DBU)H⁺BPh₄⁻ and (DBN)H⁺BPh₄⁻, give very strong single signals, m/z at 153 [(DBU)H⁺] and m/z at 125 [(DBN)H⁺], respectively (Figure 36).

5) Gas-Phase Ion Substitution Reaction

The gas-phase substitution reaction of ligands in the difluoroboron cations by other donor ligands in the FABMS ion source was proposed by Dr. Miller, in view of a few gas-phase reactions have proceeded via this method^{<133,134>}. Both of the fluoroboron cationic salt which was dissolved in matrix and the substitution reagent were placed in the two isolated sides of the targets to avoid the two parts mixing with each other before entering the ion source, as shown in Figure 37.

FIGURE 36
FAB SPECTRUM OF $[(\text{DBN})\text{H}^+](\text{BPh}_4^-)$

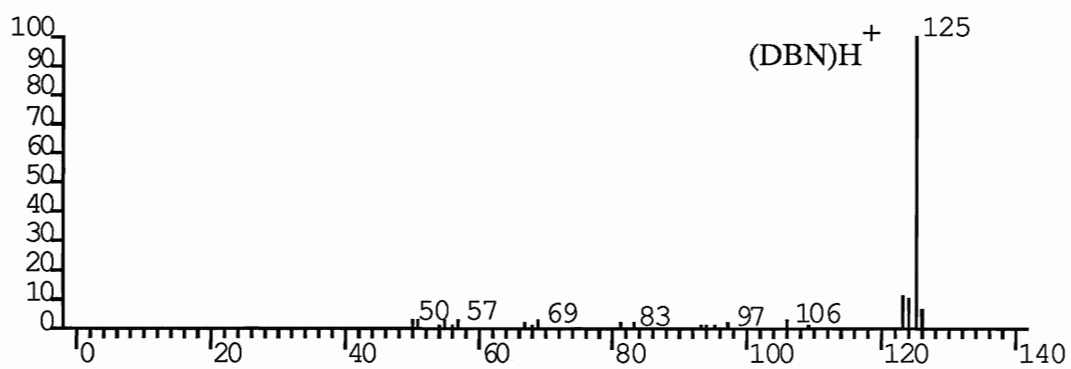
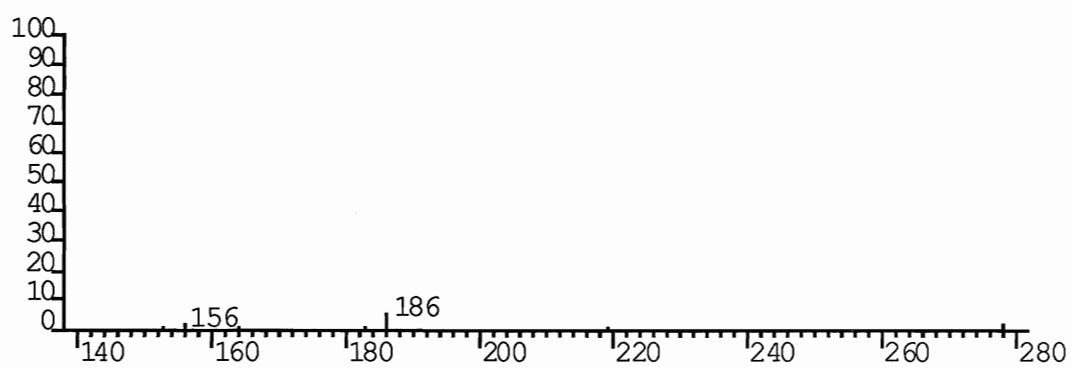
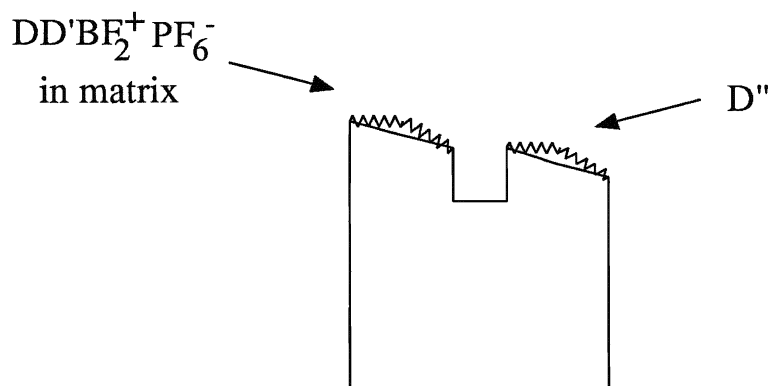


FIGURE 37
MS-30 BROCK DUAL TARGET AND SAMPLE PREPARATION



Practically, this gas-phase reaction was explored by using a non A-H bond (A: N, O or S) matrix. When NBA, as a matrix, was initially used to dissolve and support cationic salts, the free strong organic bases such as DBU and DBN were strongly protonated by the matrix to form DH^+ and their donation ability was completely lost. In view of the related substitution reactions and the known behaviour of these strong bases in the condensed-phase, a non A-H bond containing matrix(aprotic) was expected to give positive results. Fortunately, the satisfactory substitution reaction in the gas-phase was observed by using sulfolane (tetramethylene sulfone, bp. 285°C) as an aprotic matrix.

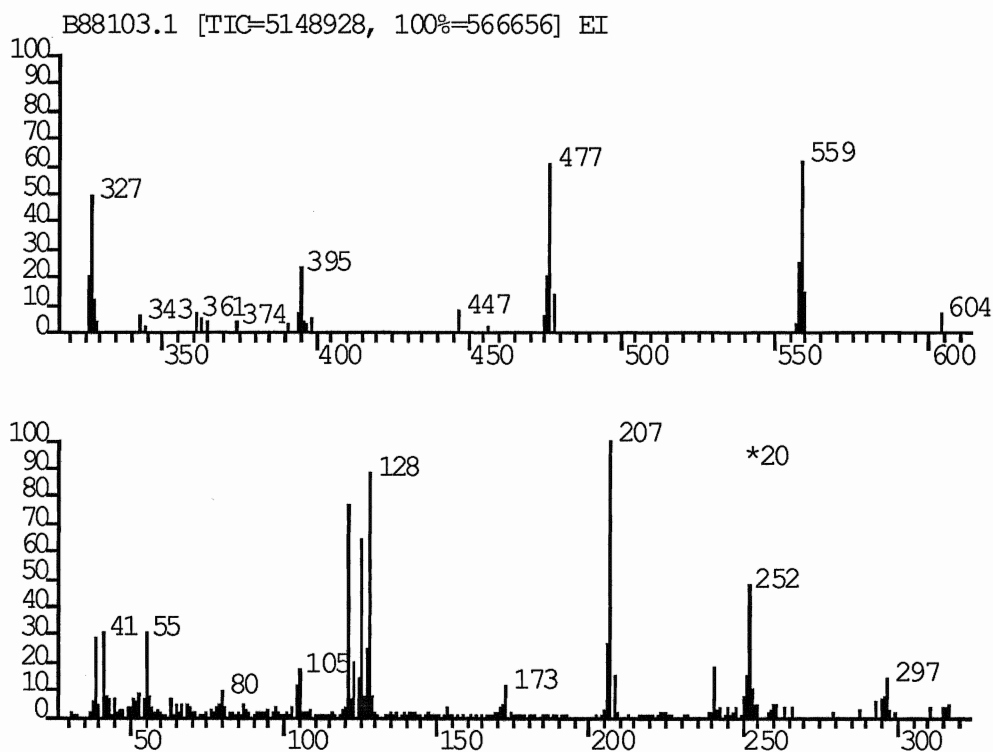
The important ions were also observed in the FAB spectra in a series of designed experiments. The experiments did not give consistent results, but qualitatively, the order of the ligand substitution reaction is $\text{Py}_2\text{BF}_2^+ > (\text{Py})(\text{Q})\text{BF}_2^+ \gg \text{Q}_2\text{BF}_2^+$. The Q_2BF_2^+ ion did not react with the strong organic bases, DBU, DBN and TMG. This order is consistent with the B-N bond strength in difluoroboron cations, which has been discussed in section 1.d. The extremely strong bases, DBU, DBN and TMG, can replace one and two pyridines from Py_2BF_2^+ to form the new cations, but quinuclidine and 2-methyl-2-oxazoline can not do so. All of the above indicates the dependence of the reactivity of ligand

substitution reaction on the basicity of both the leaving group and the entering group. As a typical example, the FAB spectrum of DBN reacting with $\text{Py}_2\text{BF}_2^+\text{PF}_6^-$ is shown in Figure 38. All major ion peaks in this spectrum are identifiable. The matrix sulfolane also took part in the reaction.

Neither $[(\text{DBN})_3\text{BF}_2^+](\text{PF}_6^-)_2$ nor $[(\text{DBU})_3\text{BF}_2^+](\text{PF}_6^-)_2$ reacted with strong bases, which is consistent with the stability of doubly charged cations in the condensed-phase.

In general, a major incentive to the investigation of gas-phase ionic reactions is their potential value as extremely simplified and generalized models of the corresponding processes occurring in solution^{<135>}. As described in Chapter VII, difluoroboron cationic hexafluorophosphate salts can only be dissolved in the common solvents acetone and nitromethane. These solvents caused remarkable side-reactions when the ligand substitution reactions of the difluoroboron cation with very strong bases took place. In the gas phase, all of the effects of the solvent can be ignored, so the reactivity of bases can be studied "accurately". However, the actual problem is not so simple. For instance, since DBN has a smaller steric hindrance and lower volatility (b.p. 95 ~ 98 °C, at 7.5 mmHg) than those of DBU (b.p. 100 °C, at 4 mmHg), it should be more reactive than DBU. But This is not so, as DBN shows a lower reactivity than DBU with Py_2BF_2^+ . We think that difluoroboron cations in the gas-phase might be in a higher energy state and might have the weaker bond strength, so that the steric effect on the ligand substitution reaction is not as important as in the condensed-phase which we have studied. But why DBU, in particular, is more reactive than DBN and TMG has not yet been answered. In view of their similar base strength, we think the effect might be found elsewhere in the donor's behaviour. Since DBN, with a five-membered ring, is easier to decompose than DBU, with a seven-membered ring, the "net amount" of DBN molecules as donors might be less than DBU in the ion source. More possibly, the difference in the volatility between the matrix and donor ligands results in a significant influence. Since the boiling point of DBU, 259 °C at 1 atm, is closest to

FIGURE 38
FAB SPECTRUM OF THE SUBSTITUTION REACTION OF
[(Py)₂BF₂⁺](PF₆⁻) IN SALFOLANE WITH DBN IN A FAB ION SOURCE



m/z	IONS	m/z	IONS
604	[(Py) ₂ BF ₂ ⁺](PF ₆ ⁻){(Py)(DBN)BF ₂ ⁺ } ⁺	252	[(Py)(DBN)BF ₂] ⁺
559	[(Py) ₂ BF ₂ ⁺] ₂ PF ₆ ⁻ ⁺	241	[(Sul+H)Sul] ⁺
477	[(Py) ₂ BF ₂ ⁺](PF ₆ ⁻){(DBN+H) ⁺ } ⁺	207	[(Py) ₂ BF ₂] ⁺
447	[(Py) ₂ BF ₂ (Sul) ₂] ⁺	173	(DBN)BF ₂ ⁺
395	[(DBN+H) ⁺] ₂ (PF ₆ ⁻) ⁺	128	(Py)BF ₂ ⁺
327	[(Py) ₂ BF ₂ (Sul)] ⁺	125	(DBN+H) ⁺
297	[(DBN) ₂ BF ₂] ⁺	121	(Sul+H) ⁺

sulfolane among DBU, DBN and TMG(53 ~ 55 °C, at 11 mmHg), DBU might volatilize simultaneously with Py_2BF_2^+ supported by the sulfolane and then be the more available to undergo reactions.

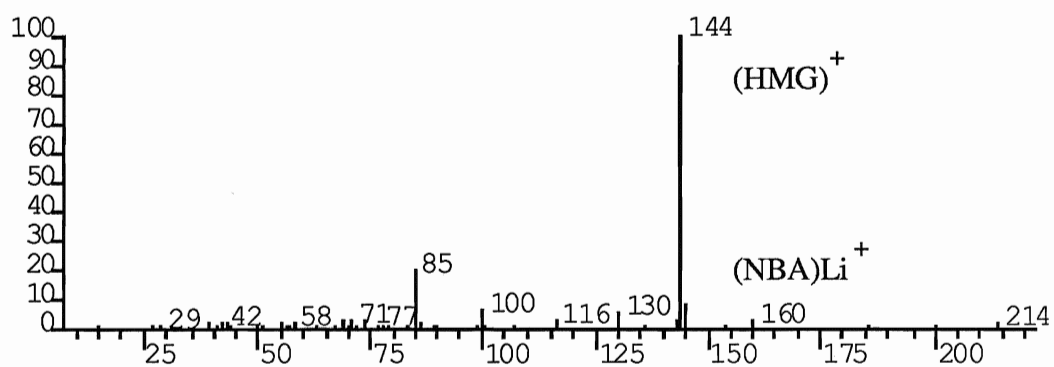
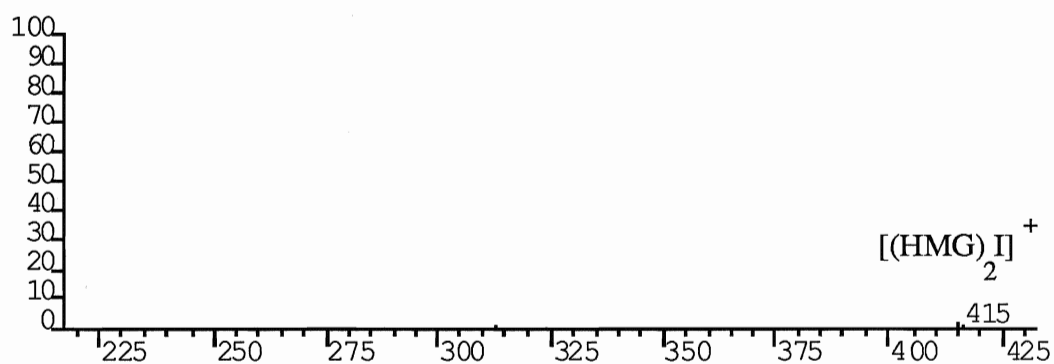
The gas-phase ligand substitution reactions of fluoroboron cations are only briefly studied in this work. (Dr. Balasanmugam is continuing this work). Since the gas-phase ion chemistry is pressure and temperature dependent, the change of these two physical parameters in the FAB ion source is worth investigating, to obtain more information.

6) Determination of Hexamethylguanidinium (HMG^+)

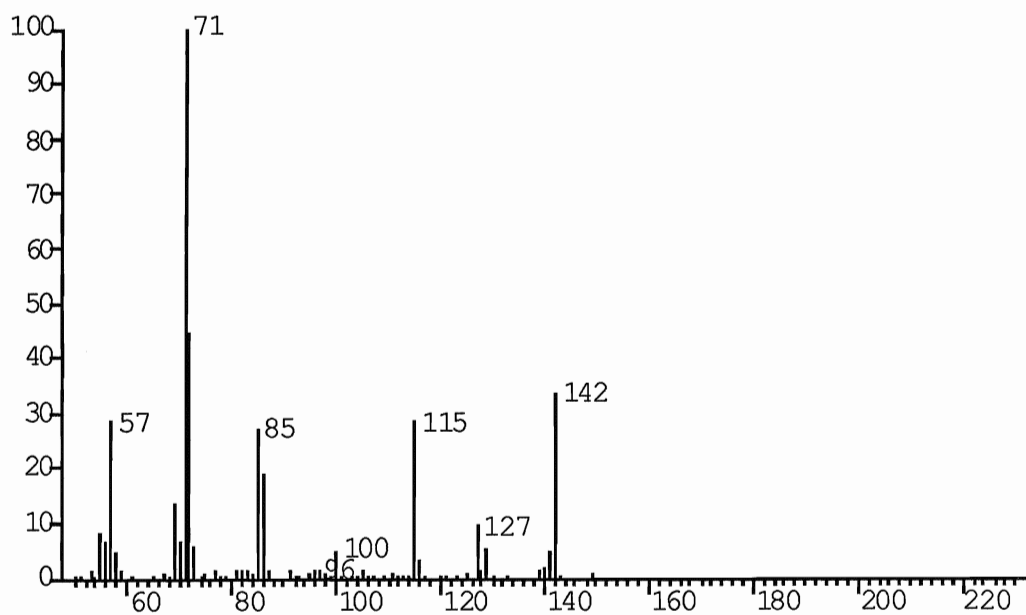
Since proton NMR did not give enough structural information about the precipitate which formed during the synthesis of pentamethylguanidine, mass spectrometry was utilized as another method to detect the molecular weight and the structure of this precipitate. Firstly, EI mass spectrometry was carried out. The peaks in the higher intensity range are m/z at 142 (34%), 129(5%), 127(9%), 115(29%), 100 (5%), 85 (27%), 72 (45%), 71 (100%) and 57 (28%). The low mass ion peaks are distinguishable as the organic fragments of PMG^+ (PMG : pentamethylguanidine, 129). The ion peaks at 127 and 142 could be I^+ and CH_3I^+ or $(\text{HMG}-2\text{H})^+$, but this is not very likely. The precipitate which was produced in the organic solvent might be ionic compounds. Secondly, FAB mass spectrometry was utilized. The FAB spectrum shows a significant peak, m/z at 144, five times higher than any other peaks, which is the exact molecular weight of HMG^+ . The peaks with m/z at 415 and 160 were interpreted as being $[(\text{HMG})_2\text{I}]^+$ and $(\text{NBA})\text{Li}^+$, respectively, which is consistent with the synthetic process. Thus, the precipitate involves HMG^+I^- and Li^+I^- . This result not only explores a key question of my synthetic work on PMG , but also exhibits the features of FABMS which can be used to study ionic organic compounds, which then allows for a comparison with EI mass spectrometry.

FIGURE 39
FAB AND EI MASS SPECTRA OF HMG⁺

FAB-MS



EI-MS



CHAPTER IX

CONCLUSIONS AND PROPOSALS

A. Conclusion

i) DBU and DBN induce a complicated redistribution reaction in D/BF₃/BCl₃ systems with all BF_nCl_{4-n}⁻, D.BF_nCl_{3-n} and fluoroboron cationic species being produced.

ii) D.BF_nCl_{3-n} species formed from strong organic bases show a very rapid displacement of chloride by the second entering ligand.

iii) Two types of fluoroboron cation salts, (D₃BF₂⁺)(X⁻)₂ and (DD'BF₂⁺)X⁻, as well as (D₂BF₂⁺)X⁻, are first isolated, and characterized by ¹⁹F and ¹¹B NMR, and FABMS.

iv) (DBU)₂BF₂⁺ shows a remarkable difference from other difluoroboron cations. The high reactivity of this cation makes it potentially useful as a starting material for preparing initially inaccessible fluoroboron containing compounds.

v) (Pyridine)₂BF₂⁺X⁻ in the condensed-phase reacts with very strong organic bases and produces (Pyridine)D'BF₂⁺ and D'₂BF₂⁺. Quinuclidine only replaces one pyridine.

vi) The application of FABMS directly to the complicated solution system is proven. FABMS is an excellent complementary technique to NMR for use with the fluoroboron cation system, and potentially, with other cationic systems in solution chemistry.

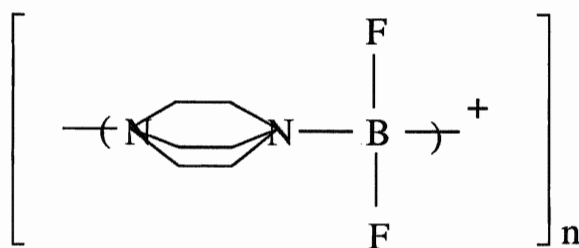
vii) Ligand substituted reactions of (Py₂BF₂⁺)(PF₆⁻) and (PyQBF₂⁺)(PF₆⁻) by the very strong organic bases, DBU DBN and TMG, in the FABMS ion source were reported as a new attempt, which demonstrates the potential application of FAB mass spectrometry to gas-phase ion chemistry and to the study of ligand substituted reactions between the gas-phase and the condensed-phase.

B. Proposals For Further Work

In the future, the present work can be developed in several different areas. X-ray determination of $(D_3BF^{2+})(X^-)_2$ will reveal the detailed structure of the doubly charged boron cations. ^{15}N NMR studies using enriched ^{15}N compounds, hopefully, will give more information about the B-N bond in fluoroboron containing adducts and fluoroboron cations. Mixed-ligand fluoroboron cations $[(D_2D'BF^{2+})(X^-)_2]$ can be isolated by choosing a suitable system. Phosphorus donor containing difluoroboron cations might have better reactivity as starting materials for making initially inaccessible fluoroboron compounds, due to the B-P bond being weaker than the B-N bond. FABMS studies of the ligand substitution reaction of fluoroboron cations in the gas-phase by using non A-H (A = O or N) bond containing matrices and under the different conditions such as changing pressure in the ion source will be very interesting topics in gas-phase chemistry.

From the point of view of my personal curiosity and interest, the following three particular projects are proposed:

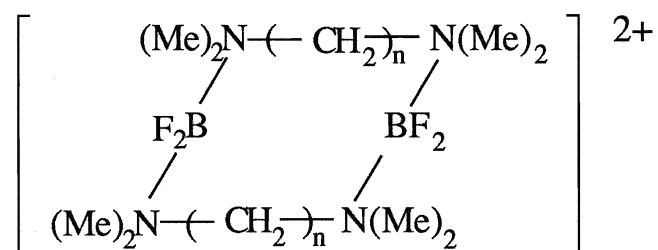
1) The study of fluoroboron cationic polymers with DABCO as building blocks (Structure IX). Some transition metal DABCO polymers have been synthesized. The first key step is finding a suitable solvent for $(DABCO).2BF_3$.



(IX)

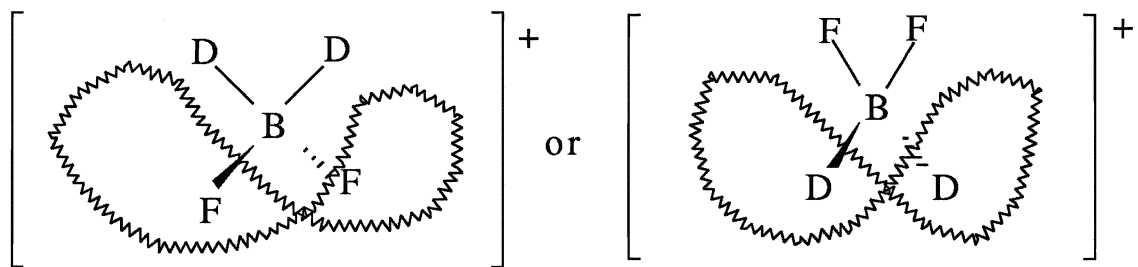
2) The study of fluoroboron cationic macrocyclo compounds with $(Me)_2N(CH_2)_nN(Me)_2$ or other two donor atoms containing ligands as building

blocks (Structure X). If these compounds can be isolated, further work on them will be very interesting.



(X)

3) The study of the second sphere coordination interaction of fluoroboron cations with crown ether or other flexible large ring compounds (Structure XI). Non-bonding interaction and the steric effect on the formation of the second sphere coordination will be a very interesting topic. In fact, we have observed the definitive peak at $m/z = 407$ ($[(\text{Pyridine})_2\text{BF}_2^+] + 15\text{-crown-5}$) in using FABMS.



(XIa)

(XIb)

References:

1. N. N. Greenwood, "Comprehensive Inorganic Chemistry" Ed. by J. C. Bailar, H. J. Emeleus, Sir R. S. Nyholm and A. F. Trotman-Dickenson, Pergamon Press, Oxford, Vol 1, 665 (1973).
2. A. G. Massey, "Adv. Inorg. Chem. Radiochem.", Ed. by H. J. Emeleus and A. G. Sharpe, 10, 1 (1967).
3. F. A. Cotton and G. Wilkinson, "Advanced Inorganic Chemistry", John Wiley & Sons, New York, 5, Chapt. 9, 289 (1980).
4. N. N. Greenwood and A. Earnshaw, "Chemistry of the Elements" Chapt. 6, Pergamon Press, New York (1984).
5. J. Emri and B. Gyori, "Comprehensive Coordination Chemistry", Ed. by Sir. G. Wilkinson R. D. Gillard and J. A. McCleverty, Pergamon Press, Oxford, Vol 3, 81 (1987).
6. D. P. N. Satchell and R. S. Satchell, Chem. Rev., 69, 251, (1969).
7. M. Zaro, J. F. Gal, S. Geribaldi and B. Videau, J. Chem. Soc., Perkin Trans. II, 57, (1983).
8. D. C. Mente, J. L. Mills and R. E. Mitchell, Inorg. Chem., 14, 123. (1975).
9. J. S. Hartman G. J. Schrobilgen and P. Stilbs, Can. J. Chem., 54, 1121 (1976).
10. J. S. Hartman and G. J. Schrobilgen, Can. J. Chem., 51, 99 (1973).
11. K. C. Janda, L. S. Bernstein, J. M. Steed, S. E. Novick and W. Klemperer, J. Chem. Soc., 100, 8074 (1978).
12. V. K. Topel and K. Hensen, Acta Cryst., C40, 828 (1984);
13. P. H. Clippard, J. C. Hanson and R. T. Taylor, J. Cryst. Mol. Struct., 1, 363 (1971); V. Hess, Acta Cryst. B25, 2338 (1969).
14. J. S. Hartman and J. M. Miller, "Adv. Inorg. Chem. Radiochem.", Ed. by H. J. Emeleus and A. G. Sharpe, 21, 147 (1978).
15. B. Benton-Jones, M. E. A. Davidson, J. S. Hartman, J. J. Klassen and J. M. Miller, J. Chem. Soc. Dalton Trans., 2603 (1972).
16. A. Fox, J. S. Hartman and R. E. Humphries, J. Chem. Soc. Dalton Trans., 1275 (1982).
17. M. J. Bula, J. S. Hartman, J. Chem. Soc. Dalton Trans., 1047 (1973); M. J. Bula, J. S. Hartman and C. V. Raman, *ibid*, 725 (1974); M. J. Bula, J. S. Hartman and C. V. Raman, Can. J. Chem., 53, 326 (1975).

18. R. G. Pearson and J. Songstad, *J. Am. Chem. Soc.*, 89, 1827 (1967).
19. G. E. Ryschkewitsch and W. J. Rademaker, *J. Magn. Reson.*, 1, 584 (1969).
20. J. M. Miller, *Inorg. Chem.*, 22, 2384 (1983).
21. J. M. Miller and T. R. B. Jones, *Inorg. Chem.*, 15, 284 (1976).
22. J. S. Hartman and J. M. Miller, *Inorg. Chem.*, 13, 1467 (1974).
23. S. G. Shore and R. W. Parry, *J. Am. Chem. Soc.*, 77, 6084 (1955); 80, 8, 12, 15 (1958).
24. H. Noth, S. Weber, B. Rasthofer, C. K. Narula and A. Konstantinov, *Pure Appl. Chem.*, 55, 1453 (1983).
25. G. E. Ryschkewitsch in "Boron Hydride Chemistry", ed by E. L. Muetterties, Academic Press, Chapt. 6, 223 (1975).
26. P. Kolle and H. Noth, *Chem. Rev.*, 85, 399 (1985).
27. R. J. Doyle, Jr., *J. Am. Chem. Soc.*, 110, 4120 (1988)
28. J. Higashi, A. D. Eastman and R. W. Parry, *Inorg. Chem.*, 21, 716 (1982).
29. G. E. Ryschkewitsch and J. W. Wiggins, *J. Am. Chem. Soc.*, 92, 1790 (1970).
30. P. Jutzi, B. Krato, M. Hursthouse and A. J. Howes, *Chem. Ber.*, 120, 1091 (1987).
31. T. D. Coyle and F. G. A. Stone, "Progress in Boron Chemistry", 1, 83 (1964).
32. E. L. Muetterties, *Pure Appl. Chem.*, 10, 53 (1965).
33. P. G. Harrison, *Coord. Chem Rev.*, 85, 193 (1988).
34. D. R. Martin, C. M. Merkel, J. P. Ruiz and J. U. Mondal, *Inorg. Chim. Acta*, 100, 293 (1985); D. R. Martin, C. M. Merkel and J. P. Ruiz, *ibid*, 115, L29 (1986).
35. N. E. Miller and E. L. Muetterties, *J. Am. Chem. Soc.*, 86, 1033 (1964).
36. B. T. Pennington, M. A. Chiusano, D. J. Dye, E. D. Martin and D. R. Martin, *J. Inorg. Nucl. Chem.*, 40, 389 (1978).
37. M. Kameda and G. Kodama, *J. Am. Chem. Soc.*, 102, 3647 (1980).
38. M. Kameda and G. Kodama, *Inorg. Chem.*, 24, 2712 (1985); 26, 2011 (1987); 26, 3968 (1987).
39. C. D. Schmulbach and I. Y. Ahmad, *Inorg. Chem.*, 8, 1414 (1969); 11, 228 (1972).
40. J. S. Hartman and G. J. Schrobilgen, *Inorg. Chem.*, 13, 874 (1974).

41. J. S. Hartman and P. Stilbs, *J. Chem. Soc., Dalton Trans.*, 1142 (1980).
42. H. Noth and S. Lucas, *Angew. Chem.*, 95, 1505 (1962).
43. G. E. Ryschkewitsch and J. M. Garrett, *J. Am. Chem. Soc.*, 90, 7234 (1968).
44. D. L. Reznicek and N. E. Miller, *Inorg. Chem.*, 4, 858 (1972).
45. G. E. Ryschkewitsch and W. H. Myers, *Syn. React. Inorg. Metal-Org. Chem.*, 5(2), 123 (1975).
46. N. Wiberg and J. W. Buchler, P. C. Keller and J. V. Rund, *J. Coord. Chem.*, 5, 129 (1976).
47. H. C. Brown, B. Singaram and J. R. Schweir, *Inorg. Chem.*, 18, 51 (1979); 18, 53 (1979).
48. J. S. Hartman, B. McGarvey and C. V. Raman, *Inorg. Chim. Acta*, 49, 63 (1981).
49. J. S. Hartman, B. McGarvey, *Inorg. Chim. Acta*, 44, L39 (1980).
50. A. Fox, J. S. Hartman, and A. T. Nguyen, unpublished work.
51. M. J. Farquharson and J. S. Hartman, *Chem. Soc., Chem. Commun.*, 256 (1984).
52. M. J. Farquharson, M. Sc. Thesis, Brock University, (1985).
53. M. J. Farquharson, unpublished work, (1985).
54. F. V. Sowa, U. S. Patent, 2,655,524 (1951); S. Prasad and N. P. Singh, *Z. Anorg. Chem.*, 346, 217 (1966).
55. C. Makosky, G. L. Galloway, and G. E. Ryschkewitsch, *Inorg. Chem.*, 6, 1972 (1967).
56. M. A. Mathur and G. E. Ryschkewitsch, *Inorg. Chem.*, 19, 887 (1980).
57. M. A. Mathur and G. E. Ryschkewitsch, *Inorg. Chem.*, 19, 3054 (1980).
58. R.C. Mehrotra, in "Comprehensive Coordination Chemistry", Ed. by Sir G. Wilkinson, R. D. Gillard and J. A. McCleverty, Pergamon Press, Oxford, Vol 2, 269, (1987).
59. J. Oszapowicz and E. Raczynska, *J. Chem. Soc., Perkin Trans. II*, 1643 (1984).
60. J. Oszapowicz and K. Ciszowski, *J. Chem. Soc., Perkin Trans. II*, 663(1987).
61. E. Raczynska, J. Oszapowicz and M. Walczak, *J. Chem. Soc., Perkin Trans. II*, 1087 (1985).
62. F. A. Cotton, T. Inglis, M Kilner and T. R. Webb, *Inorg. Chem.*, 14, 2023 (1975); A. Bino, F. A. Cotton and W. Kaim, *ibid*, 18, 3569 (1979).

63. W. Reppe, *Justus Liebigs Ann. Chem.* 596, 210 (1967).
64. H. Oediger and F. Moller, *Angew. Chem.* 79, 53 (1967); H. Oediger and F. Moller, *Angew. Chem. Int. Ed. Engl.* 6, 76 (1967).
65. D. H. R. Barton, J. D. Elliott and S. D. Gero, *J. Chem. Soc. Perkin Trans. I*, 2085 (1982).
66. I. Hernecz " *Adv. Heterocyclic chem.* " ed. A. R. Katritzky. Academic press, Orlando, Vol. 42, 84 (1987).
67. H. Oediger, F. Moller, and K. Eiter, *Synthesis*, 591 (1972).
68. R. E. Erickson, "DBU - Scope of Search", Abbott Laboratories, Jan. 25, 1983
69. K. Eiter, F. Lieb, H. Dissenlnkoetter and H. Oediger, *Justus liebigs Ann. Chem.* 658 (1978).
70. A. Caminade, C. Couret, J. Escudie and M. Koenige, *J. Chem. Soc. Chem. Commun.*, 1621 (1984).
71. S. Kim and H. Chang, *Bull. Chem. Soc. Jpn.*, 58, 3669 (1985).
72. M. K. Blanchette, W. Choy, J. T. Davis, A. P. Essensfeld, S. Masamune, W. R. Roush and T. Saki, *Tetrahedron Lett.*, 25, 2183 (1984).
73. K. R. Grundy, *Inorg. Chim. Acta*, 53, L225, (1981).
74. S. Lofås and P. Ahlberg, *J. Chem. Soc., Chem. Commun.* 998 (1981); S. Lofås and P. Ahlberg, *J. Heterocycl. Chem.*, 21, 583, (1984)
75. H. Hoberg, Y. Reres and A. Milchereit, *J. Organomet. chem.*, 307, C41 (1986); 317, C25 (1986).
76. R. Reagrani and P. Dixneuf, *J. Organomet. Chem.*, 344, C11 (1988).
77. H. Eshtiagh-Hosseini, H. W. Kroto, J. G. Nixon, M. J. Mach and M. J. Taylor, *J. Chem. Soc., Chem. Commun.*, 199 (1981).
78. J. S. Angyal and W. K. Warburton, *J. Chem. Soc.*, 2492 (1951).
79. G. J. Durant, *Chem. Soc. Rev.*, 14, 375 (1985).
80. P. J. Taylor and A. R. Wait, *J. Chem. Soc., Perkin Trans. II*, 1765 (1986).
81. G. Wieland and G. Simchen, *Liebigs Ann. Chem.* 2178 (1985).
82. H. Kessler and D. Leibfritz, *Tetrahedron*, 26, 1085 (1970).
83. H. Kessler and D. Leibfritz, *Chem. Ber.*, 184, 2158 (1971).
84. H. Lecher and F. Graf, *Chem. Ber.* 56B, 1326 (1923).
85. A. N. Sinyakov, A. I. Lomakin and S. G. Dopov, *Bioorg. Khim.*, 10 (1), 68, (1984).
86. K. Kamio, K. Okurro and K. Watanabe, *CA*: 106 p68470r, (1986).

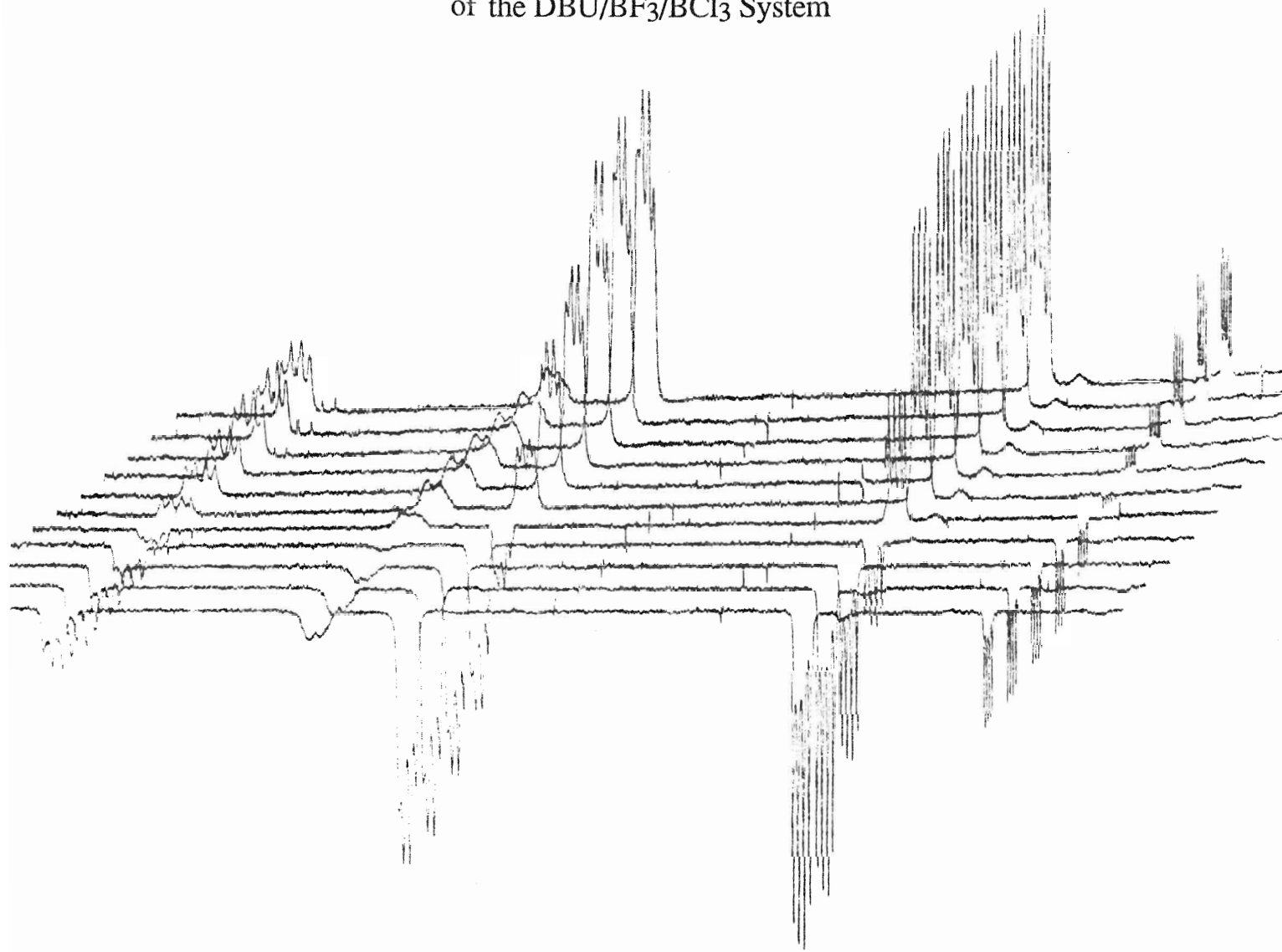
87. D. H. R. Barton J. D. Elliott and S. D. Gero, *J. Chem. Soc., Chem. Commun.*, 1136 (1981).
88. W. Kantlehner, E. Haug, W. Mergen, P. Speh, T. Maier, J. J. Kapassakalidis, H-J. Bruauner and H. Hagen, *Liebigs Ann. Chem.*, 108 (1984).
89. R. Snaith, K. Wade and B. K. Wyatt, *J. Chem. Soc. (A)*, 380 (1970).
90. I. Pattison, K. Wade and B. K. Wyatt, *J. Chem. Soc. (A)*, 837 (1968).
91. W. Clegg, R. Snaith, H. M. M. Shearer, K Wade and G. Whitehead, *J. Chem. Soc., Dalton Trans.*, 1309 (1983).
92. S. C. Chaudury and D. Kummer, *J. Organomet. Chem.*, 339, 241 (1988).
93. G. J. Schrobilgen, M. Sc, thesis, Brock University, (1971).
94. E. M. Purcell, H. C. Torrey, and R. Pound, *Phys. Rev.*, 69, 37 (1946); F. Bloch, W. W. Hansen, and M. Packard, *Phys. Rev.*, 69, 127 (1946).
95. A. E. Derome, "Modern NMR Techniques For Chemistry Research", Pergamon Press, Oxford (1987).
96. E. Oldfield and R. J. Kirpatrick, *Science*, 227, 4694 (1985); D. J. O'Donnell, V. J. Bartuska, A. R. Palmer, and D. W. Sindorf, *Am. Lab.* 18, 96 (1986).
97. E. M. Bradbury and C. Nicolili, "NMR in the Life Sciences", Plenum Press, New York, Vol. 107, (1986).
98. R. K. Harris and B. E. Mann "NMR and the Periodic Table", Academic Press, London (1978).
99. P. Laszlo "NMR of Newly Accessible Nuclei", Academic Press, New York, Vol. 2, (1983).
100. R. Benn and A. Ruffinska, *Angew. Chem. Int. Ed. Engl.*, 25, 861 (1986).
101. T. L. James, (Nuclear Magnetic Resonance in Biochemistry", Academic Press, New York, (1975); E. D. Becker "High Resolution NMR", 2nd Ed., Academic Press, New York (1980); R. K. Harris, "Nuclear Magnetic Resonance Spectroscopy", Pitman, Toronto (1983); W. Kemp, "NMR in Chemistry, A Multinuclear Introduction", Macmillan, Hong Kong (1986).
102. N. F. Ramsey and E. M. Purcell, *Phys. Rev.*, 85, 143 (1952).
103. C. Brevard and P. Granger, "Handbook of High Resolution Multinuclear NMR", John Wiley & Sons, New York, (1981).

104. H. Noth and B. Wrackmeyer, "Nuclear Magnetic Resonance Spectroscopy of Boron Compounds", NMR 14, Ed. by P. Diehl, E. Fluck, and R. Kosfeld, Springer-Verlag, Berlin, (1978).
105. M. Barber, R. S. Bordoli, R. D. Sedgwick, A. N. Tyler, J. Chem. Soc., Chem. Commun., 325 (1981); D. J. Surman, J. C. Vickerman, J. Chem. Soc., Chem. Commun., 324 (1981).
106. C. Fenselau and R. J. Colter, Chem. Rev., 87, 501 (1987).
107. E. D. Pawn, Mass Spectrom. Rev., 5, 191 (1986).
108. R. L. Cochran, Appl. Spectroscopy Rev., 22, 137 (1986).
109. K. Balasubramanian, S. K. Viswanadham, D. M. Hercules, R. J. Cotter, D. Heller, A. Benninghoven, W. Sichtermann, V. Anders, T. Keough, R. D. Macfarlane, and C. J. McNeal, Appl. Spectroscopy, 41, 821 (1987).
110. J. M. Miller, J. Organomet. Chem., 249, 299 (1983).
111. J. M. Miller, Adv. Inorg. Chem. Radiochem., 28, 1 (1984).
112. M. I. Bruce and M. J. Liddell, Appl. Organomet. Chem. 1, 191 (1987).
113. I. A. Kahawa, J. Selbin, T. C.-Y. Hsieh, D. W. Evans, K. M. Pamidimukkula and R. Laine, Inorg. Chim. Acta, 144, 275 (1988).
114. D. F. Shriver, "The Manipulation of Air-Sensitive Compounds", McGraw-Hill, New York, (1969).
115. San-Abbott Limited, "Subject to Revision-DBU", Tokyo, Japan, Jan., 1980.
116. J. R. McDivitt and G. L. Humphrey, Spect. Acta, 30A, 1021 (1974); J. M. Van Paasschen and R. A. Geanangel, Can. J. Chem., 53, 723 (1974); H. C. Brown, Inorg. Chem., 18, 51 (1979); H. C. Brown and B. Singaram, Inorg. Chem., 19, 455 (1980).
117. A. Nguyen, Unpublished Work, 1983.
118. J. S. Hartman and G. J. Schrobilgen, Inorg. Chem., 11, 940 (1972).
119. R. J. Gillespie and J. S. Hartman, Can. J. Chem., 46, 2147 (1968).
120. G. A. Webb, "NMR of Newly Accessible Nuclei", Ed. by P. Laszlo, Academic Press, New York, Vol. 1, 79, (1983).
121. M. R. Bendall, D. M. Doddrell, Aust. J. Chem., 31, 1141 (1978).
122. I. M. Ishmail, S. J. S. Kerrison, and P. J. Sadler, J. Chem. Soc., Chem. Commun., 1175 (1980).
123. R. E. Wasylshen and N. Burford, Can. J. Chem., 65, 2707 (1987).
124. K. L. Leighton and R. E. Wasylshen, Can. J. Chem. 65, 1469 (1987).

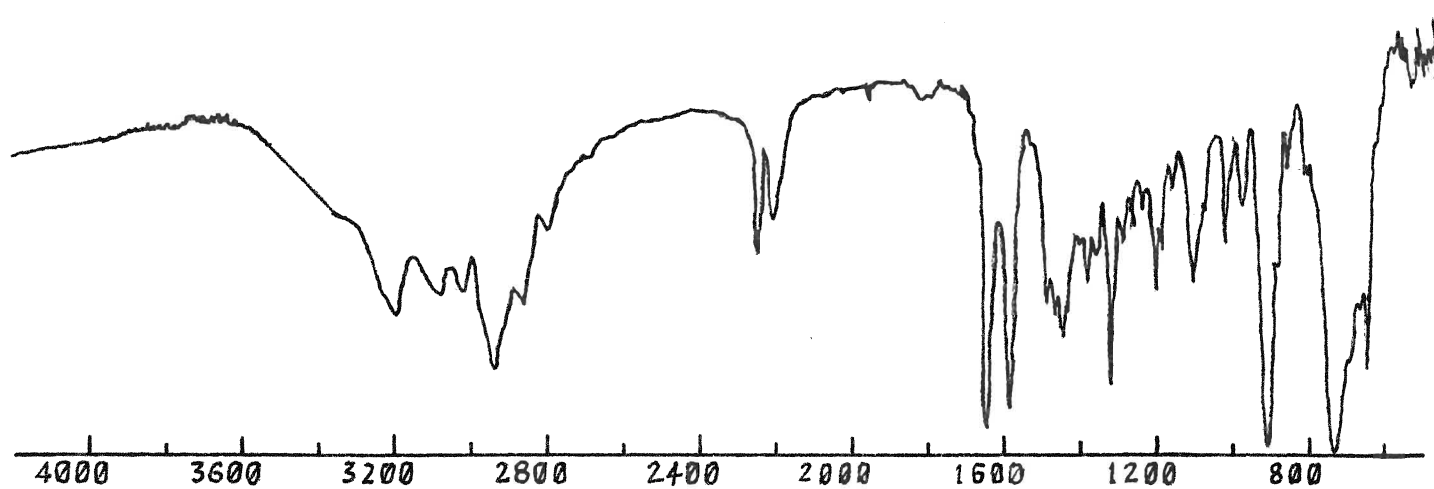
125. G. J. Martin and J-P. Gouesnard, "¹⁵N-NMR Spectroscopy", Springer-Verlag, Berlin, (1981).
126. R. R. Yetman, M. Sc. Thesis, Brock University, 1975.
127. T. Sielisch and M. Cowie, *Organometalics*, 7, 707 (1988).
128. E. Tolun and J. F. J. Todd, *Org. Mass Spect.*, 23, 105 (1988)
129. P. R. Ashton, D. Fenton, R. N. Prasad, M. Jindal and M. Jain, *Inorg. Chim Acta*, 146, 99 (1988).
130. R. L. Cerny, M. Bursey, D. L. Jameson, M. R. Malachowski and T. N. Sorrell, *Inorg. Chim. Acta*, 89, 89 (1984).
131. K. R. Jennings, T. J. Kemp, and B. Sieklucka, *Inorg. Chim. Acta*, 141, 163 (1988).
132. J. M. Miller, K. Balasanmugan, J. Nye, G. B. Deacon and N. C. Thomas, *Inorg. Chem.*, 26, 560 (1987); G. Bojeson, *Org. Mass Spect.*, 20, 413 (1985).
133. K. Balasanmugam, J. M. Miller and A. Fulcher, Submitted to *Anal. Chem.*, in May 1988.
134. K. Balasanmugan, J. M. Miller, A submitted to *Anal. Chem.*, 1988.
135. F. Cacace, *Accounts Chem. Res.*, 21, 215 (1988).

Appendix 1

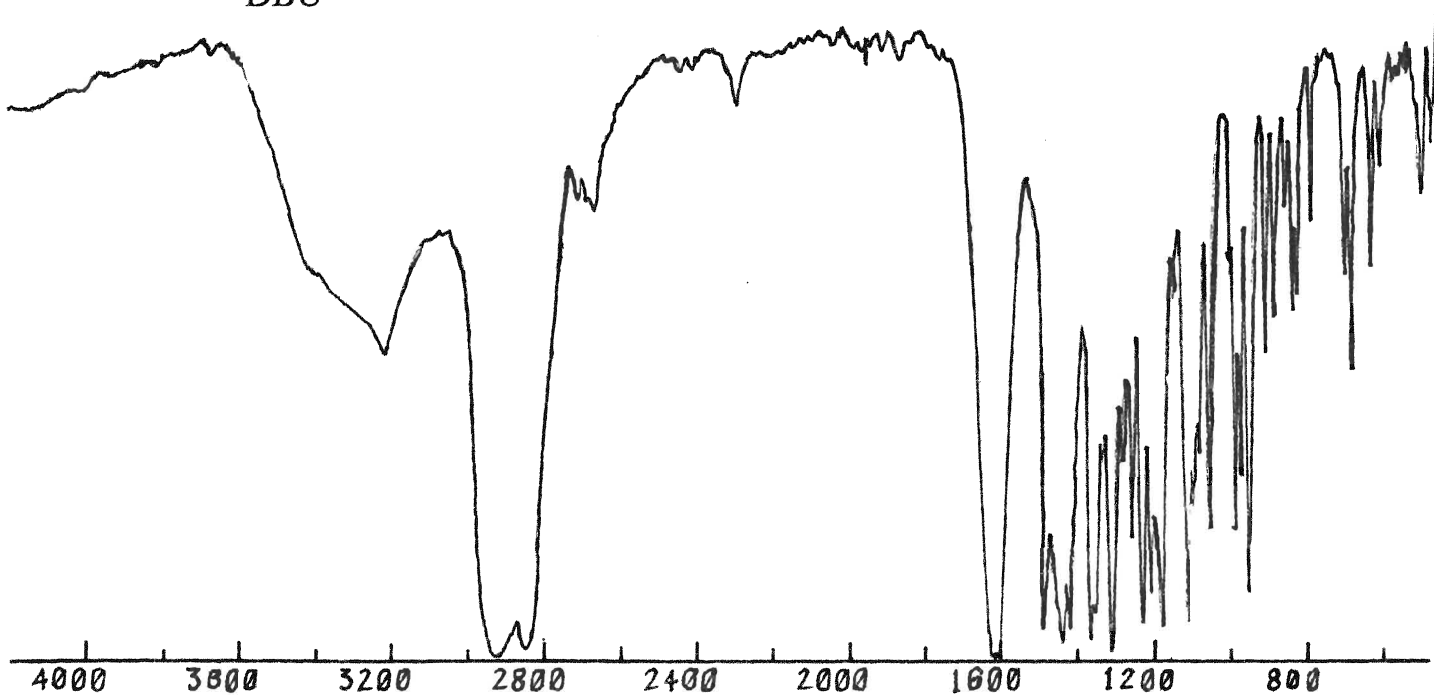
A Stacked Plot Out of Inversion Recovery Experiment
of the DBU/BF₃/BCl₃ System



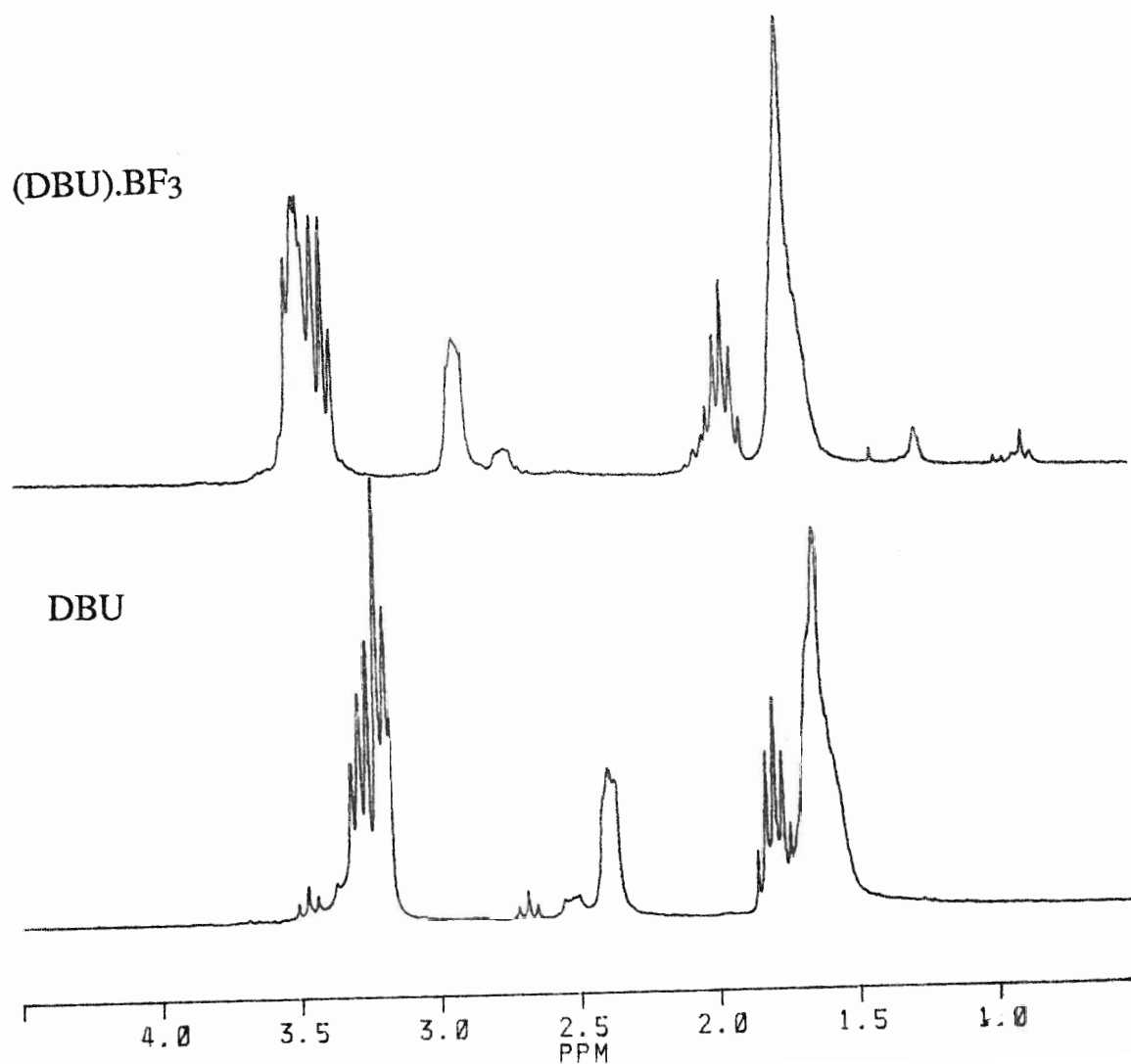
Appendix 2

FT IR Spectra of DBU and the DBU/BF₃/BCl₃ SystemThe DBU/BF₃/BCl₃ System

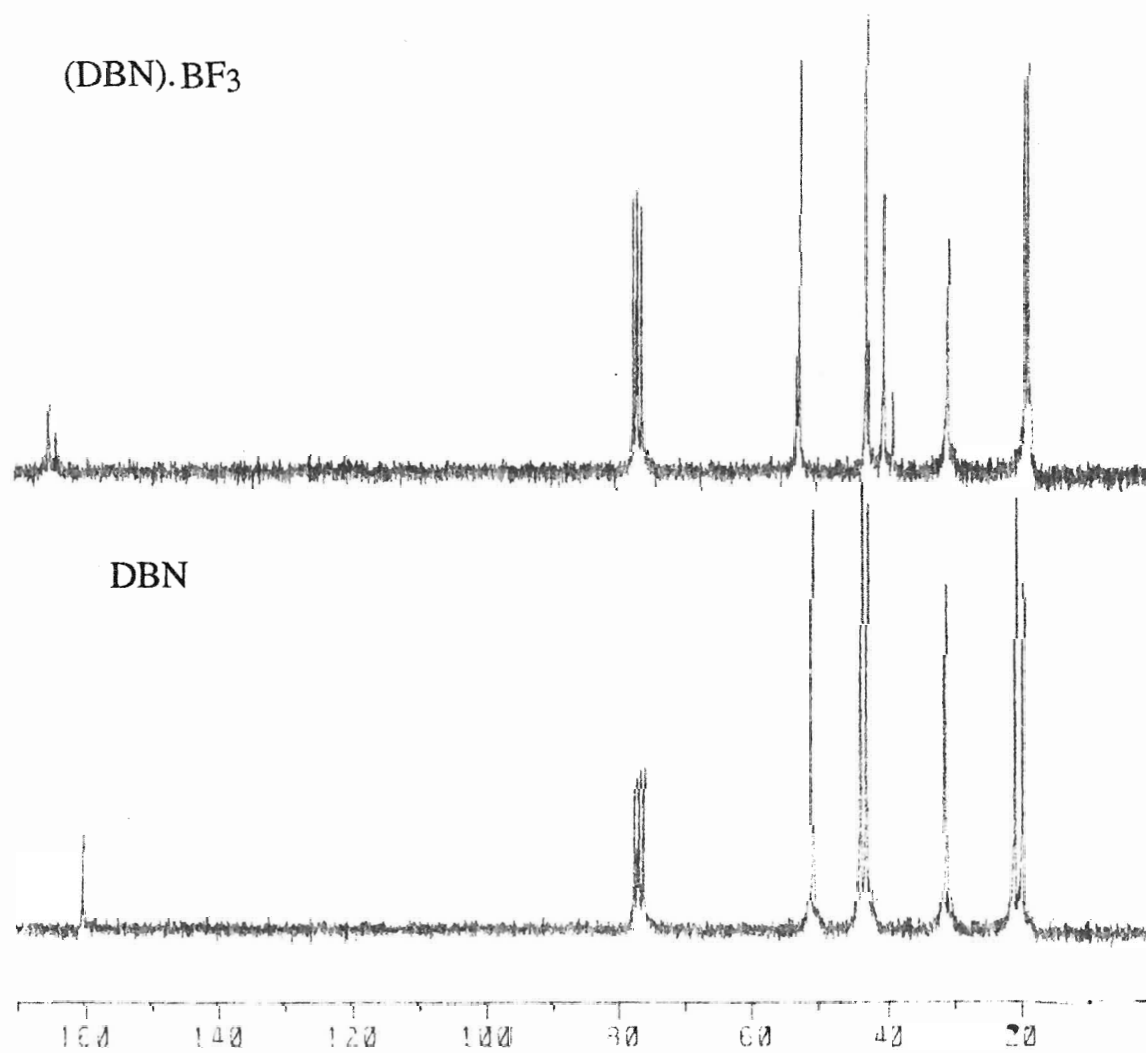
DBU



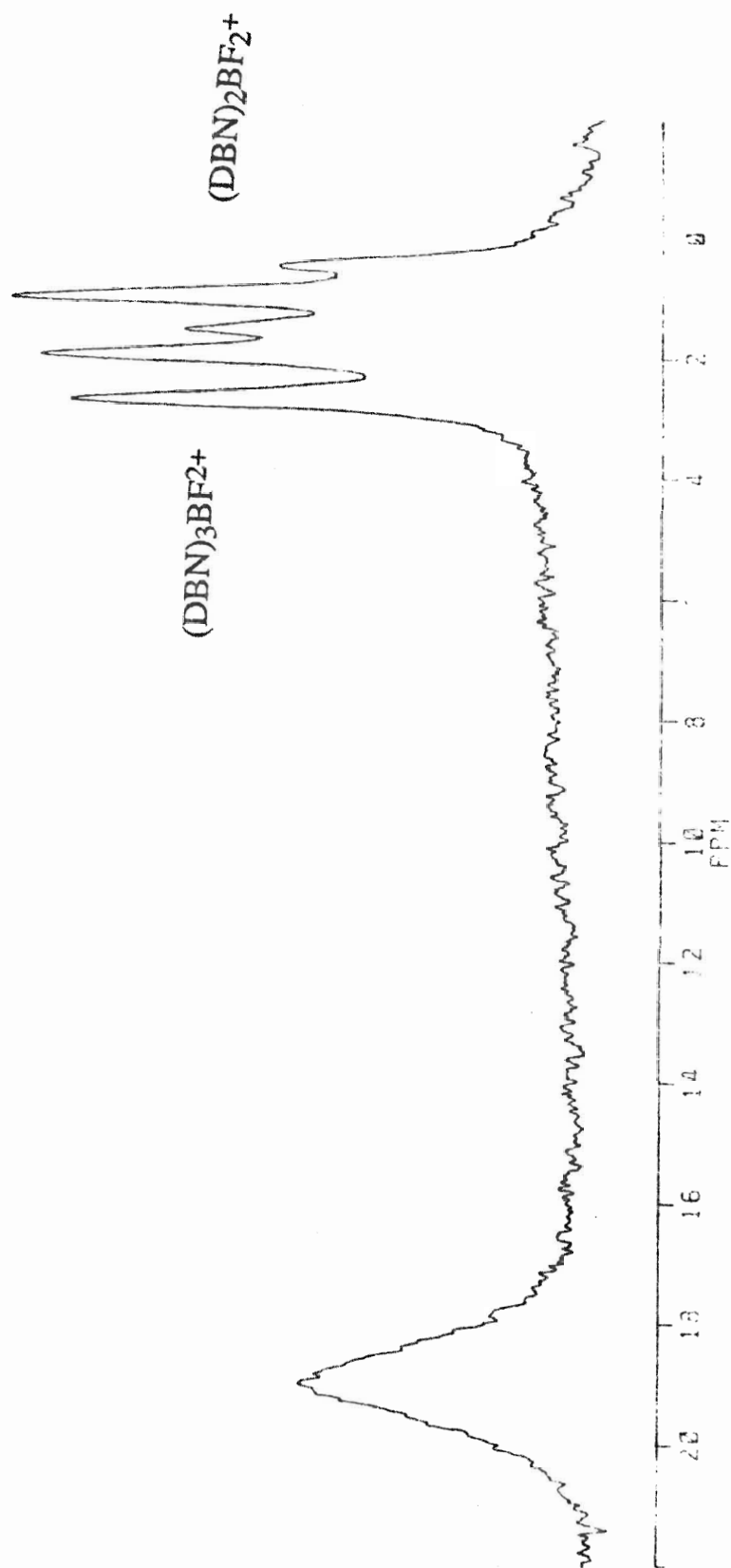
Appendix 3
 ^1H Spectra of DBU and $(\text{DBU})\cdot\text{BF}_3$



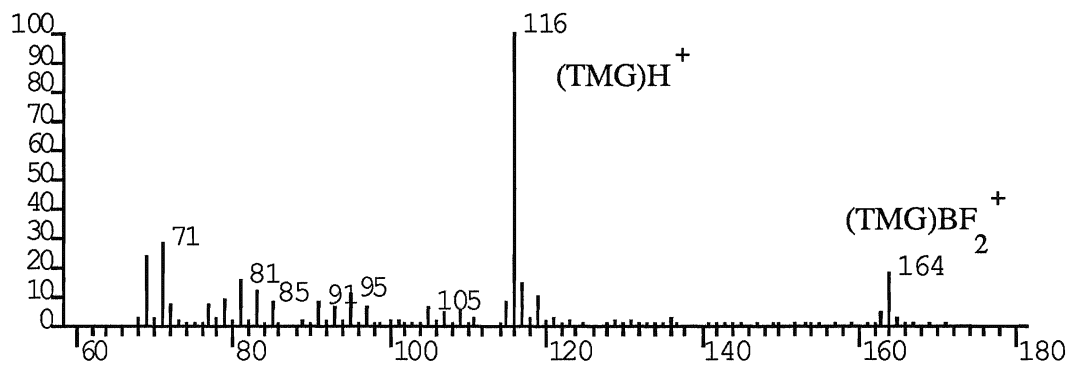
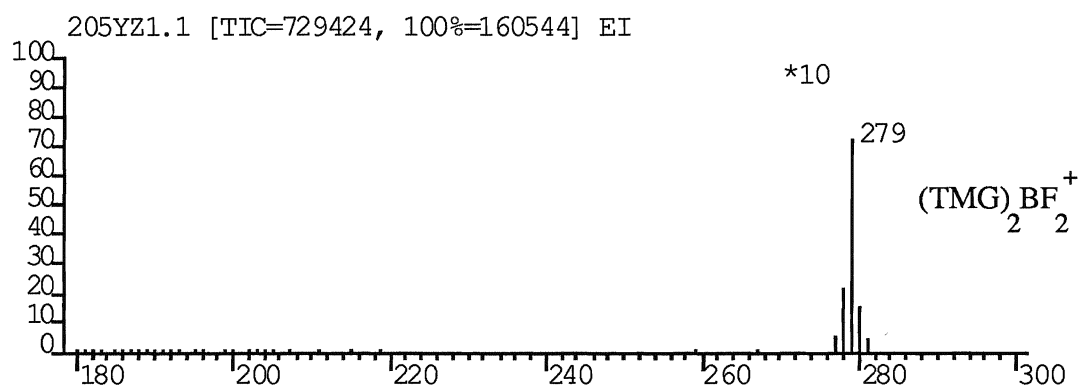
Appendix 4
 ^{13}C Spectra of DNB and (DNB).BF₃



Appendix 5
 ^{11}B Spectrum of the $\text{DBN}/\text{BF}_3/\text{BCl}_3$ System in Water
Following Extraction from CDCl_3



Appendix 6
FAB Spectrum of $(\text{TMG})_2\text{BF}_2^+$ in Solution



Appendix 7

FAB Spectrum of the DBU/BF₃/BCl₃/Quinuclidine System